ERDC/CHL TR-13-13

US Army Corps
of Engineers®
Engineer Research and
Development Center

ERDC
INNOVATIVE SOLUTIONS
for a safer, better world

Coastal Inlets Research Program

Preliminary Analysis of Morphology Change, Waves, and Currents for Navigation at Tillamook Inlet, Oregon

Zeki Demirbilek, Honghai Li, Lihwa Lin, Tanya M. Beck,
and Hans R. Moritz

September 2013

Coastal and Hydraulics Laboratory

The US Army Engineer Research and Development Center (ERDC) solves the nation's toughest engineering and environmental challenges. ERDC develops innovative solutions in civil and military engineering, geospatial sciences, water resources, and environmental sciences for the Army, the Department of Defense, civilian agencies, and our nation's public good. Find out more at www.erdc.usace.army.mil.

To search for other technical reports published by ERDC, visit the ERDC online library at http://acwc.sdp.sirsi.net/client/default.

ERDC/CHL TR-13-13
September 2013

Preliminary Analysis of Morphology Change, Waves, and Currents for Navigation at Tillamook Inlet, Oregon

Zeki Demirbilek, Honghai Li, Lihwa Lin, and Tanya M. Beck

Coastal and Hydraulics Laboratory
US Army Engineer Research and Development Center
3909 Halls Ferry Road
Vicksburg, MS 39180-6199

Hans R. Moritz

Portland District
333 SW 1st Avenue #200
Portland, OR 97204

Final report

Prepared for US Army Engineer District, Portland
333 SW First Avenue
10th Floor
Portland, OR 97204-3495

Under Coastal Inlets Research Program

Monitored by Coastal and Hydraulics Laboratory
US Army Engineer Research and Development Center
3909 Halls Ferry Road, Vicksburg, MS 39180-6199

Abstract

This report documents preliminary investigations of morphologic change and numerical modeling of wave and current conditions that affect entrance channel navigation at Tillamook Inlet, Oregon. It is believed that unfavorable conditions are caused by a combination of three primary factors: a large ebb shoal, the Pacific coast high-energy wave climate, and a narrow dual-jetty entrance that forms a high current environment. A limited analysis of two bathymetry surveys for representative summer and winter months in 2005 and 2010 indicated that the geometry of ebb shoal outside the entrance of the inlet has been changing, exhibiting an asymmetric orientation relative to the entrance in 2005 which became symmetric by 2010. The historical morphologic evolution of the ebb shoal was evaluated in an attempt to determine possible relationships between the ebb shoal changes and changes to waves and currents in the entrance channel at Tillamook. The numerical modeling analysis was limited to one selected summer month and one winter month, with the sole purpose being the investigation of potential relationships between the geometry (shape, footprint, and elevation) of the ebb shoal and local wave and current conditions during these two selected months. Results indicated that both the geometry of ebb shoal and the entrance jetties together influence the magnitude of waves and currents at the inlet area (through the entrance channel and over the shoal). The two jetties forming the narrow inlet entrance played a critical role in the evolution of the ebb shoal, controlling the spatial variation and severity of waves and currents at the entrance and over the ebb shoal. Wave conditions at Tillamook Inlet may be improved by changing the geometry of the ebb shoal or jetties or both.

Contents

Abstract ii

Figures and Tables v

Preface ix

Unit Conversion Factors xi

1 Introduction 1

1.1 Study area 1
1.2 Navigation at Tillamook Inlet 4
1.3 Study Plan 7
1.3.1 Purpose 7
1.3.2 Motivation 8
1.3.3 Approach 9

2 Data 12

2.1 Bathymetric Surveys 12
2.2 Tides 12
2.3 River Flows 13
2.4 Winds and Waves 13
2.5 Sediments and Littoral Transport 16

3 Analysis of Historical Morphology Change 17

3.1 Historical Evolution 17
3.2 Volume Change 18
3.3 Morphologic Characteristics 24
3.4 Role of Environmental Forces on Morphology 25

4 Wave Modeling 30

4.1 Bathymetry and Coastline Data 31
4.2 Model Input Winds and Wave Data 32
4.3 Wave Model Domain 32
4.4 Types of Wave Simulations 34
4.5 Wave Modeling Results 34
4.5.1 Seasonal Mean Wave Conditions 34
4.5.2 Symmetric and Asymmetric Ebb Shoal Simulations for a Summer Month 40
4.5.3 Symmetric and Asymmetric Ebb Shoal Simulations for a Winter Month 46
4.6 Hypothetically shortened South Jetty 51
4.6.1 Seasonal Mean Wave Conditions 52
4.6.2 Simulations for August and December 2010 55
4.7 Discussion and Summary of Results 58

5 Combined Wave and Flow Modeling 61

5.1 Details of Combined Wave and Flow Modeling 61
5.1.1 Model Setup 61
5.1.2 Model Forcing Conditions 61
5.2. Modeling Results 64
5.2.1 Water Levels and Currents 64
5.2.2 Summer and Winter Monthly Simulations 66
5.2.3 Simulations of Peak Flood and Ebb Conditions 69
5.3 Simulations for a hypothetically shortened South Jetty 71
5.3.1 Currents 71
5.3.2 Summer and Winter monthly simulations for hypothetically shortened South Jetty 72
5.3.3 Peak flood and ebb simulations for hypothetically shortened South Jetty 74
5.4 Discussion and Summary of Results 76

6 Conclusions 78
6.1 Morphology Change Analysis 79
6.2 Numerical Modeling 81

References 85

Appendix A: Description of CMS 87

Report Documentation Page

Figures and Tables

Figures

Figure 1-1. Study area location map for Tillamook Inlet and Bay, OR, and Port of Garibaldi. 2
Figure 1-2. The September 2010 bathymetry with authorized navigation channel (black), and the USCG preferred south channel (grey)..... 3
Figure 1-3. North Jetty (right) and South Jetty (left) of Tillamook Inlet..... 5
Figure 1-4. Vessel traffic intensity at Tillamook Inlet, 2010 - October 2012..... 6
Figure 2-1. Annual discharge for the Wilson River from 1980 to 2011..... 13
Figure 2-2. Annual discharge for the Trask River from 1997 to 2011. 14
Figure 2-3. Wind speed roses at the NDBC buoy 46029 for 2002 to 2004..... 14
Figure 2-4. Wave roses for the NDBC buoy 46029 for 2002 to 2004..... 15
Figure 3-1. The 1957 bathymetric contours (NOS; vertical datum is NAVD88) with the outlines of authorized navigation channel (black polygon), and present-day USCG navigation channel (grey polygon). 18
Figure 3-2. The 1984 to 2000 bathymetric contours of NWP surveys (NAVD88) with the outlines of authorized navigation channel (black polygon), and present-day USCG navigation channel (grey polygon). 19
Figure 3-3. The 2002 to 2010 bathymetric contours of NWP surveys (NAVD88) and the outlines of authorized navigation channel (black polygon), and present-day USCG navigation channel (grey polygon). 20
Figure 3-4. Baseline bathymetry (NAVD88) with plane and parallel contours offshore of the jetty tips. 21
Figure 3-5. Calculated total volume from 1957 to 2010..... 22
Figure 3-6. Evaluation of distance offshore as the length between the original South Jetty tip and the 10-m contour NAVD88. 25
Figure 3-7. The offshore distance of ebb shoal for bathymetric surveys from 1982 to 2010, with symmetric morphology highlighted in red. 26
Figure 3-8. Correlation between the offshore distance of the 10-m contour and the ebb shoal volume. 26
Figure 3-9. Monthly mean significant wave heights for 2001 to 2006. 28
Figure 3-10. Monthly mean significant wave heights for 2006 to 2011. 29
Figure 4-1. CMS-Wave grid for asymmetric ebb shoal grid domain and bathymetry based on September 2005 survey, NGDC shoreline and GEODAS database..... 32
Figure 4-2. Symmetric ebb shoal grid domain and bathymetry based on June 2010 survey, NGDC shoreline and GEODAS database..... 33
Figure 4-3. Hypothetically shortened South Jetty bathymetry contours. 33
Figure 4-4. Calculated wave steepness field for incident wave of (a) 2 m, 8 sec, (b) 3 m, 10 sec, and (c) 4 m, 12 sec, all with shore-normal wave direction, using the June 2010 symmetrical ebb shoal grid. 36

Figure 4-5. Calculated wave dissipation field for incident wave of (a) 2 m, 8 sec, (b) 3 m, 10 sec, and (c) 4 m, 12 sec, all with shore-normal wave direction, using the June 2010 symmetrical ebb shoal grid. 37

Figure 4-6. Calculated surfzone similarity field for incident wave of (a) 2 m, 8 sec, (b) 3 m, 10 sec, and (c) 4 m, 12 sec, all with shore-normal wave direction, using the June 2010 symmetrical ebb shoal grid. 38

Figure 4-7. Calculated Ursell number field for incident wave of (a) 2 m, 8 sec, (b) 3 m, 10 sec, and (c) 4 m, 12 sec, all with shore-normal wave direction, using the June 2010 symmetrical ebb shoal grid. 39

Figure 4-8. Calculated monthly maximum wave steepness fields for (a) asymmetric ebb shoal bathymetry (August 2005 waves), and (b) symmetric ebb shoal bathymetry (August 2010 waves). 41

Figure 4-9. Calculated monthly mean wave steepness fields for (a) asymmetric ebb shoal bathymetry (August 2005 waves), and (b) symmetric ebb shoal bathymetry (August 2010 waves)..... 42

Figure 4-10. Calculated monthly maximum wave dissipation fields for (a) asymmetric ebb shoal bathymetry (August 2005 waves), and (b) symmetric ebb shoal bathymetry (August 2010 waves). 43

Figure 4-11. Calculated monthly mean wave dissipation fields for (a) asymmetric ebb shoal bathymetry (August 2005 waves), and (b) symmetric ebb shoal bathymetry (August 2010 waves). 44

Figure 4-12. Calculated monthly maximum Ursell number fields for (a) asymmetric ebb shoal bathymetry (August 2005 waves), and (b) symmetric ebb shoal bathymetry (August 2010 waves). 45

Figure 4-13. Calculated monthly mean Ursell number fields for (a) asymmetric ebb shoal bathymetry (August 2005 waves), and (b) symmetric ebb shoal bathymetry (August 2010 waves)..... 46

Figure 4-14. Calculated monthly maximum wave steepness fields for (a) asymmetric ebb shoal bathymetry (December 2005 waves), and (b) symmetric ebb shoal bathymetry (December 2010 waves). 47

Figure 4-15. Calculated monthly mean wave steepness fields for (a) asymmetric ebb shoal bathymetry (December 2005 waves), and (b) symmetric ebb shoal bathymetry (December 2010 waves). 48

Figure 4-16. Calculated monthly maximum wave dissipation fields for (a) asymmetric ebb shoal bathymetry (December 2005 waves), and (b) symmetric ebb shoal bathymetry (December 2010 waves). 49

Figure 4-17. Calculated monthly mean wave dissipation fields for (a) asymmetric ebb shoal bathymetry (December 2005 waves), and (b) symmetric ebb shoal bathymetry (December 2010 waves). 50

Figure 4-18. Calculated monthly maximum Ursell number fields for (a) asymmetric ebb shoal bathymetry (December 2005 waves), and (b) symmetric ebb shoal bathymetry (December 2010 waves). 51

Figure 4-19. Calculated monthly mean Ursell number fields for (a) asymmetric ebb shoal bathymetry (December 2005 waves), and (b) symmetric ebb shoal bathymetry (December 2010 waves). 52

Figure 4-20. Calculated wave steepness fields of three incident waves for the hypothetically shortened South Jetty. 53

Figure 4-21. Calculated wave dissipation fields of three incident waves for the hypothetically shortened South Jetty. 54

Figure 4-22. Calculated Ursell number fields of three incident waves for the hypothetically shortened South Jetty. 55

Figure 4-23. Calculated monthly maximum wave steepness fields for symmetric ebb shoal bathymetry with (a) August 2010 waves and (b) December 2010 waves - hypothetically shortened South Jetty. 56

Figure 4-24. Calculated monthly maximum wave dissipation fields for symmetric ebb shoal bathymetry with (a) August 2010 waves and (b) December 2010 waves - hypothetically shortened South Jetty. 57

Figure 4-25. Calculated monthly maximum Ursell number fields for symmetric ebb shoal bathymetry with (a) August 2010 waves and (b) December 2010 waves - hypothetically shortened South Jetty. 58

Figure 5-1. CMS domain and telescoping grid. 62

Figure 5-2. The symmetric ebb shoal grid (based on June 2010 bathymetry) and asymmetric ebb shoal grid (based on September 2005 bathymetry). 62

Figure 5-3. Existing (left) and hypothetically shortened (right) South Jetty configurations. 62

Figure 5-4. Water level data for August 2005 at South Beach and Yaquina River, OR. 63

Figure 5-5. Wind data for August and December 2005 at NDBC Buoy 46029. 64

Figure 5-6. River flow discharges for December 2005 and 2010 from USGS gauges at Trask (Sta 14302480) and Wilson (Station 14301500) rivers, OR. 64

Figure 5-7. Calculated water surface elevation at Garibaldi, August 2010. 65

Figure 5-8. Calculated current field on 12 August 2010 at 21:00 GMT (flood current) and on 13 August 2010 at 03:00 GMT (ebb current). 65

Figure 5-9. Calculated current field on 27 December 2010 at 12:00 GMT (flood current) and 18:00 GMT (ebb current). 66

Figure 5-10. Calculated monthly mean wave steepness (top), wave dissipation (middle), and Ursell number (bottom) for August and December 2005. 67

Figure 5-11. Calculated maximum wave steepness (top), wave dissipation (middle), and Ursell number (bottom) for August and December 2005. 67

Figure 5-12. Calculated monthly mean wave steepness (top), wave dissipation (middle), and Ursell number (bottom) for August and December 2010. 68

Figure 5-13. Calculated maximum wave steepness (top), wave dissipation (middle), and Ursell number (bottom) for August and December 2010. 68

Figure 5-14. Calculated wave steepness (top), wave dissipation (middle) and Ursell number (bottom) during a flood current on 12 August 2010 at 21:00 GMT and an ebb current on 13 August 2010 at 03:00 GMT. 69

Figure 5-15. Calculated wave steepness (top), wave dissipation (middle), and Ursell number (bottom) during a flood current on 27 December 2010 at 12:00 GMT and an ebb current on 27 December 2010 at 18:00 GMT. 70

Figure 5-16. Calculated wave steepness (top), wave dissipation (middle), and Ursell number (bottom) during an ebb current in 24 December 2010 at 03:00 GMT. 71

Figure 5-17. Calculated current fields for the hypothetically shortened South Jetty on 12 August 2010 at 21:00 GMT (flood current) and 13 August 2010 at 03:00 GMT (ebb current). 72

Figure 5-18. Calculated current fields for the hypothetically shortened South Jetty on 27 December 2010 at 12:00 GMT (flood current) and 18:00 GMT (ebb current)..... 73

Figure 5-19. Monthly mean wave steepness (top), wave dissipation (middle), and Ursell number (bottom) fields for the hypothetically shortened South Jetty in August and December 2010. 73

Figure 5-20. Maximum wave steepness (top), wave dissipation (middle), and Ursell number (bottom) fields for the hypothetically shortened South Jetty in August and December 2010. 74

Figure 5-21. Wave steepness (top), wave dissipation (middle), and Ursell number (bottom) for the hypothetically shortened South Jetty: a) flood current in 12 August 2010 at 21:00 GMT and b) ebb current in 13 August 2010 at 03:00 GMT. 75

Figure 5-22. Wave steepness (top), wave dissipation (middle), and Ursell number (bottom) for the hypothetically shortened South Jetty: a) flood current on 27 December 2010 at 12:00 GMT and b) ebb current on 27 December 2010 at 18:00 GMT. 75

Figure A-1. The CMS framework and its components. 88

Tables

Table 2-1. General characteristics of tides for NOAA Station 9437540 at Garibaldi. 12

Table 2-2. Computed wave parameters for NOAA Buoy 46029 for ten years (2000-2010). 15

Table 3-1. Bathymetric datasets used in this study and volumetric evolution of the ebb shoal. 22

Preface

A preliminary analysis of morphology change and numerical modeling estimates of waves and currents was conducted at Tillamook Inlet located approximately 90 miles west of Portland, OR. Under the guidance outlined in Engineering Circular 11-2-204 (USACE 2013), the Corps must pursue an on-going program to rehabilitate, modernize, or replace structures and components, and maintain channels exhibiting a deteriorating ability to meet system demands. These decisions are based on performance-based and risk-informed criteria. While surveys and wave conditions used in this limited scope study are partial data sets, the information obtained from this study is critical to assessing the present structural and functional conditions of the Tillamook jetties, which then informs future investment strategies.

The entrance connects to Tillamook Bay, a shallow estuary that consists of tidal channels and broad inter-tidal mudflats. This study was performed by the Coastal and Hydraulics Laboratory (CHL) of the US Army Corps Engineer Research and Development Center (ERDC) at the request of the US Army Engineer District, Portland (NWP). The study started with a historical morphologic analysis followed by modeling of waves and currents from approximately 80-m depth contour, through the approach channel, over the ebb shoal and into the entrance channel. Waves and tides move through the entrance channel protected by two rubble-mound jetties into the well-sheltered shallow back-bay areas of the estuary.

Historical morphology changes at Tillamook were caused by waves, tides, river inflows, and sedimentation. The effects were examined with the Coastal Modeling System (CMS), an integrated coastal modeling system composed of a spectral wave model and a two-dimensional depth-averaged hydrodynamic model that includes sediment transport calculations. The goal of this limited scope study was to characterize the combined effect of waves and currents in relation to the morphology of the entrance channel for two ebb shoal geometries during one summer and one winter month condition. The roles of the various physical forcings that affect navigation at Tillamook Inlet were investigated. This report provides the details of these tasks, the results, and major findings of the study.

The Coastal Inlets Research Program (CIRP) conducted this study with funding by the Operation and Maintenance (O&M) Navigation business line of the Headquarters, US Army Corps of Engineers (HQUSACE). The CIRP is administered for Headquarters by the US Army Engineer Research and Development Center (ERDC), Coastal and Hydraulics Laboratory (CHL), Vicksburg, MS, under the Navigation Program of HQUSACE. James E. Walker is HQUSACE Navigation Business Line Manager overseeing the CIRP. W. Jeff Lillycrop, CHL, is the ERDC Technical Director for Navigation. Dr. Julie Dean Rosati, CHL, is the CIRP Program Manager. The study was conducted by Tanya M. Beck, Drs. Honghai Li and Lihwa Lin, all of Coastal Engineering Branch (CEB), and Dr. Zeki Demirbilek, of Harbors, Entrances, and Structures Branch (HESB). The report was reviewed by Heidi P. Moritz of USACE Portland District and Dr. Julie Dean Rosati. Hans R. Moritz of the Portland District provided information and coordination in support of this study, and reviewed the report. This work was conducted under the general administrative supervision of Drs. Jeffrey P. Waters and Jackie Pettway, Chiefs of CEB and HESB, respectively, and Dr. Rose Kress, Chief of the Navigation Division. Funding for the study was provided by Jeff Lillycrop, the Navigation Technical Director. Jose Sanchez and Dr. Bill Martin were the Deputy and Director of CHL during this study period, respectively.

At the time of publication of this report, COL Kevin Wilson, EN, was Commander and Executive Director of ERDC. Dr. Jeffery P. Holland was ERDC Director.

Unit Conversion Factors

Multiply	By	To Obtain
cubic yards	0.7645549	cubic meters
feet	0.3048	meters
yards	0.9144	meters

1 Introduction

This study was performed for Tillamook Inlet, Oregon by the Coastal and Hydraulics Laboratory (CHL) of the USACE Engineer Research and Development Center (ERDC) at the request of the US Army Engineer District, Portland, hereafter, the Portland District (NWP). The objective of this limited scope preliminary investigation was to analyze characteristics of waves and currents during one summer and one winter month in relation to the morphology of the ebb shoal located seaward of the entrance to Tillamook Inlet. The roles of the various physical forcings affecting navigation at Tillamook Inlet were investigated, including analysis of historical morphology change of the ebb shoal and numerical modeling of waves and currents. An analysis of storm climate and oceanographic conditions of the Pacific North West was not in the scope of this study. A limited in scope modeling effort was conducted using the 2005 and 2010 bathymetric surveys, which characterize two recent representative morphologic conditions for a summer and winter month. The purpose of this chapter is to present an overview of the study.

1.1 Study area

The study area is Tillamook Inlet (Figure 1-1), located on the Pacific Northwest coast of Oregon, about 90 miles west of Portland. Five rivers drain into Tillamook Bay, and this shallow estuary is connected to the Pacific Ocean through the navigation channel that passes through a jetty-entrance that joins with an ebb shoal and the Pacific Ocean at approximately the 80-m depth contour. The channel is well-defined from the entrance to Port of Garibaldi, the channel's termination point in Tillamook Bay. The average depth in the shallow Tillamook estuary is less than 2 m, and its dynamics are controlled by rivers, surface water flows, and tides. Tillamook Bay is meso-tidal, with a diurnal tidal range of 2 m and extreme tidal range of 4.1 m (Komar 1997). The National Oceanic and Atmospheric Association (NOAA) have a water level gauge at Port of Garibaldi (NOAA Station 9437540). Tillamook Bay has mixed semi-diurnal tides and a mean tide range of about 2 m.

Figure 1-1. Study area location map for Tillamook Inlet and Bay, OR, and Port of Garibaldi.

The navigation channel is depicted in Figure 1-2. The depth and width of the navigation channel are monitored from the entrance to Garibaldi. The channel is comparatively deeper at the entrance than it is in the middle and back bay (estuary). Depth at the entrance ranges between 8 to 13 m relative to mean lower low water (MLLW). There are no markers defining the channel past beyond the tips of jetties over the ebb shoal and out in the Pacific Ocean. As such, the width and depth of the unmarked channel seaward of the entrance over the entire ebb shoal and beyond are not specified. Consequently, there is no prescribed inbound/outbound vessel route for traffic moving over the ebb shoal, where depths vary between 8 to 15 m. Additional information about the Tillamook Inlet navigation channel is available from the NWP website[1].

Because the inlet is naturally self-scouring, the dual-jetty entrance segment of the channel has not been dredged since 1976 following the completion of the South Jetty in 1970. The North Jetty was first

[1] http://www.nwp.usace.army.mil/Locations/OregonCoast/TillamookBay.aspx

Figure 1-2. The September 2010 bathymetry with authorized navigation channel (black), and the USCG preferred south channel (grey).

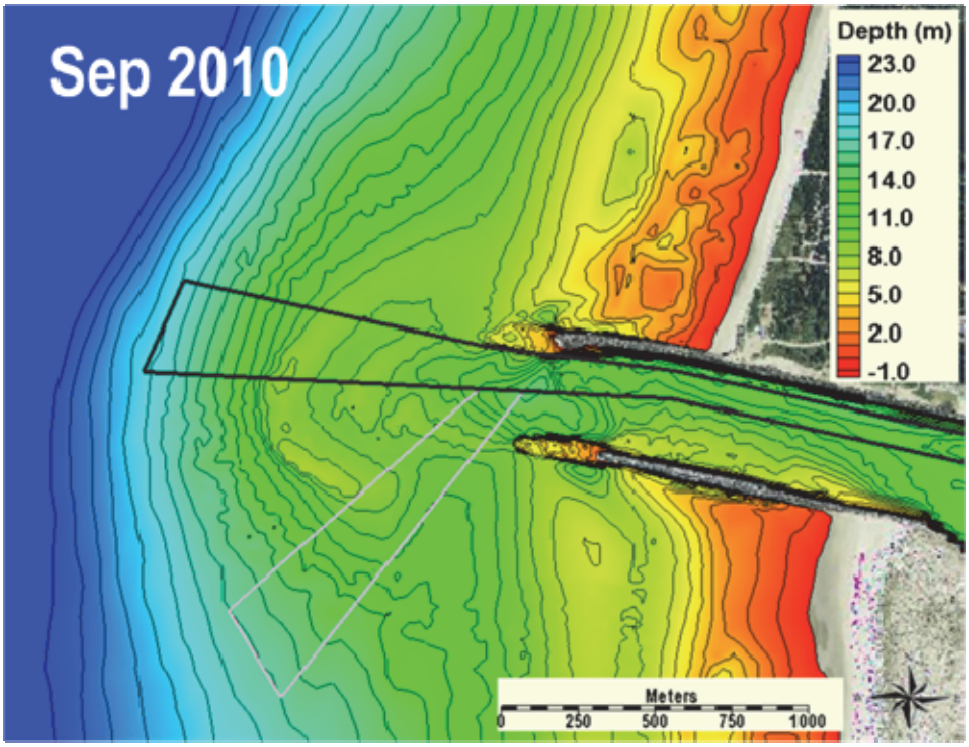

constructed in 1914 and completed in 1931. Annual surveys indicate that the entrance has not shoaled to the 6-m MLLW depth limit to require dredging. Both jetty heads have degraded over the years, and as of 2010, the north and south jetties had receded landward approximately 160 m and 300 m, respectively. Based on the Coastal Navigation Structures (CNS) Structural Condition Rating (SCR) criteria outlined in EC 11-2-204, the South Jetty meets the completely degraded condition criteria. In 2006, annual surveys, local knowledge of wave severity, degradation of jetties, and change in the entrance channel morphology collectively led the US Coast Guard (USCG) to reevaluate optimal approaches to the inlet. This resulted in a new turn in the channel direction marked by lights and buoys that directed vessels abruptly toward a south-oriented navigation channel. The USCG recommended channel is shown by a polygon of the hypothetical channel perimeter in grey color on Figure 1-2.

The spatial variation of waves and currents occurring over the ebb shoal is dependent partly on the morphology of the ebb shoal that changes year to year. Because of the dynamic nature of seasonally evolving ebb shoal geometry, the resulting wave and current magnitudes over the ebb shoal and in the entrance channel can vary year around. The interaction between

waves and currents in these areas can develop large steep waves and strong currents.

Because of these concerns, the present study was conducted with the goal to identify local wave and current conditions in Tillamook Inlet. Consequently, the primary motivation behind this study was a better understanding of the cause-effect relationship between wave conditions at Tillamook Inlet and characteristics of the ebb shoal, hydrodynamics of entrance, role of the jetties, and interaction between the ebb shoal, entrance, and estuary. The first objective of this study was an analysis of the characteristics of short- and long-term morphology changes at Tillamook Inlet using historical survey records. Sediment transport and morphology change modeling was not considered in this study. The second objective of the study was to evaluate effects of ebb shoal changes on estimated waves and currents at the entrance. The third objective was to develop estimates of waves and currents for the months of August and December representing summer and winter seasons. These estimates were obtained by transforming offshore waves from Buoy 46029 in 197 ft depth over the August 2005 and September 2010 bathymetries.

1.2 Navigation at Tillamook Inlet

Tillamook Inlet is the only navigable link that connects ports within Tillamook Bay estuary to the Pacific Ocean. In the 20th Century, steamboat ships would haul timber from Tillamook Bay north to the Columbia River. The inlet was historically located at the northern end of the present day Tillamook Bay and was held stable by a rocky headland. To help control the position of the entrance channel at the inlet, North Jetty was first installed in 1914 and extended to the full length in 1931. By 1918, the ebb shoal had migrated approximately 300 m offshore of the partially-completed North Jetty tip. Completion of the 1,740 m North Jetty in 1931 straightened and stabilized the channel adjacent to the jetty but did not create a deep navigable channel beyond the North Jetty tip.

A series of large destructive fires severely damaged forests surrounding Tillamook Bay in the 1930s and 1950s. These events introduced a significant amount of sediment into the local rivers that was deposited into Tillamook Bay, shut down the port in Bay City (Figure 1-1), and increased shoaling of the entrance channel. Although sedimentation of the Bay slowed in the 1960s, the navigation problems persisted, and Congress authorized construction of the South Jetty in 1965. The 2,440-m-long South Jetty was

finished in 1979. The authorized channel between the jetties is 1,520 m long, 5.5 m (18 ft, MLLW) deep, and 61 m wide. The entrance channel outside the jetties is also 5.5 m (18 ft) deep and has no prescribed width (Figures 1-2 and 1-3). Both the entrance and main navigation channels have remained deep since 1976, requiring no dredging.

Figure 1-3. North Jetty (right) and South Jetty (left) of Tillamook Inlet.

Subsequent to the construction of the jetties, the adjacent shorelines on the north and south sides of the entrance of inlet adjusted to the local effects of jetties, waves, currents, and longshore sediment transport. The jetties were constructed to mainly improve navigation, minimize dredging requirements for the Federal deep-draft navigation channel, and train the tidal current that carries material from the entrance area to the ocean. Over the past 50 yrs, while the offshore beach profile has remained relatively uniform, depths over the ebb shoal have continued to change, but remained steadily above 8 m. The depths over the ebb shoal have been deep enough not to pose risk to the vessels passing over it. Consequently, no dredging was necessary to deepen any part of the ebb shoal. The adjacent shorelines north and south of the inlet were initially affected after jetties were in place, but they have stabilized.

In 2006, the USCG recommended that passage through the present day navigation channel landward of the jetty tips follow the North Jetty and take a southerly turn near the submerged tip of the South Jetty. The mariners familiar with this area refer to this area as the "South Hole", implying that there is a lull or depression in the waves over this part of the ebb shoal when boats enter and exit the entrance channel. Figure 1-4 exhibits the inbound and outbound traffic routes for 2010 to the present time through Tillamook Inlet as reported by the USCG's Nationwide Automatic Identification System (NAIS). The lighter blue colors represent dense traffic areas in Figure 1-4, highlighting the recommended USCG navigable transit routes and the concentration of traffic through the south-oriented undefined channel.

Figure 1-4. Vessel traffic intensity at Tillamook Inlet, 2010 - October 2012.

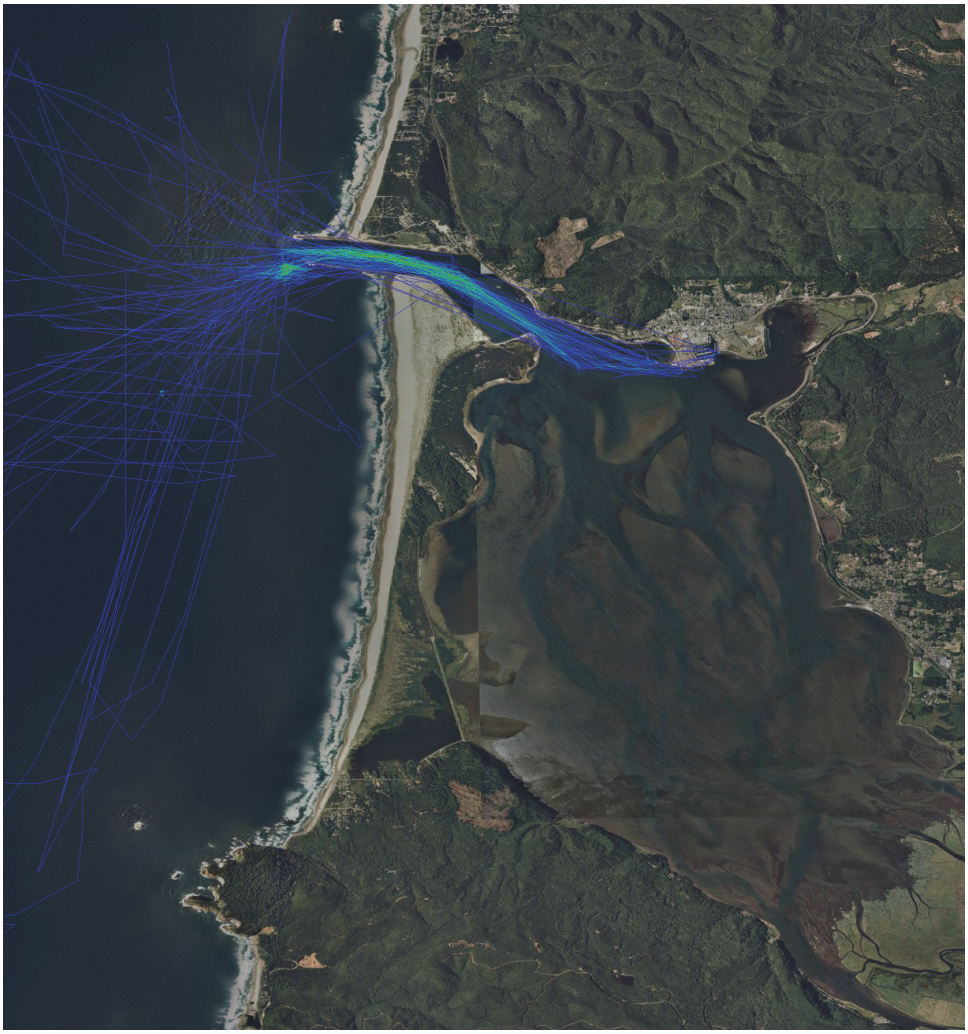

The USCG uses nav-aid buoys currently to guide boaters on a path west to east from the open sea over the ebb shoal. Local boaters extremely familiar with this inlet may not follow these buoys directing them to come straight across the mid-grounds of the ebb shoal, considered to be the most active area over the ebb shoal. In fact, boaters believe the mid-section of ebb shoal is filled in over the years and has a hump, and there is less depth in the channel straight out than to the south or north. Consequently, the USCG is considering improvements to navigational aids to guide boaters into the bay by realigning the entrance buoys to direct boaters to approach the ebb shoal from the southwest instead of heading straight over the roughest waters at the jetty opening. Local boaters know to take a southerly approach, this is their preferred way to come in and go out the entrance. Only during very mild or calm conditions do boaters consider coming from the north or down the middle of ebb shoal. Mariners unfamiliar with the ebb shoal who follow the current USCG navigational aids encounter navigation problems. To avoid such problems, the USCG is considering re-directing traffic in a southwest direction near the submerged tip of the South Jetty. Estimates of waves and currents provided in Chapters 4 and 5 should be useful to improvements of navigation at Tillamook Inlet.

1.3 Study Plan

1.3.1 Purpose

This report investigates the time-varying and spatially-varying nature of wave action affecting the jettied inlet to Tillamook Bay, Oregon, in terms of the processes that can affect ocean waves approaching the inlet. The report and the work featured within represents an initial step for investigating the complex nature of wave conditions at the ocean entrance to Tillamook Bay, as these processes may affect navigation at the inlet. Should the need arise, incremental successor evaluations can build upon the models, spatial data, and findings produced by this report. Additional evaluations may be prompted by a need for potential future jetty repairs, development of improved navigation aids or channel re-alignment, analysis of sediment transport pathways, or shoreline evolution assessment. This evaluation and future evaluations are critical to define the structural and functional condition of the jetties, which are the basis to informing the performance-based, risk-informed budgeting criteria and process.

Tillamook Bay is located along the northern coast of Oregon, where the coastal ocean wave environment can be affected by the interaction of

locally generated sea and swell waves generated from distant storms. The results from this report represent an initial-first step assessment, toward understanding how wave action at Tillamook Bay inlet may be affected by the variation of the following:

1. Ebb tidal shoal configuration (morphology),
2. Offshore wave conditions,
3. Inlet current patterns, and
4. Continued future landward recession of the South Jetty.

The information contained within this report is based on a collaborative effort between the US Army Engineering Research and Development Center and Portland District. The authors express appreciation for project briefing and onsite support provided by the US Coast Guard-MLB Garibaldi (MC Michael Saindon) and Port of Garibaldi (Kevin Greenwood). This report was compiled during Sept-Dec 2012 using funding from the USACE Navigation Asset Management Portfolio for Research, Development, and Transfer. The expertise for work synthesis was provided by the Coastal Inlets Research Program.

1.3.2 Motivation

The present configuration of the ocean entrance to Tillamook Bay is characterized by a narrow dual-jetty inlet (1,200 ft wide) and a large ebb shoal located immediately oceanward (within 1-mile west) of the jettied entrance. The top elevation of ebb tidal shoal is below the federally-authorized depth for the inlet (5.5 m MLLW), yet incoming ocean waves can be destabilized by the depth-limiting condition of the prominent ebb tidal shoal. The inlet's narrow jetty configuration functions to constrict tidal flow through the inlet, increasing the current velocity, especially during the ebb (outgoing) tide. Increased current velocity prevents sediment deposition within the inlet's navigation channel, which has eliminated the need for dredging. This was an intended outcome of the dual-jetty system at Tillamook Bay. However, the interaction of strong ebbing currents with incoming ocean waves passing over the inlet's ebb shoal can amplify and confuse the wave environment at the inlet entrance. During some conditions, ocean waves approaching the inlet may become very steep and break at locations where mariners are attempting to transit the seaward approach to the inlet. This condition is made more problematic by the presence of submerged-relic jetties, which extend 122-274 m further offshore than what is indicated by the present visible surface expression of

each jetty head. The submerged parts of each jetty reach an elevation of 1.5 to 3 m MLLW and can enhance wave breaking near the inlet, as waves pass over the submerged structures. Vessels passing over the submerged jetty sections can ground and founder on the relic structures.

The confounding effects that the inlet's ebb shoal, enhancement of strong tidal currents, and presence of submerged relic jetty sections interact to affect navigation at the ocean side of Tillamook Bay inlet. The primary objective for this study was to develop an evaluation framework for improving our understanding of factors that affect the wave and current environment at Tillamook Inlet. That primary objective of defining how the structural condition impacts the functionality of the jetties can then be used to support and inform program objectives and performance measures to reflect the near term realities of a constrained budget environment.

1.3.3 Approach

The above purpose and motivation of this study would require a comprehensive analysis of the morphology change, waves, currents, and their interaction that affect navigation at the Tillamook Inlet. The approach used in this study is only a preliminary analysis that needs to be followed by a more complete investigation. The present study focused on the investigation of two related issues: a) an analysis of short- and long-term morphologic changes at the Tillamook Inlet based on historical survey records to determine how the ebb shoal adjusts itself to the environmental forces that change during winter and summer months, and b) to what extent estimates of waves and currents are different for the months of August and December using the 2005 and 2010 bathymetric surveys. The implementation of approach and associated tasks are described briefly next, and details are provided in Chapters 2 through 5. The approach was implemented in four specific Tasks as follows:

1. Morphological analysis. Details are presented in Chapter 3.
2. Numerical modeling of only waves. Chapter 4 describes details of this modeling task.
3. Numerical modeling of waves with flow (circulation). The details of this task are provided in Chapter 5.
4. Modeling with a hypothetically shortened South Jetty. Wave-only results for the hypothetically shortened South Jetty are included in the Chapter 3, and waves with flow are provided in Chapters 4 and 5.

Task 1. Historical survey records were used in the analysis of ebb shoal morphology changes, with the intent to identify short- and long-term morphologic changes that have occurred at Tillamook Inlet, as well as to determine if and how the ebb shoal had adjusted itself to the seasonally changing environmental forces during the winter and summer months. Geographic Information System (GIS) tools were used in the morphology change analysis to calculate area, volume, and geometry (footprint) changes that have occurred over the last three decades. It is important to note that morphology change was not considered in the numerical modeling of this study which would have required the calculation of sediment transport and morphology change.

The morphologies associated with bathymetric surveys from the 1980s to 2010 were reviewed, and two representative bathymetric datasets were selected from the recent decade for numerical modeling of waves and currents using the Coastal Modeling System (CMS). A 1957 survey was included for a perspective on the pre-South Jetty condition. The GIS analysis of these datasets provided historical morphology change of the inlet, including volume change and shape parameters. This information is needed in the assessment of various environmental and physical forcing factors that have a significant impact on seasonal to decadal changes of the inlet's modern-day morphology. The physical forcing factors considered include the river discharges affecting tidal prism, sea level trends (USACE 2011), and wave energy.

Tasks 2 through 4. Details of the numerical modeling tasks are provided in Chapters 3, 4, and 5. Wave and current estimates were obtained by numerical modeling using the CMS. Sediment transport and morphology change modeling were not considered in this study. The CMS includes wave, flow, and sediment transport modeling tools for coastal inlets and navigation projects, and development and enhancement of CMS capabilities continues to evolve as a research and engineering tool for desk-top computers. The CMS uses the Surface-water Modeling System (SMS) interface for grid generation and model setup, as well as plotting and post-processing (Zundel 2006). See Appendix A for additional information about the CMS and its capabilities.

Two alternatives were considered in the CMS modeling: existing inlet configuration with two representative ebb shoal morphologies and a hypothetically shortened South Jetty configuration. Wave and current

modeling was performed for the months of August and December for both the 2005 and 2010 bathymetric surveys. Three NOAA offshore buoys (46041, 46029 and 46050) are available in proximity of the Tillamook Inlet. The offshore winds and wave data from the closest Buoy 46029 were used in the CMS modeling tasks. Details of the wave and flow modeling performed for the months of August (summer) and December (winter) using the 2005 and 2010 bathymetric surveys are described in Chapters 4 and 5 of this report.

Chapter 4 describes the waves-only simulations which were conducted to represent wave and wind conditions during slack or low tidal flows. The height and direction of waves approaching the Tillamook Inlet navigation channel change due to wave shoaling, refraction, diffraction, reflection, and breaking. Waves propagating through the entrance interact with bathymetry, surrounding land features, currents and coastal structures. These changes to waves affect bed shear stresses and sediment mobility around this inlet. The CMS-Wave, a spectral wave model, was used in this study given the large modeling domain over which wave estimates were required.

The coupled wave-current simulations described in Chapter 5 include winds, tides, and river inflows to represent more realistic conditions. CMS-Flow, a two-dimensional shallow-water wave model, was used for hydrodynamic modeling (calculation of water level and current) in this study. This circulation model provides estimates of water level and current given the waves, tides, winds, and river discharges as boundary conditions. In this study, the coupled CMS-Flow and CMS-Wave models used the same grid domains. The CMS-Flow modeling task included specification of winds, tides, and river flows (discharges) to the model. The effects of waves on the circulation were investigated by using wave forcing as input to CMS-Flow and have been included in the simulations performed for this study. For the combined wave and flow modeling, three wave conditions (H_s = 2 m with T_p = 8 sec, H_s = 3 m with T_p = 10 sec, and H_s = 4 m with T_p = 12 sec) were used to investigate the effects of flow on waves. These test runs were done in part for setting up the CMS-Flow for simulations using the actual field conditions in 2005 and 2010 for the months of August (summer) and December (winter). Details of these simulations are presented in Chapter 5.

2 Data

2.1 Bathymetric Surveys

Time-series digital surveys of the entrance channel to Tillamook were analyzed in GIS to determine the shape, size, and temporal characteristics of the ebb shoal. The Portland District provided surveys from 1982 to 2009 in digital format. Additional datasets were gathered from the National Oceanic Services (http://oceanservice.noaa.gov/), including a 1957 digital single-beam survey, a 2010 multi-beam survey of the entrance channel from the US Geological Survey (USGS), and a USACE 2010 lidar survey (http://shoals.sam.usace.army.mil/). The NOS and JALBTCX data had complete coverage and were used in the morphology change study. The data quality of NOS and JALBTCX datasets were not investigated in this study. All datasets were converted to the North American Vertical Datum of 1988 (NAVD 88). The survey data collected by the District varied in coverage from year to year, and only the ten best surveys from 1984 to 2010 could be used in this analysis.

2.2 Tides

Table 2-1 lists measured mean and diurnal tidal ranges inside Tillamook Bay at Port of Garibaldi. Overall, Tillamook Bay has mixed semi-diurnal tides, with a 1.7 m MLLW mean tidal range in the lower bay, 2.4 m average highest daily tide, and 3.6 m extreme tide (Table 2-1). The average Tillamook Bay water level is 0.25 m lower during the summer period.

Table 2-1. General characteristics of tides for NOAA Station 9437540 at Garibaldi.

General Characteristic	Value	Description
Mean Tidal Range	1.90 m	NOAA (2012a)
Great Diurnal Tidal Range	2.53 m	NOAA (2012a)

Low-pressure fronts are common in this part of the northeast Pacific Ocean during the months of October and March. These winter storm events are similar to hurricanes that impact the Gulf of Mexico and East coast of the USA. These storms have sustained wind speeds of 10 m/sec to 35 m/sec and capable of generating large wind-waves that can cause water levels to rise rapidly in the Tillamook Bay. These water level variations combined with

increased river flows draining into the estuary can affect several inter-tidal mudflats that are present in this shallow estuary (Figure 1-4).

2.3 River Flows

Five rivers drain into Tillamook Bay, and clockwise from north to south they are the Miami, Kilchis, Wilson, Trask, and Tillamook rivers (see Figure 1-4). The Wilson and Trask rivers contribute the highest volume of water and have been regularly monitored by the USGS since the 1980s and 1990s, respectively. The annual discharges for the Wilson and Trask rivers are shown in Figures 2-1 and 2-2. The Pacific Northwest experienced intense climatic events in the late 1990s that resulted in higher than average rainfall. There were not sufficient data to perform a reliable analysis of the morphology change in the Tillamook Bay estuary to examine how mudflats might have changed by flooding events and other climate changes.

2.4 Winds and Waves

The three NOAA offshore buoys in proximity of Tillamook are 46041, 46029, and 46050. The closest buoy to Tillamook Inlet is 46029, and the offshore wind and wave data used in this study were obtained from this buoy. Wind roses in Figure 2-3 show that majority of wind directions are parallel to shoreline. While a higher percentage of winds are from N-NNW, stronger winds are from S-SSE.

Figure 2-1. Annual discharge for the Wilson River from 1980 to 2011.

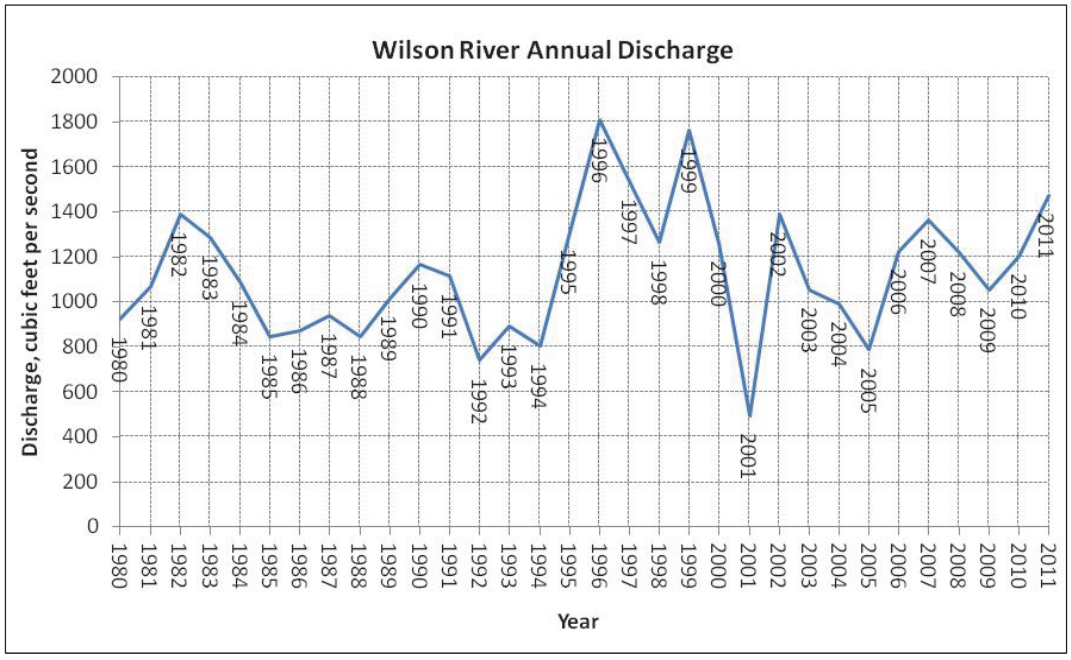

Figure 2-2. Annual discharge for the Trask River from 1997 to 2011.

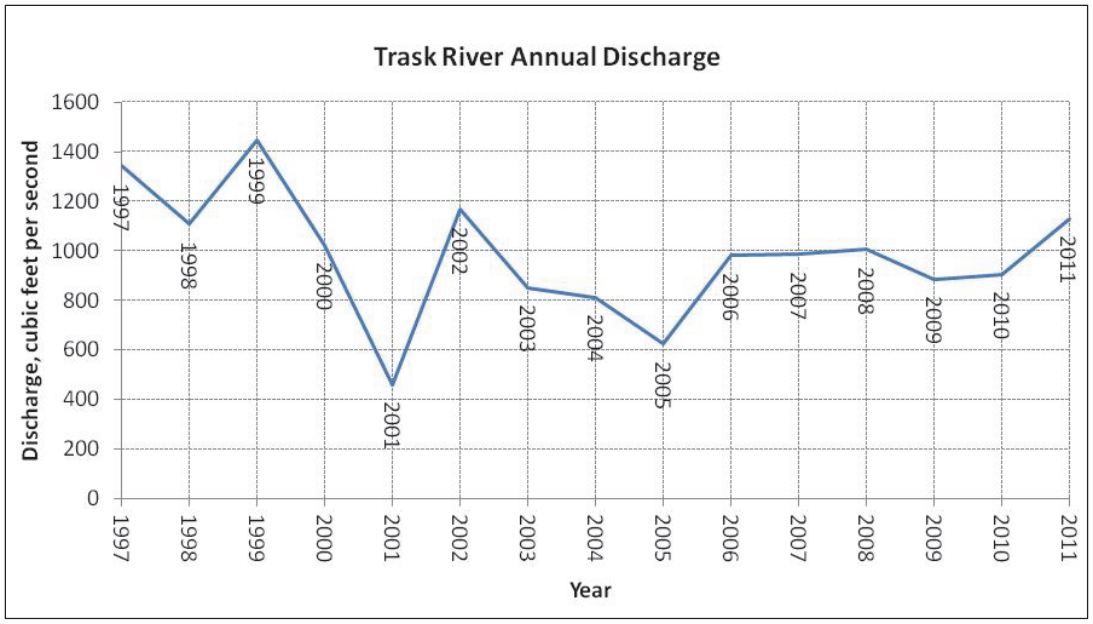

Figure 2-3. Wind speed roses at the NDBC buoy 46029 for 2002 to 2004.

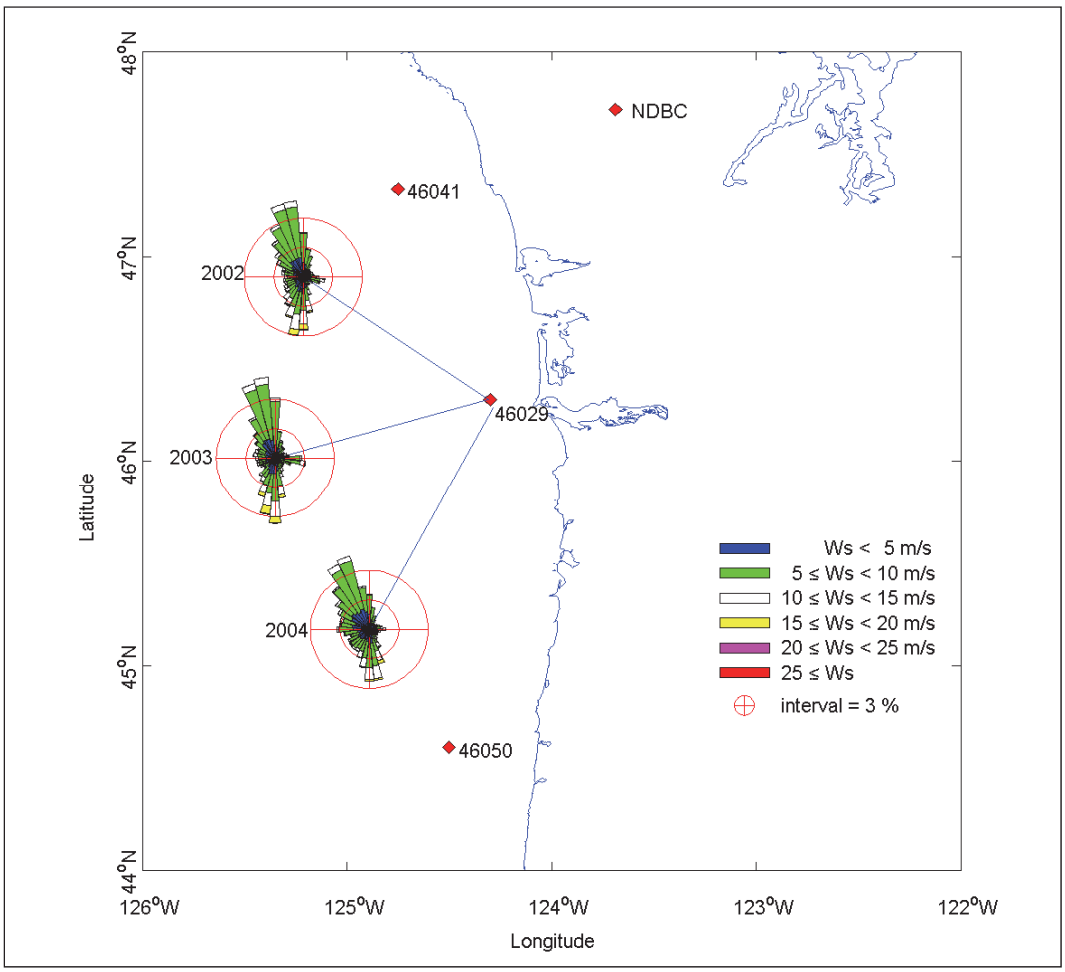

Figure 2-4 shows examples of wave roses for the buoy 46029 for three consecutive years: 2002, 2003 and 2004. These show that waves for 2002 to 2004 occur primarily from the NNW-W sector. The wave heights at the offshore buoy varied, and large wave heights in excess of 5 m had occurred. Tillamook Inlet is directly exposed to such large waves. The wave parameters calculated for a period of 10 yrs (2000-2010) are listed in Table 2-2. These sample wave data are for recent years and may not represent the long-term wave climate in the study area.

Figure 2-4. Wave roses for the NDBC buoy 46029 for 2002 to 2004.

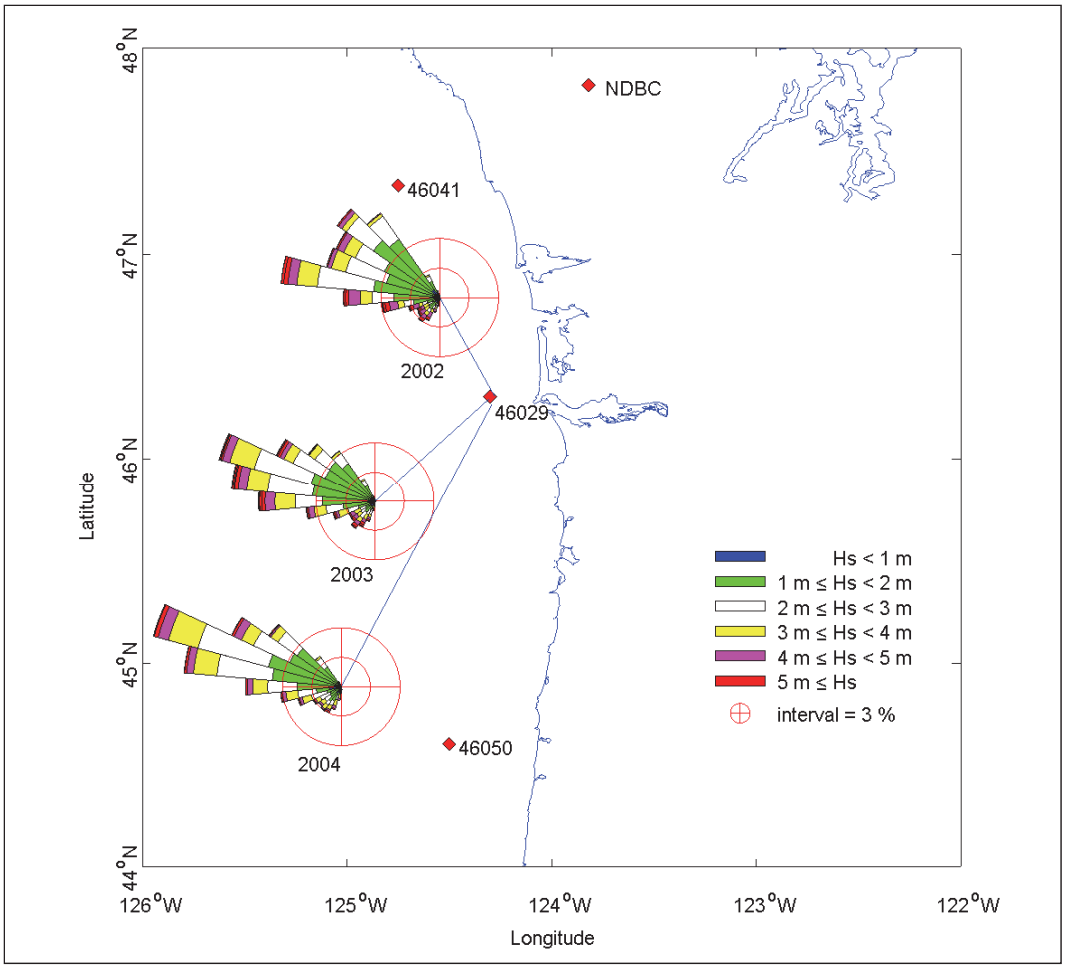

Table 2-2. Computed wave parameters for NOAA Buoy 46029 for ten years (2000-2010).

General Characteristic	Value	Description
Mean Significant Wave Height	3 m	NDBC (2012)
Mean Peak Wave Period	7 sec	NDBC (2012)
Mean Wave Direction	360 deg	NDBC (2012)

Figures 2-3 and 2-4 show that this region of the North Pacific Ocean is characterized by a high-energy wave climate with moderate summer waves and energetic waves during the passages of extra-tropical storms in the winter. The largest waves are mostly from the NW in the summer and from SW during the extra-tropical passages of storms in winter months. These dominant incident wave directions are important as the wave-induced longshore transport affects changes to the morphology of the ebb shoal, including geometry, position, and alignment of the ebb shoal in relation to the entrance, which could critically influence the spatially-varying wave pattern developing over the ebb shoal and in the entrance channel.

The numerical wave modeling was performed based on wave measurements from Buoy 46029. Wind, tide, and river flow inputs were included in the model simulations.

2.5 Sediments and Littoral Transport

Although sediment transport and morphology change were not modeled numerically in this study, general sediment information at Tillamook Bay is provided here for information. Sediments from the entrance channel and boat basin were collected in 2007 and earlier data are also available (USACE 2007). The grain-size composition had a range of 32.5 percent to 68.4 percent with a mean of 43.3 percent, and contained poorly graded sand with shell hash. The fine-grain size distribution for silt and clay had a range of 31.6 percent to 67.5 percent with a mean of 56.7 percent, and consisted of a general silt-sand grain composition (USACE 2007). Sediment data for the ebb shoal and nearshore were not available to this study. Visual estimates from a site visit on August 2012 indicated that the ebb shoal and entrance channel areas had similar sandy sediments. There are outcrops of in-situ rocks along the adjacent beach to the north, and north along the Bay channel.

3 Analysis of Historical Morphology Change

3.1 Historical Evolution

The results of the analysis on the recent historical morphology change of the ebb shoal include plots of morphology, morphology change, volume change calculations, and comparisons to times-series wave and river discharge data. The digital bathymetric datasets (all vertical datum herein are referenced to NAVD88) used are illustrated in Figures 3-1, 3-2, and 3-3. Figure 3-1 illustrates the earliest digital dataset for 1957 analyzed in this study, and clearly shows a straight and perpendicular channel approximately 5-8 m deep adjacent to a single jetty to the north. The Tillamook Burn, a catastrophic series of large forest fires in the Northern Pacific Coast Range of Oregon from 1933-1951,[1] may have contributed to bathymetric conditions in 1957. After burning of vegetation, upland sediment would be more readily transported into the rivers and offshore to increase volume of the ebb shoal as shown in the 1957 bathymetry. The morphology of ebb shoal was a shallow platform directly connected to the northern and southern beaches, indicating no strong flood tidal currents at the entrance to the channel. The wide shallow open reach between the North Jetty tip and the southern beaches would have provided uninhibited access for much of the flood current into the main channel and bay.

Nearly thirty years later, the bathymetry from the 1980s to 2000 (Figure 3-2) indicated that although the general planform aerial extent of the ebb shoal had not changed substantially following the construction of the South Jetty, the morphology and depth of the delta had. The outer shield of the ebb shoal had deepened substantially to 6 to 8 m (NAVD88) at its shallowest, and the shallow bypassing bar connecting the shoal to the adjacent south beach was no longer found in subsequent measured datasets. The area adjacent to the jetty tips was deeper and characteristic of a flood-marginal channel, although in some years there was no apparent flood channel to the north.

[1] http://en.wikipedia.org/wiki/Tillamook_Burn

Figure 3-1. The 1957 bathymetric contours (NOS; vertical datum is NAVD88) with the outlines of authorized navigation channel (black polygon), and present-day USCG navigation channel (grey polygon).

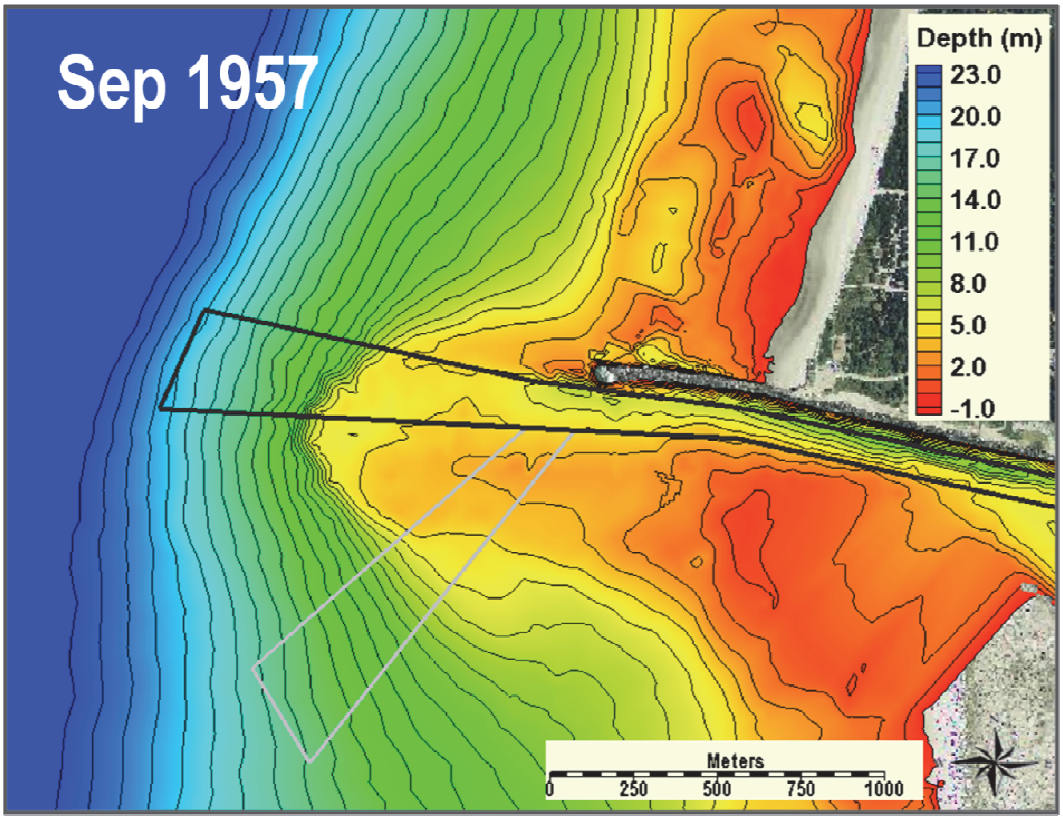

Figure 3-3 illustrates the evolution of the bathymetry and ebb shoal from 2002 to 2010. The morphodynamics of the ebb shoal are similar to the previous decades in terms of depth and planform area. The bathymetries displayed in Figure 3-3 are predominantly symmetric about the navigation channel position (in black), with some years tending to increased shoaling along the northern side of the ebb shoal. The deeper south access channel area remains deep near the South Jetty tip. The details of the general morphodynamics of the ebb shoal are presented in Section 3.3.

3.2 Volume Change

Volume change calculations were based on the volumetric difference between each bathymetric dataset that covers only the ebb shoal with a baseline nearshore slope. The Base grid was created by delineating continuous nearshore contours just offshore of the jetty tips to create a "no delta" bathymetry. Walton and Adams (1976) developed this methodology to evaluate the positive and negative volumetric change over plane and parallel contours due to the presence of tidal inlets. Figure 3-4 illustrates

Figure 3-2. The 1984 to 2000 bathymetric contours of NWP surveys (NAVD88) with the outlines of authorized navigation channel (black polygon), and present-day USCG navigation channel (grey polygon).

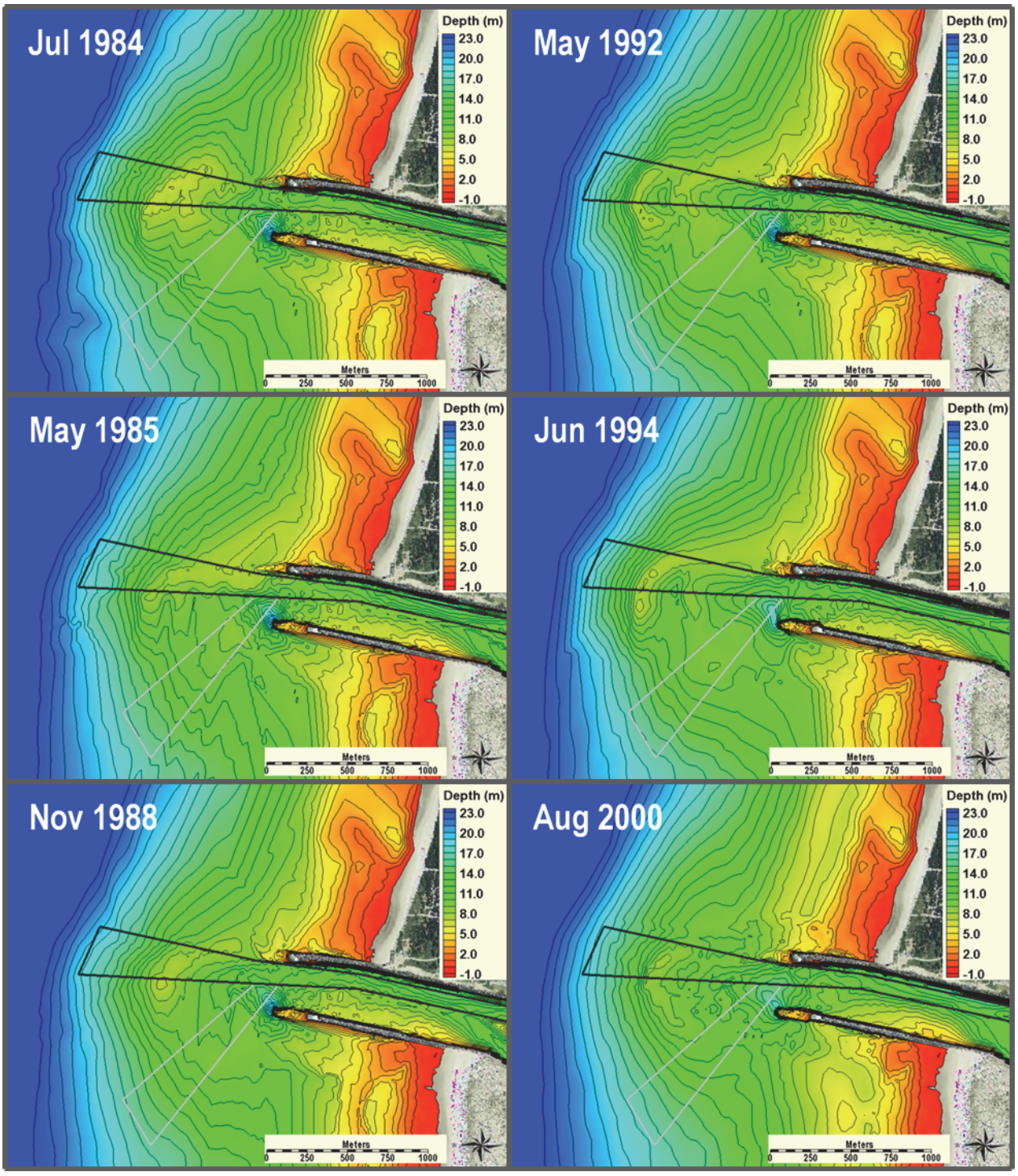

Figure 3-3. The 2002 to 2010 bathymetric contours of NWP surveys (NAVD88) and the outlines of authorized navigation channel (black polygon), and present-day USCG navigation channel (grey polygon).

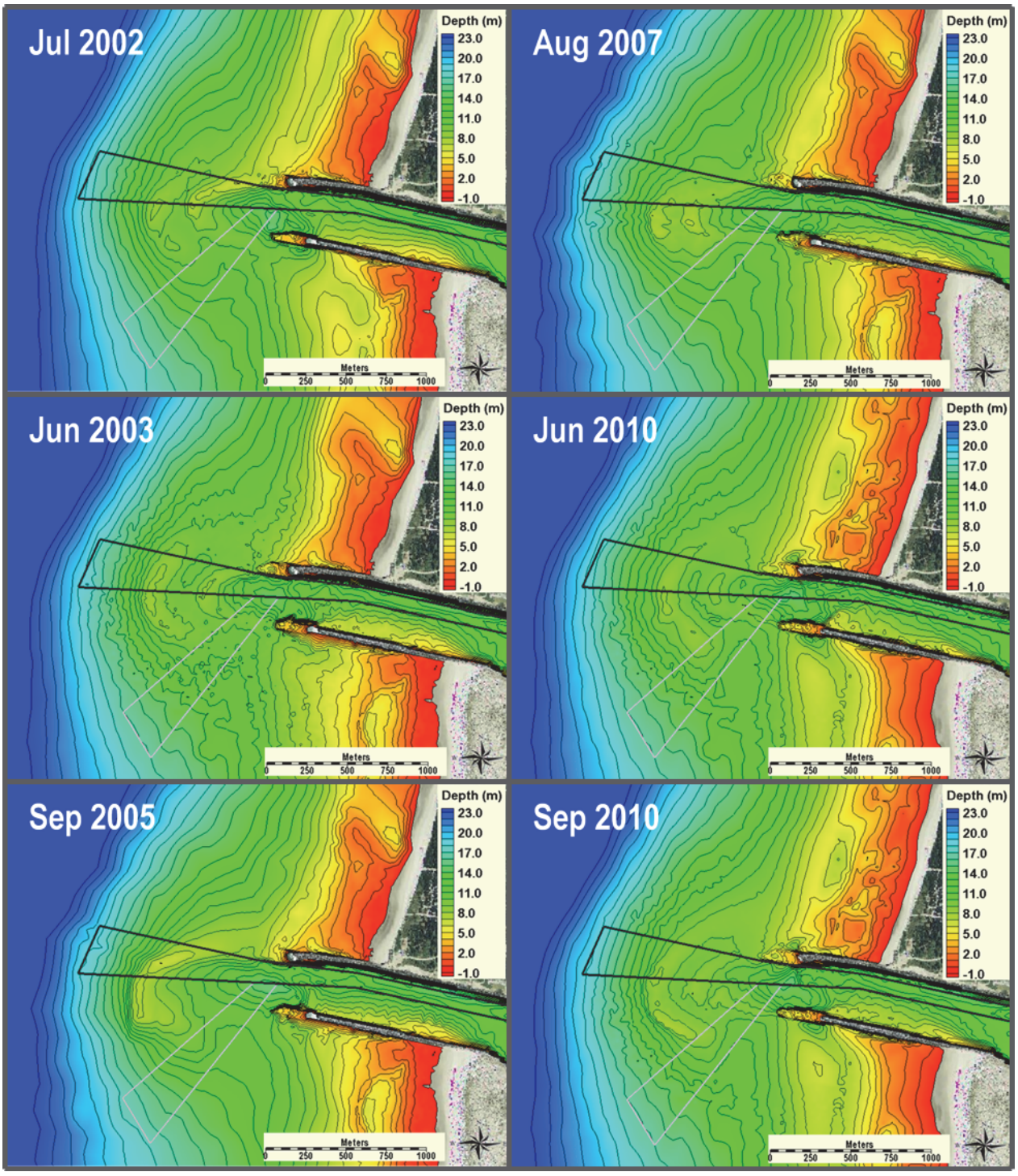

Figure 3-4. Baseline bathymetry (NAVD88) with plane and parallel contours offshore of the jetty tips. The yellow polygon indicates the area over which volume change was calculated.

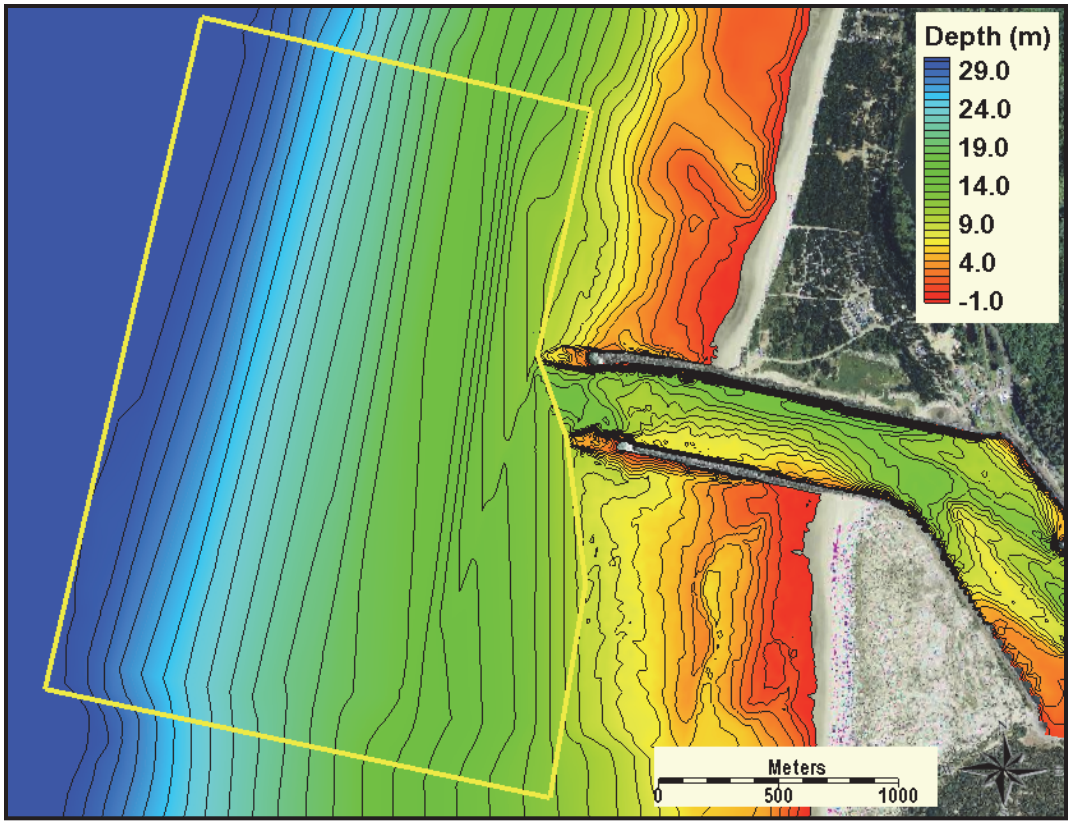

the plane and parallel contours as well as the region (yellow polygon) over which volume change was calculated. The polygon area delineated in yellow extends 1 km beyond the distinct ebb shoal, 1.5 km laterally north and south of the inlet, and extending no shallower than the jetty tips to exclude volume changes measured, or not measured, in the alongshore. This expansive aerial extent was designed to capture all potential ebb shoal morphology change during the analysis. Changes within the entrance navigation channel, bay navigation channel, and flood-tidal delta were not calculated due to insufficient data; therefore, these areas have not experienced significant change since the 1980s.

Table 3-1 lists the bathymetric datasets used in this analysis, including the surveyor, general coverage, and the type of survey, as well as the net volume of the ebb shoal and the rate of volumetric change. The rates of volumetric change were estimated based on the difference in ebb shoal volume from the previous survey. Figure 3-5 shows the total volumes calculated from surveys of 1957 and 1984-2010. The available datasets do not encompass volumetric changes from high wave events, or monthly or seasonal time

Table 3-1. Bathymetric datasets used in this study and volumetric evolution of the ebb shoal.

Date	Surveyor	Survey Location	Survey Type	Volume (m^3)	Rate of Change (m^3/year)
Sep 1957	NOS	Nearshore & Entrance	Single-beam Survey	14,964,657	
Jul 1984	NWP	Entrance	Single-beam Survey	6,166,320	-323,553
May 1985	NWP	Entrance	Single-beam Survey	8,597,230	2,856,319
Nov 1988	NWP	Entrance	Single-beam Survey	8,686,400	25,737
May 1992	NWP	Entrance	Single-beam Survey	7,125,980	-441,977
Jun 1994	NWP	Entrance	Single-beam Survey	8,099,350	467,128
Aug 2000	NWP	Entrance	Single-beam Survey	9,123,432	164,038
Jul 2002	NWP	Entrance	Single-beam Survey	9,587,190	249,150
Jun 2003	NWP/USGS	Entrance	Single-beam & Multi-beam Surveys	11,319,592	1,797,799
Sep 2005	NWP	Entrance	Single-beam Survey	8,581,620	-1,207,393
Aug 2007	NWP	Entrance	Single-beam Survey	9,291,896	378,243
Jun 2010	NCMP	Nearshore & Entrance	LIDAR	11,263,775	688,645
Sep 2010	NOS	Nearshore & Entrance	Multi-beam Survey	11,493,877	1,164,092

NOS = National Ocean Service (NOAA)

NWP = US Army Corps of Engineers, Portland District

USGS = US Geological Survey

NCMP = National Coastal Mapping Program, US Army Corps of Engineers

Figure 3-5. Calculated total volume from 1957 to 2010.

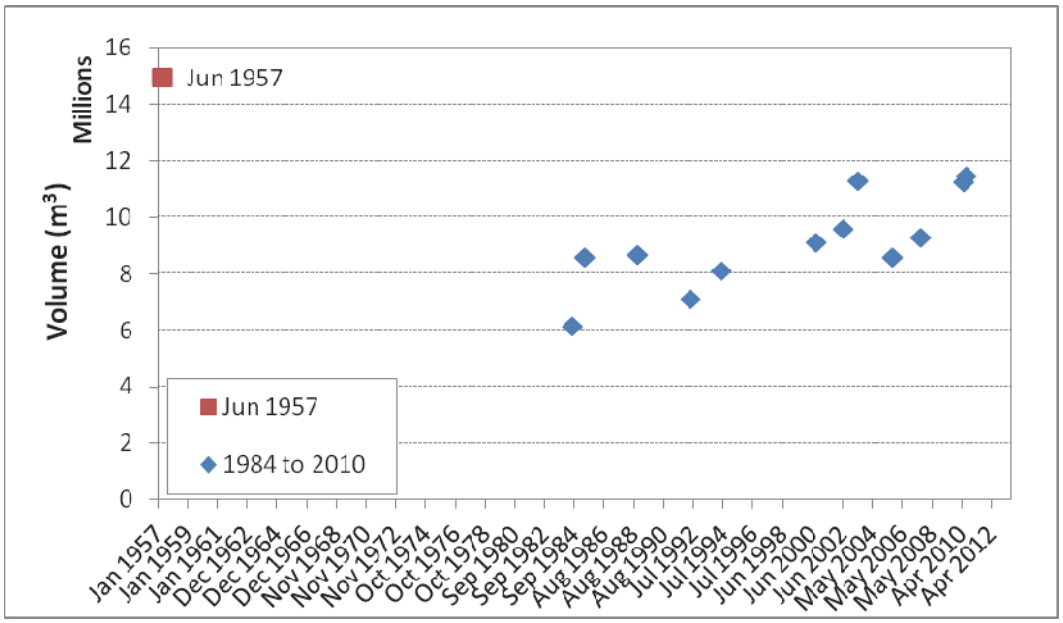

scales, and, therefore, only yearly volumetric change is analyzed herein. The June 1957 survey conducted by the NOS (Figure 3-5) indicated a shallow, shore-perpendicular ebb shoal, and the total volume was approximately 15 million cubic meters (MCM) or 19.5 million cubic yards (MCY). From 1957 to 1982, the ebb shoal decreased in volume to 6.1 MCM which likely was caused by construction of the South Jetty which helped focus the ebb flows over the shoal.

A significant amount of sediment was released into Tillamook Bay following the Tillamook Burn in the 1930s-1950s, and this may have contributed to the size of the ebb shoal in 1957. The first digital NWP survey (Figure 3-2) that had near complete coverage of the ebb shoal and enough of the adjacent nearshore was in 1984. The volume of the ebb shoal in 1984 was small compared to 1957, and this may have been attributed to either a reestablishment of the ebb shoal following completion of the South Jetty in 1979 or because of low density measurements which did not adequately represent the shoal. From 1985 to 2002, the volume of ebb shoal varied between 7 MCM and 9 MCM. The rate of volume change varies substantially by an order of magnitude. For example, between August 2000 and July 2002, the ebb shoal had accreted at a rate of 250 KCM/YR (thousand cubic meters per year) between those two years. However, the shoal can accrete at rates of 1-3 MCM a year as measured from July of 2002 to June of 2003. The subsequent surveys indicated that volume decreased to 8.5 MCM by 2005, and then increased to 11.4 MCM by September 2010 (Table 3-1 and Figure 3-5).

The multi-beam and lidar surveys for 2003 and 2010 provided the highest density of measurements and coverage. In 2010, detailed morphology change for a two month period in mid-summer indicated a rapid change in ebb shoal volume. Mid-summer waves are typically less energetic than in winter months, which may provide the conditions to allow sediment to deposit on the ebb shoal. Alternatively, there are potential uncertainties in the accuracy of previous lidar datasets along the Pacific Northwest Coast (personal communication with Portland District), which may indicate that this volume discrepancy is artificial. The results of the lidar volume calculations are meant to provide qualitative perspective to a two-month period of morphologic change. Additionally, only the multi-beam datasets were utilized in the wave modeling analysis in this study.

3.3 Morphologic Characteristics

The morphology of the ebb shoal has been relatively stable over the last three decades following the equilibration of the shoals after the South Jetty was completed in 1979. However, there are significant differences in the location of the deepest channel scour and the symmetry of the entrance bar (Figures 3-2 and 3-3). As observed in the 2000 bathymetry, the deep scour pit (+7 m) typically associated with the South Jetty during the 1980s and 1990s began migrating towards the center of the entrance channel. In the last decade, this scoured area remains centrally-located (evident in the 2010 bathymetry) and at relatively shallower depths of 5-6 m.

The portion of the ebb shoal offshore of the jetties, however, was found to have two main, alternating characteristic states: an asymmetric offshore bar, extending from the shallow sea bed near the North Jetty tip curved toward the south but not connected or close to the South Jetty, and, a symmetric offshore bar with deep flood marginal channels adjacent to both jetty tips and no clear indication of connection to either jetty. There is some variation found among the two dominant morphologies, the result of transitioning, however, the inadequate temporal coverage of the surveys limit further discussion of transition time scales. In Figures 3-2 and 3-3 there are six distinct symmetric ebb shoal entrance bars found in the available bathymetries datasets 1992, 2000, 2003, 2007, and 2010 (June and September); and there are six distinct asymmetric entrance bars: 1984*, 1985, 1988, 1994, 2002, and 2005. (*The surveys from 1982 to 1984 had very low coverage, but 1984, which was missing data over the northern portion of the shoal near the North Jetty, was included because it contained good coverage of the distance offshore and was assumed to be asymmetric). Larger, more symmetric entrance bars have been more common in the survey data of the past decade (2000 to 2010). This is supported by local observations of more active shoaling and breaking of waves along the southern portion of the ebb shoal, indicating extension of the shoal further south (Sept. 2010, Figure 3-3). The occurrence of this gradual trend is concurrent with the migration to a centrally-located scour pit.

The symmetry of the ebb shoal has varied at the least on a yearly time scale; however, the lack of data cannot support a temporal scale for the apparent trends. Figure 3-6 shows the measured distance offshore from the tip of the South Jetty (referenced to the June 2003 bathymetry survey) to the 10-m depth contour, a measure of perpendicular growth, for symmetric and asymmetric ebb shoals. This measure has been used to quantify the

Figure 3-6. Evaluation of distance offshore as the length between the original South Jetty tip and the 10-m contour NAVD88.

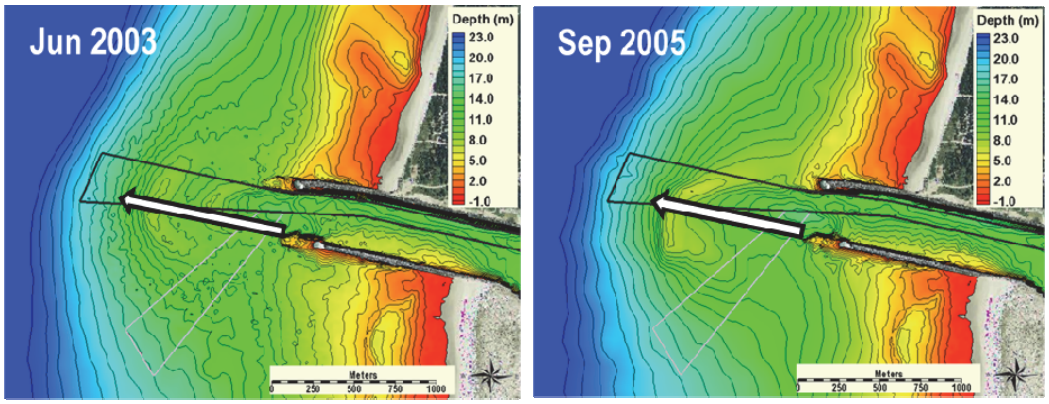

asymmetry of ebb shoals in Carr-Betts et al. (2012), and can demonstrate the skewness of an entrance bar under combined tidal and wave forcing. A stronger tidal current or river discharge will move sediment further offshore. Figure 3-7 is a plot of available bathymetric datasets from 1982 to 2010 that shows no correlation between symmetry, highlighted in red, and the offshore distance of the ebb shoal. The dates of the surveys are also displayed in Figure 3-7, indicating the captured seasons which consist of Spring, Summer, and Fall. The variance in distance offshore as well as symmetry could not be correlated to a particular time of the year due to limited data. However, there is a slight correlation between the offshore distance of the 10-m contour and the ebb shoal volume because as the offshore distance increases, the ebb shoal volume decreases (Figure 3-8). Note that the connection between these two variables is not clear, though it may be related to the effects of excessive shoaling due to larger waves during a particular year that induce a landward migration of the shoal and increase the volume due to increased littoral transport. There are also potentially seasonal differences in this data as well as differences connected to changes in jetty length or storm climate that may inform this data.

3.4 Role of Environmental Forces on Morphology

Significant modulations to the ebb shoal at Tillamook Inlet can be caused by combined environmental forcing from natural processes such as winds, tides, waves and riverine discharges. The amplification of these processes occurring at the inlet can affect the symmetry, size, and larger morphologic characteristics of the nearshore bars and the ebb shoal. Energetic waves can affect the shape of the ebb shoal, as well as the amount of littoral materials provided to the shoal from adjacent beaches. High riverine discharges could create greater ebb currents with potential to transport sediments further

Figure 3-7. The offshore distance of ebb shoal for bathymetric surveys from 1982 to 2010, with symmetric morphology highlighted in red.

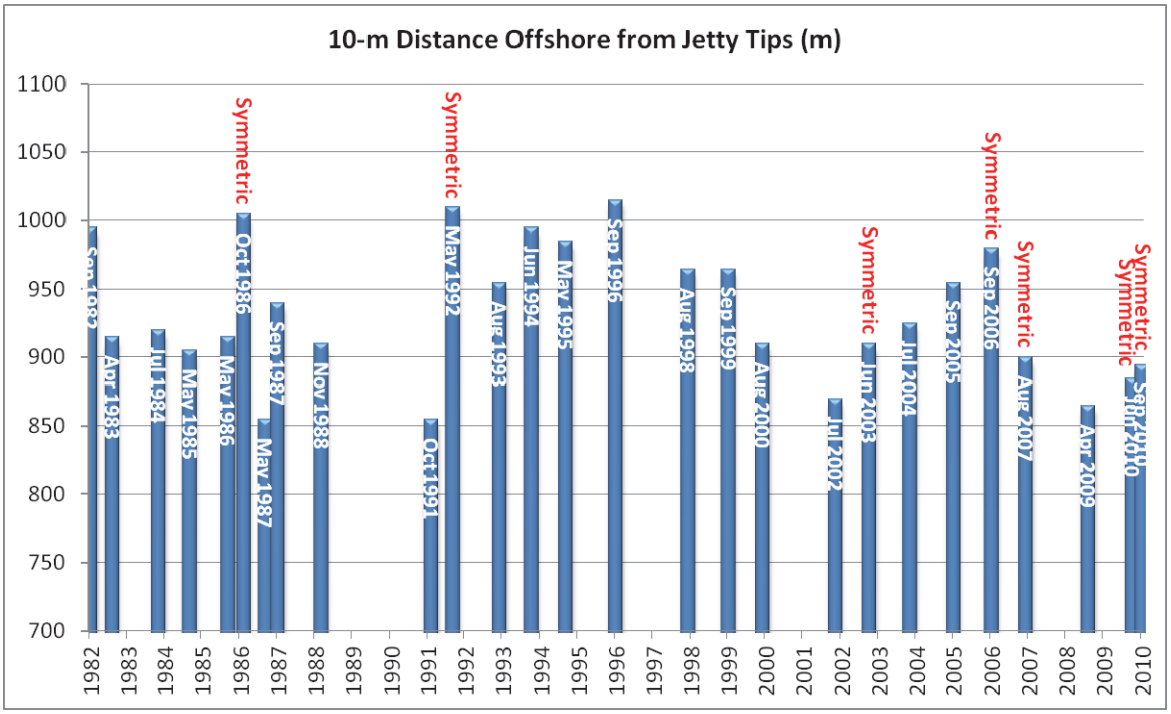

Figure 3-8. Correlation between the offshore distance of the 10-m contour and the ebb shoal volume.

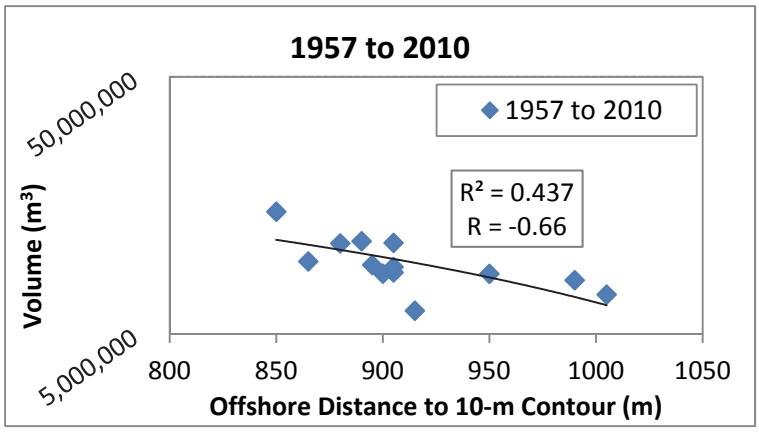

offshore beyond the littoral zone, or could bring sediment to deposit on the ebb shoal. Cause-effect relationships cannot be determined by the available survey data. However, long-term trends in ebb shoal symmetry and volume may be correlated to monthly mean significant wave heights and river discharges. The study area can be also significantly influenced by El Nino and La Nina years. These cycles of extreme storm climate combining both elevated water levels as well as strong storm events may also influence the morphology at the entrance from year to year.

Figures 3-9 and 3-10 show the examples of monthly mean significant wave heights for 10 years from 2001 to 2011. The seasonal differences in monthly mean wave heights indicate 1-2 m range in the summer months, while the significant wave heights from fall to spring range from 3-13 m. The high energetic winter seasons between 2001 and 2011 occurred in 2001-2002, 2006-2007, and 2009-2010 (El Nino years). There appears a connection between higher waves and the ebb shoal symmetry or asymmetry, where ebb shoal is more symmetric following energetic winter seasons. Based on the limited data used in the present study, the calculated offshore distance of ebb shoal is not well correlated to energetic seasons, as observed in the shorter offshore distances of 2000-02 and longer offshore distances of 2006-07.

Riverine discharge from 2000 to 2011 (Figures 2-4 and 2-5) was relatively constant on an average-annual basis, with some minor exceptions. The years of 1993-1994, 2001, and 2005 had less freshwater discharge than average years. The river discharge was particularly low in 1992 and the distance of the 10-m contour ebb shoal was +1000 m. This contradicts the hypothesis of increased ebb shoal volume decreasing with the offshore distance of the ebb shoal. River discharge data for 1996-1999 were available; however, the bathymetric data were limited in these years and a comparison to morphologic parameters for the ebb shoal was inconclusive. Although a significant volume of sediment may be transported out of the bay during precipitation events and waning stages of storms, these sediments consist of fine-grain materials that may not settle on the ebb shoal and may not affect the volume and morphology of the ebb shoal.

Figure 3-9. Monthly mean significant wave heights for 2001 to 2006.

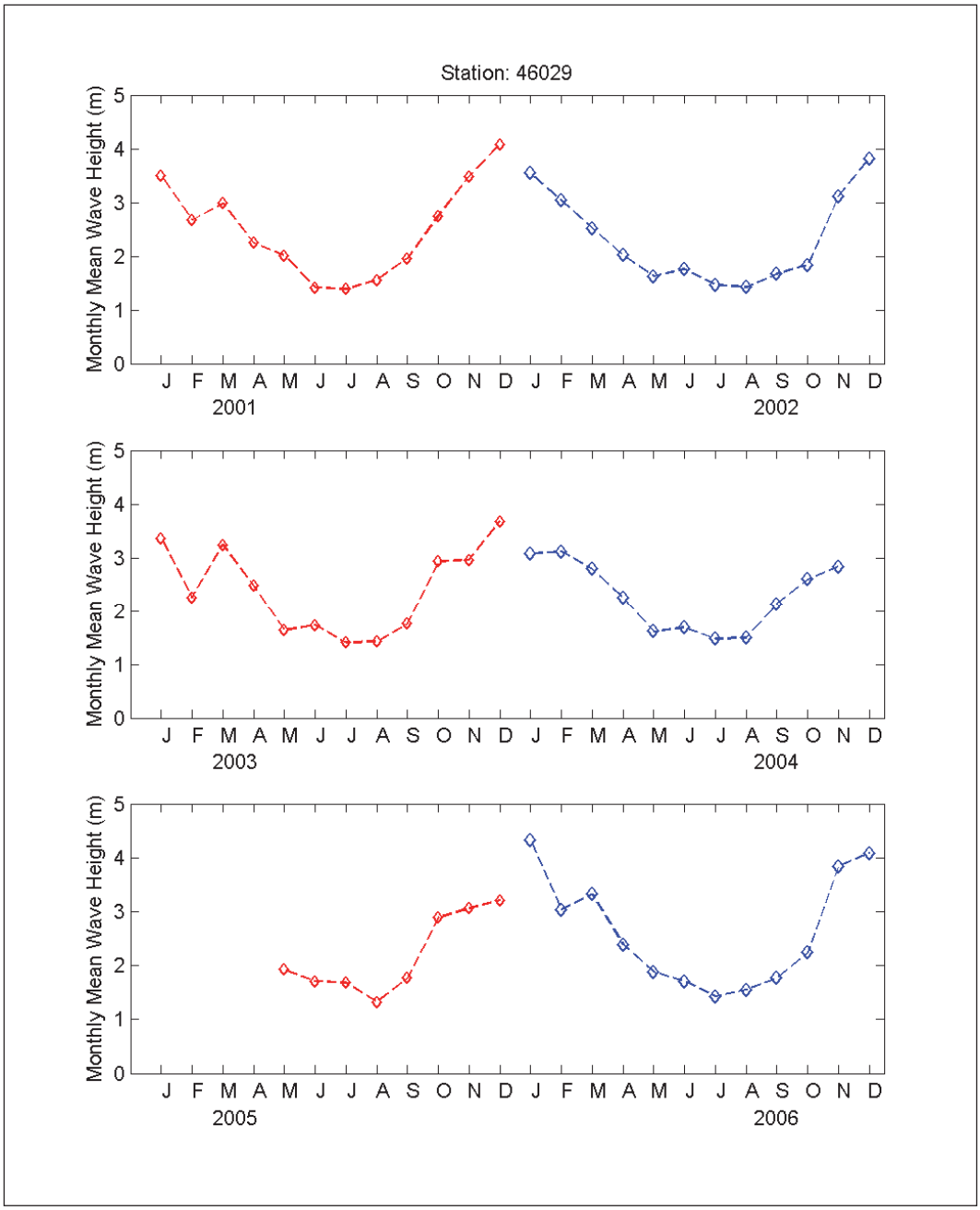

Figure 3-10. Monthly mean significant wave heights for 2006 to 2011.

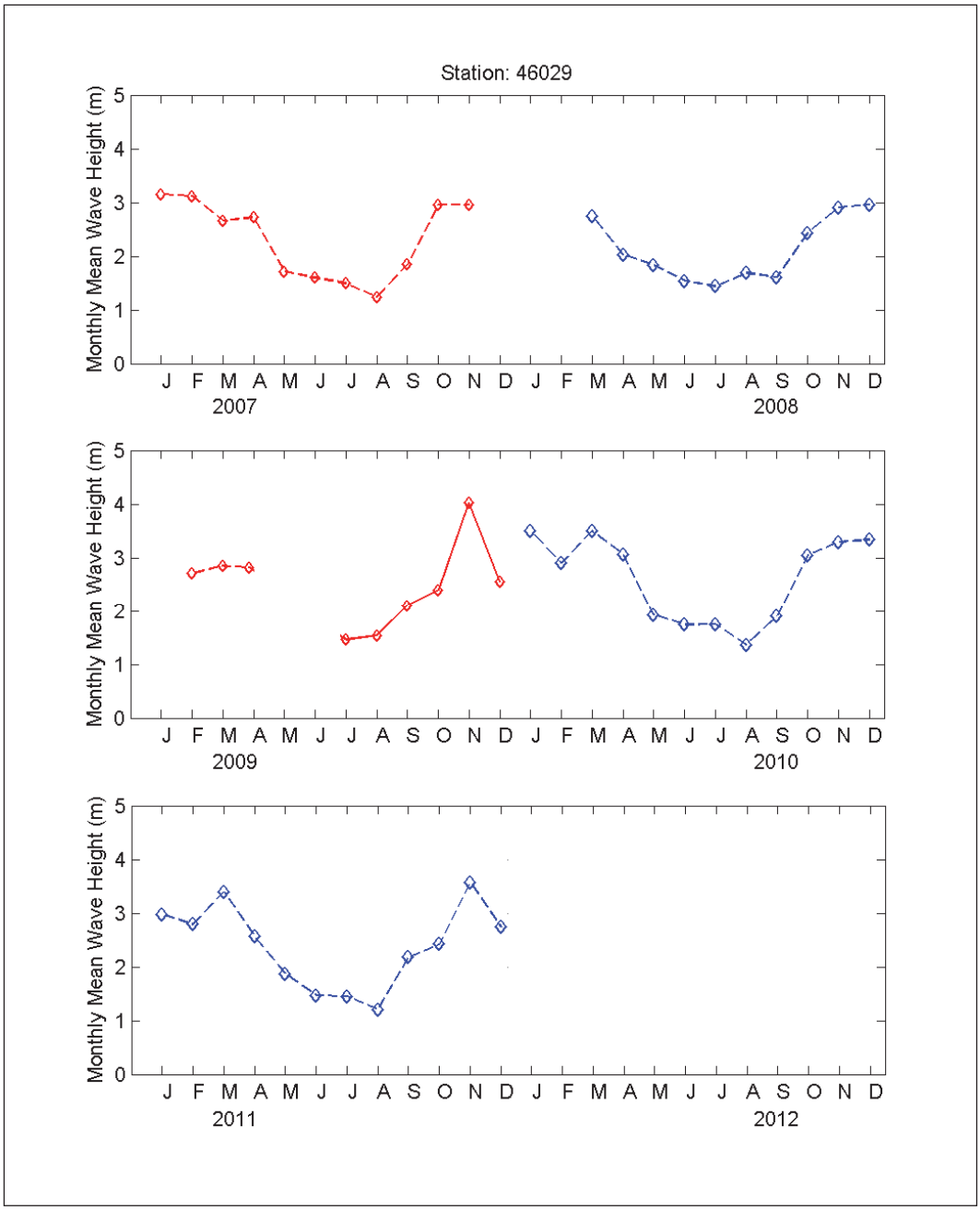

4 Wave Modeling

Wave modeling was conducted for the Tillamook Inlet complex, which includes the bay, nearshore areas around the immediate vicinity of the Inlet (approach channel, ebb shoal, adjacent beaches, and entrance channel), and the main navigation channel into the bay using CMS-Wave. Wave transformation with refraction, shoaling, and breaking was simulated without tides to provide estimates of wave-related parameters of interest to the navigable region at Tillamook, which likely are more dominant during slack or low-tidal flows. The calculated wave-related parameters of interest were as follows:

- significant wave height, H_s (m)
- spectral peak period, T_P (sec)
- mean wave direction, $\bar{\theta}$ (deg)
- wave steepness $\zeta = H_s / L_p$, where L_p is the spectral peak wavelength calculated at the local depth
- wave breaking intensity expressed in terms of wave dissipation (m^3/sec), the wave energy loss in the wave propagation direction
- surf-zone similarity parameter $\xi = s / \sqrt{H_s / L_p}$, where s is the local bed slope in the wave propagation direction
- Ursell number $U_r = (H_s/h)\,(L_p/h)^2 = H_s L_p^2 / h^3$, where h is the local water depth

Each of the parameters or combinations of these may be used in navigation projects. Among these parameters, wave steepness, and breaking intensity are of particular interest in terms of gaining a better understanding of wave conditions at the entrance. Wave modeling results are provided using these parameters.

The Ursell number helps to identify the roles of wave "nonlinearity" measured by height and "shallowness" as measured by depth over wavelength ratio. It is widely used to characterize linear versus nonlinear waves at any water depth. The Ursell number has high values in shallow water as waves shoal. Typical values of the Ursell number for navigable depths in shallow water range between 10 and 50. This is an ideal parameter for assessing hazard and risk levels for navigation. Calculated U_r values range

from zero to hundreds. Careful interpretation of Ursell values is required; large values of U_r may represent non-navigable shallow depths or could correspond to long waves in very deep water, which would be the least hazardous to navigation.

It has been shown in the Coastal Engineering Manual (Demirbilek and Vincent 2010), that a steadily-progressing wave train is uniquely defined by three physical dimensions: the mean water depth h, the wave crest-to-trough height H, and wave length L, such that waves can be expressed in terms of two dimensionless quantities, usually H/h and L/h for shallow waves. In many situations the wave period is known rather than the wave length. In most coastal applications waves travel on a finite current and wave speed; hence, the measured wave period depends on the current, because waves travel faster with the current than against it. The mean steepness measures the geometrical nonlinearity of the wave field due to nonlinear wave–wave interactions. The mean steepness is high (0.04-0.05) for large waves (H_s > 4 m). The Ursell number measures the dynamic nonlinearity due to the finite water depth effects and is larger for waves with high skewness, indicating an increase in nonlinearity that leads to an increase in wave asymmetry.

4.1 Bathymetry and Coastline Data

Coastline information for Tillamook Inlet and Bay was extracted for this study from a geo-referenced image file downloaded from Google Earth 5 (http://earth.google.com). The coastline digital data are available from the National Geophysical Data Center (NGDC, http://rimmer.ngdc.noaa.gov).

Bathymetry data for the nearshore area surrounding Tillamook Inlet were mainly based on the September 2005 and June 2010 surveys. The offshore bathymetry data were obtained from GEOphysical DAta System (GEODAS), developed and managed by the National Geophysical Data Center (http://www.ngdc.noaa.gov/mgg/bathymetry/relief.html). The land elevation data were downloaded from USGS Geographical Digital Elevation models (DEM, http://edc2.usgs.gov/geodata/index.php). Figure 4-1 shows the depth contours (in meters relative to mean sea level (MSL)) for the wave model domain from the combination of the September 2005 survey, NGDC shoreline, and GEODAS dataset.

Figure 4-1. CMS-Wave grid for asymmetric ebb shoal grid domain and bathymetry based on September 2005 survey, NGDC shoreline and GEODAS database.

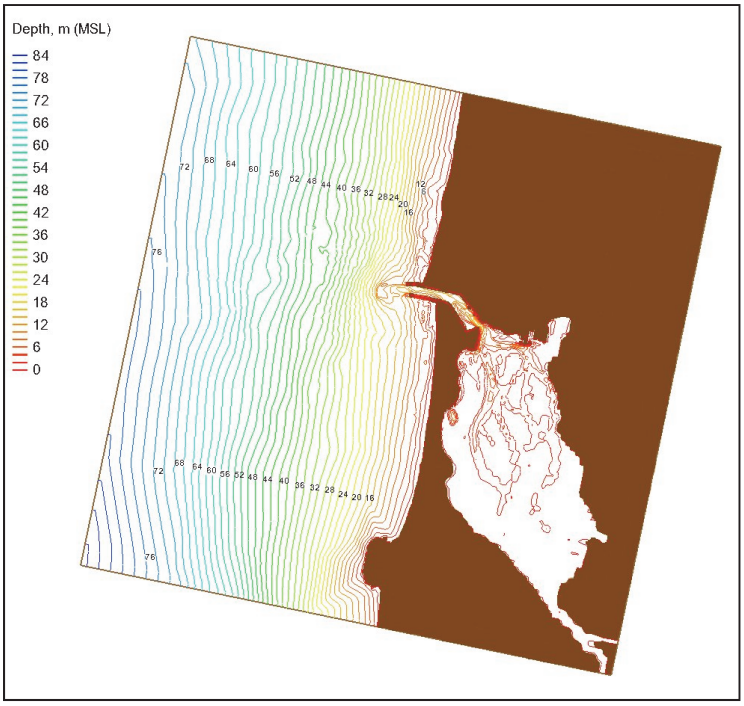

4.2 Model Input Winds and Wave Data

Incident wave conditions were based on directional wave data collected by the National Data Buoy Center (NDBC 2012) Buoy 46029, located approximately 60 miles northeast of Tillamook Inlet. The buoy wave data were transformed to the seaward boundary of the CMS-Wave grid using a simplified wave transformation for shore-parallel depth contours. Wind speed and direction data collected from Buoy 46029 were used as atmospheric input to wave modeling for wind and wave interactions.

4.3 Wave Model Domain

Three CMS-Wave grids were generated for wave modeling: (1) an asymmetric ebb shoal grid (based on September 2005 survey), (2) a symmetric ebb shoal grid (based on June 2010 survey), and (3) a hypothetically shortened South Jetty grid. All three grids cover the same square domain of 17.6 × 17.6 km with varying cell sizes from 10-m spacing. The asymmetric ebb shoal grid (Figure 4-1) was generated from the September 2005 survey that shows a crescent shape ebb shoal that extends seaward from the North Jetty to the inlet outer bar. The symmetric ebb shoal grid was generated from the June 2010 survey, showing a symmetric, isolated

ebb shoal seaward of the inlet entrance. The hypothetically shortened South Jetty grid is based on the June 2010 symmetric ebb shoal grid with a truncated South Jetty recessed landward by 230 m (750 ft). This case was simulated to evaluate whether removing a section of the South Jetty would affect navigation in the channel. The offshore boundary of the grid domain is at the 80-m isobath. Figure 4-2 shows the symmetric ebb shoal grid domain and bathymetry. Figure 4-3 shows the local inlet entrance bathymetry contours for the hypothetically shortened South Jetty grid.

Figure 4-2. Symmetric ebb shoal grid domain and bathymetry based on June 2010 survey, NGDC shoreline and GEODAS database.

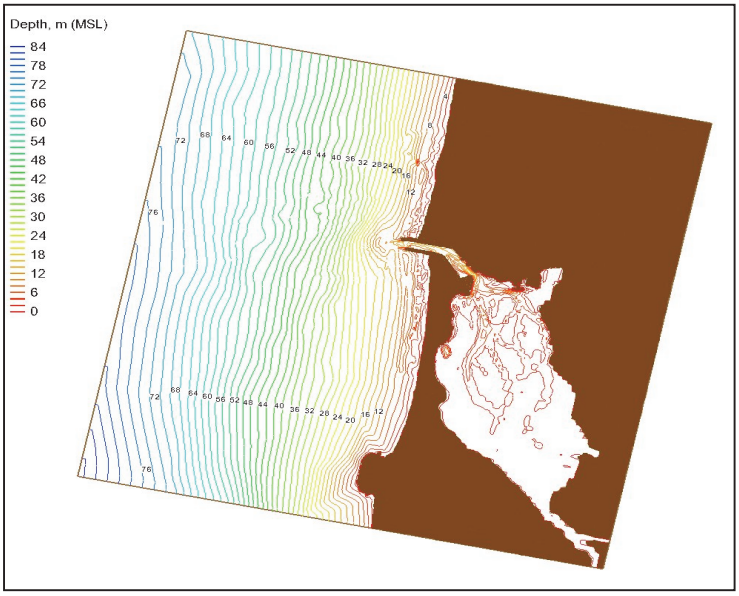

Figure 4-3. Hypothetically shortened South Jetty bathymetry contours.

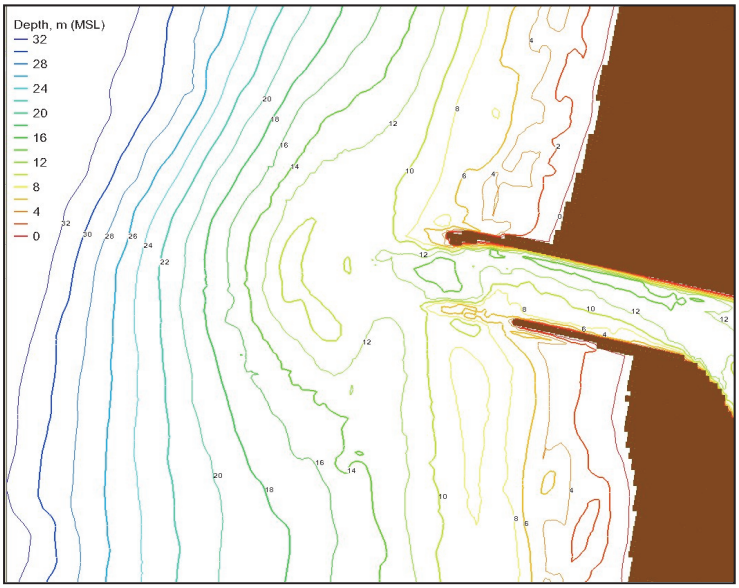

4.4 Types of Wave Simulations

Wave simulations were conducted for selected seasonal mean wave conditions (Figures 3-9 and 3-10) and for a typical summer month (August) and a winter month (December) using the 2005 and 2010 bathymetric grids. Note that for comparing wave estimates for the summer month (August) in 2005 and 2010, because there was no survey data available for August 2010, the simulations for 2010 were made with the June 2010 grid. The selected seasonal mean wave conditions include three incident waves with the mean direction normal to the local shoreline: 1) 2-m significant height and 8-sec peak period for summer, 2) 3-m significant height and 10-sec period for spring and fall, and 3) 4-m significant height and 12-sec period for winter. The incident waves were represented by the TMA spectrum (Bouws et al. 1985) with a standard spectral peak enhancement factor of 3.3 and the cosine-square directional distribution using a wide spreading parameter value of 10 (Longuet-Higgins and Stewart 1963).

The typical summer and winter months selected for wave simulations were from August 2005, August 2010, December 2005, and December 2010. The incident wave climate was strikingly similar between August 2005 and August 2010, the mean significant wave height was 1.3 m for August 2005 and 1.4 m for August 2010. The incident wave climate for December 2005 was also similar to December 2010, and had a 3.2 m mean significant wave height for December 2005 and 3.3 m for December 2010. However, more severe storm waves with greater wave heights occurred in December 2005 than in December 2010. The maximum significant wave height was 8 m in December 2005 and 6 m in December 2010. The August and December 2005 simulations were conducted with the asymmetric ebb shoal grid, while the symmetric ebb shoal grid was used for August and December 2010 simulations. All wave simulations were run using CMS-Wave with the default wave breaking criteria, a combination of extended Goda formula (Sakai et al. 1989) and limiting steepness by Miche (1951).

4.5 Wave Modeling Results

4.5.1 Seasonal Mean Wave Conditions

The seasonal mean wave conditions were simulated to determine the sensitivity and appropriateness of using wave-related parameters as the measures of a navigation safety index. The wave-related parameters considered were wave steepness, wave dissipation, surf-zone similarity

parameter, and the Ursell number. The simulations were run using the symmetrical ebb shoal grid (e.g., June 2010 grid).

Figure 4-4 shows calculated wave steepness (H_s / L_p) fields for three incident shore-normal waves with different significant heights and peak periods: (a) H_s = 2 m, T_p = 8 sec, (b) H_s = 3 m, T_p =10 sec, and (c) H_s = 4 m, T_p = 12 sec. Note that the contour range in these figures and other wave steepness figures in this chapter are limited to the maximum contour of 0.05. Values of wave steepness greater than this threshold, over the ebb shoal and adjacent areas, are associated with large waves breaking in shallow depths (Demirbilek and Vincent 2010). The maximum steepness for individual waves can be approximately twice the spectral wave steepness for an irregular sea state (Longuet-Higgins and Stewart 1963; Demirbilek and Vincent 2010). Because the wave steepness in the present study is based on significant wave height (not individual waves), a wave steepness of H_s / L_p = 0.03 is used.

The wave steepness calculations show that the threshold value of 0.03 is exceeded outside the inlet and around the ebb shoal for incident wave heights greater than 3 m. Within the oceanward reach of the inlet, wave steepness can become greater than 0.03. The model results show values of higher wave steepness immediately seaward of the jetty tips, indicating complex wave conditions exist in these areas.

Figure 4-5 shows calculated wave dissipation for incident waves of (a) H_s = 2 m, T_p = 8 sec, (b) H_s = 3 m, T_p =10 sec, and (c) H_s = 4 m, T_p = 12 sec. Similar to wave steepness, the wave dissipation is greater for larger incident waves over and surrounding the ebb shoal, and consequently this parameter could be used as another measure to characterize wave conditions at the inlet. The wave dissipation is negligible outside the breaker zone. However, inside the surf zone with wave increasing shoaling and breaking, wave energy can dissipate drastically where the values of wave dissipation exceed 0.01 m^3/sec^3. The wave energy dissipation value of 0.01 m^3/sec^3 is used in this study as a limit to characterize wave conditions.

The model results show stronger wave dissipation outside the inlet and around the ebb shoal for incident wave heights greater than 3 m. The model results show higher values of wave dissipation immediately seaward of jetty tips, which indicate that large breaking waves occur in these areas.

Figure 4-4. Calculated wave steepness field for incident wave of (a) 2 m, 8 sec, (b) 3 m, 10 sec, and (c) 4 m, 12 sec, all with shore-normal wave direction, using the June 2010 symmetrical ebb shoal grid.

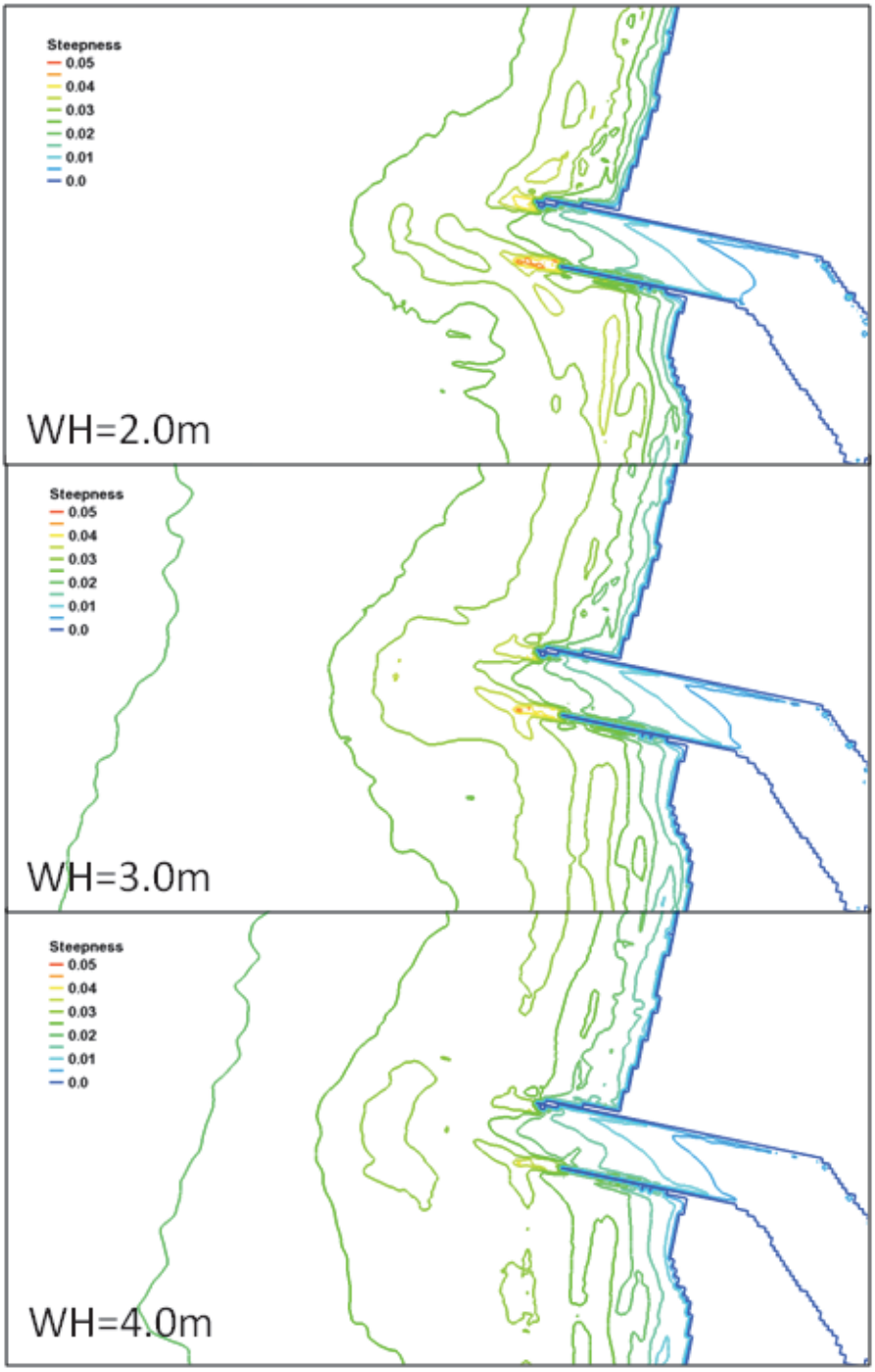

Figure 4-5. Calculated wave dissipation field for incident wave of (a) 2 m, 8 sec, (b) 3 m, 10 sec, and (c) 4 m, 12 sec, all with shore-normal wave direction, using the June 2010 symmetrical ebb shoal grid.

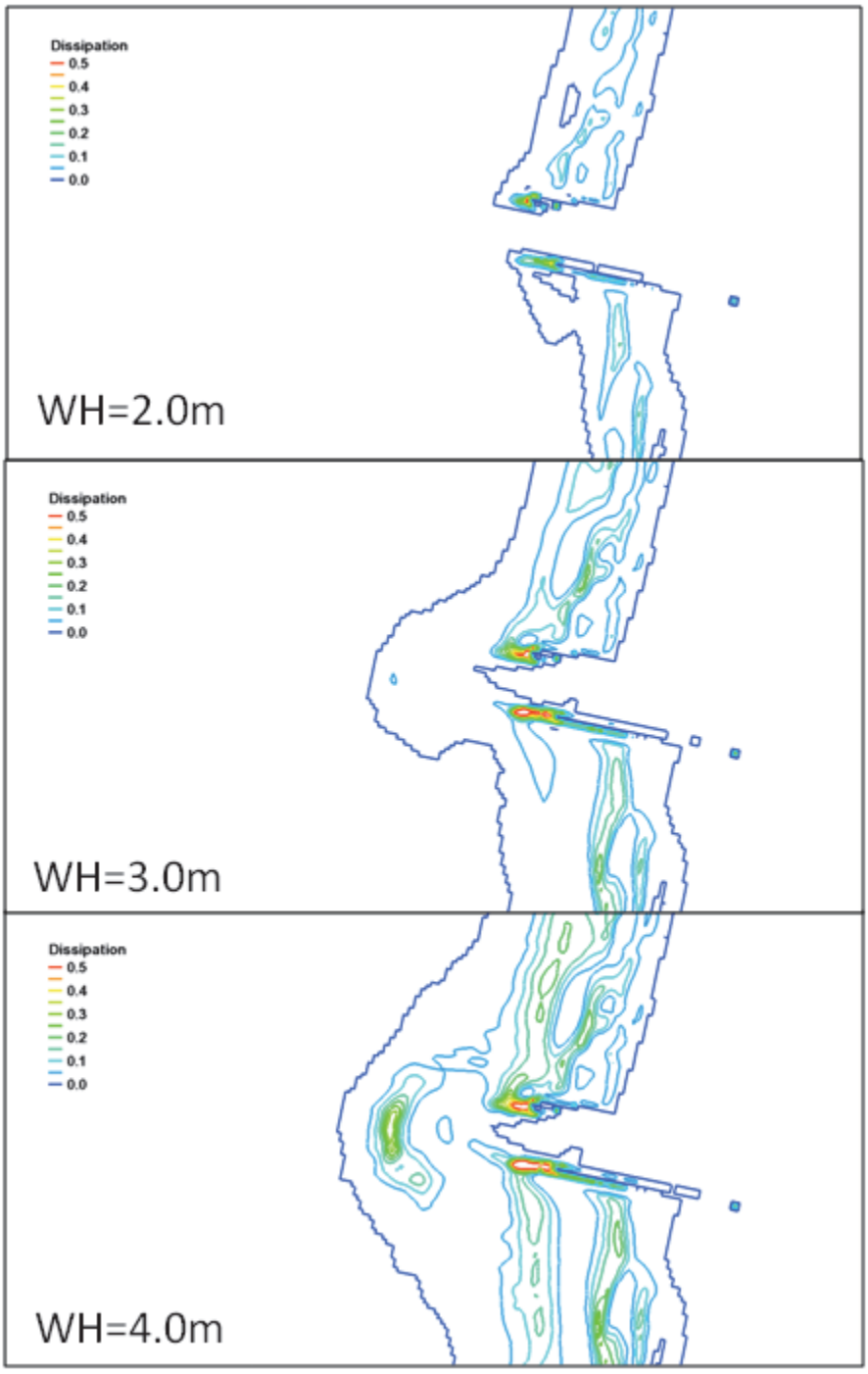

Figure 4-6 shows calculated surf-zone similarity parameter fields for incident waves of (a) H_s = 2 m, T_p = 8 sec, (b) H_s = 3 m, T_p =10 sec, and (c) H_s = 4 m, T_p = 12 sec. Note that the contour range in these figures is limited to the maximum contour of 2. The value greater than 2 is not contoured as

higher values are more associated with greater bottom slope change. Since the surf-zone parameter is affected by bottom slope and varies inversely with the square root of wave height, it is less sensitive to the incident wave heights. The model results show the surf-zone parameter may not be a good safety indicator for navigation, and thus it will not be calculated or shown for the remaining simulations in this study.

Figure 4-6. Calculated surfzone similarity field for incident wave of (a) 2 m, 8 sec, (b) 3 m, 10 sec, and (c) 4 m, 12 sec, all with shore-normal wave direction, using the June 2010 symmetrical ebb shoal grid.

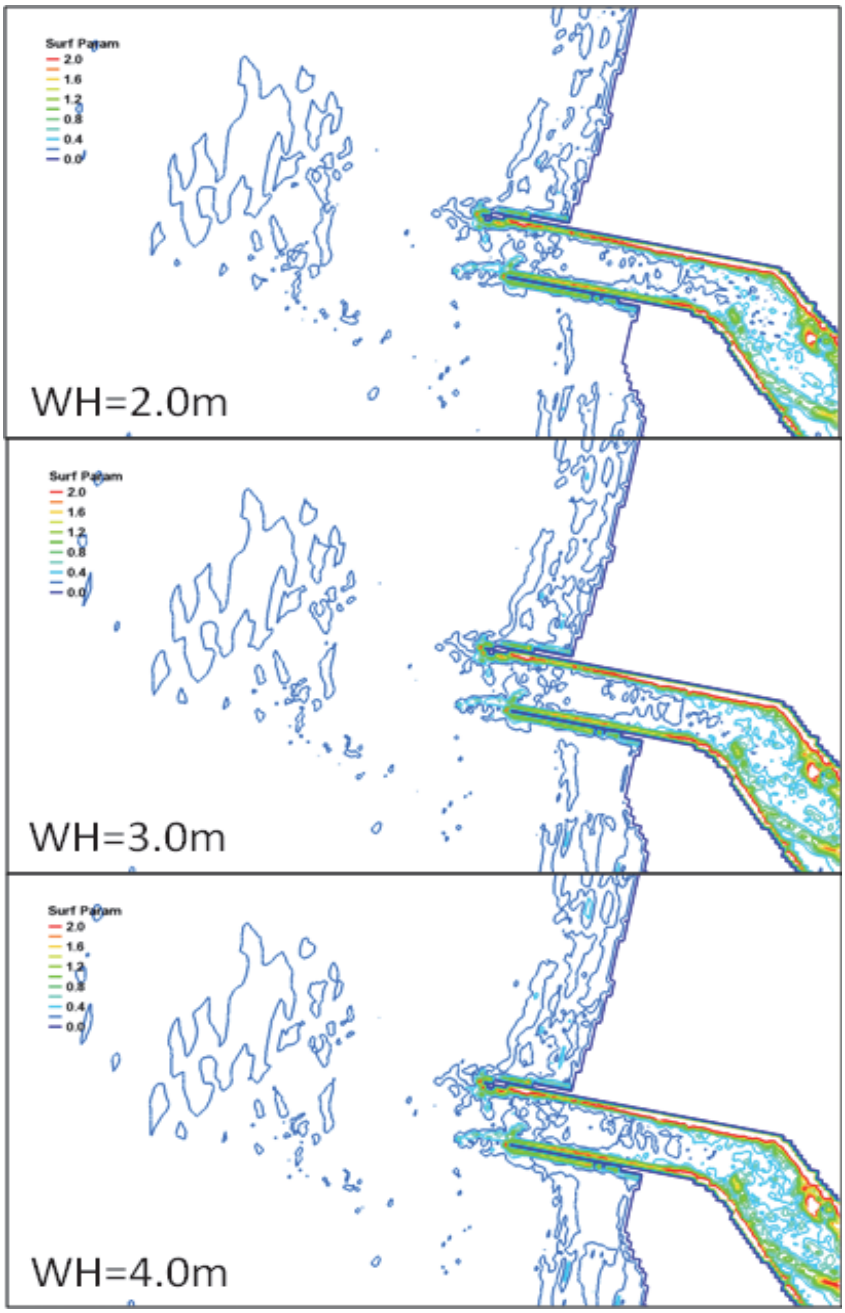

Figure 4-7 shows calculated Ursell number fields for incident waves of (a) H_s = 2 m, T_p = 8 sec, (b) H_s = 3 m, T_p =10 sec, and (c) H_s = 4 m, T_p = 12 sec. Note that the contour range for the Ursell number in these figures is limited to the maximum contour of 100. The values greater than 100 are not contoured because these represent interaction of nonlinear waves with bottom in shallower depths.

Figure 4-7. Calculated Ursell number field for incident wave of (a) 2 m, 8 sec, (b) 3 m, 10 sec, and (c) 4 m, 12 sec, all with shore-normal wave direction, using the June 2010 symmetrical ebb shoal grid.

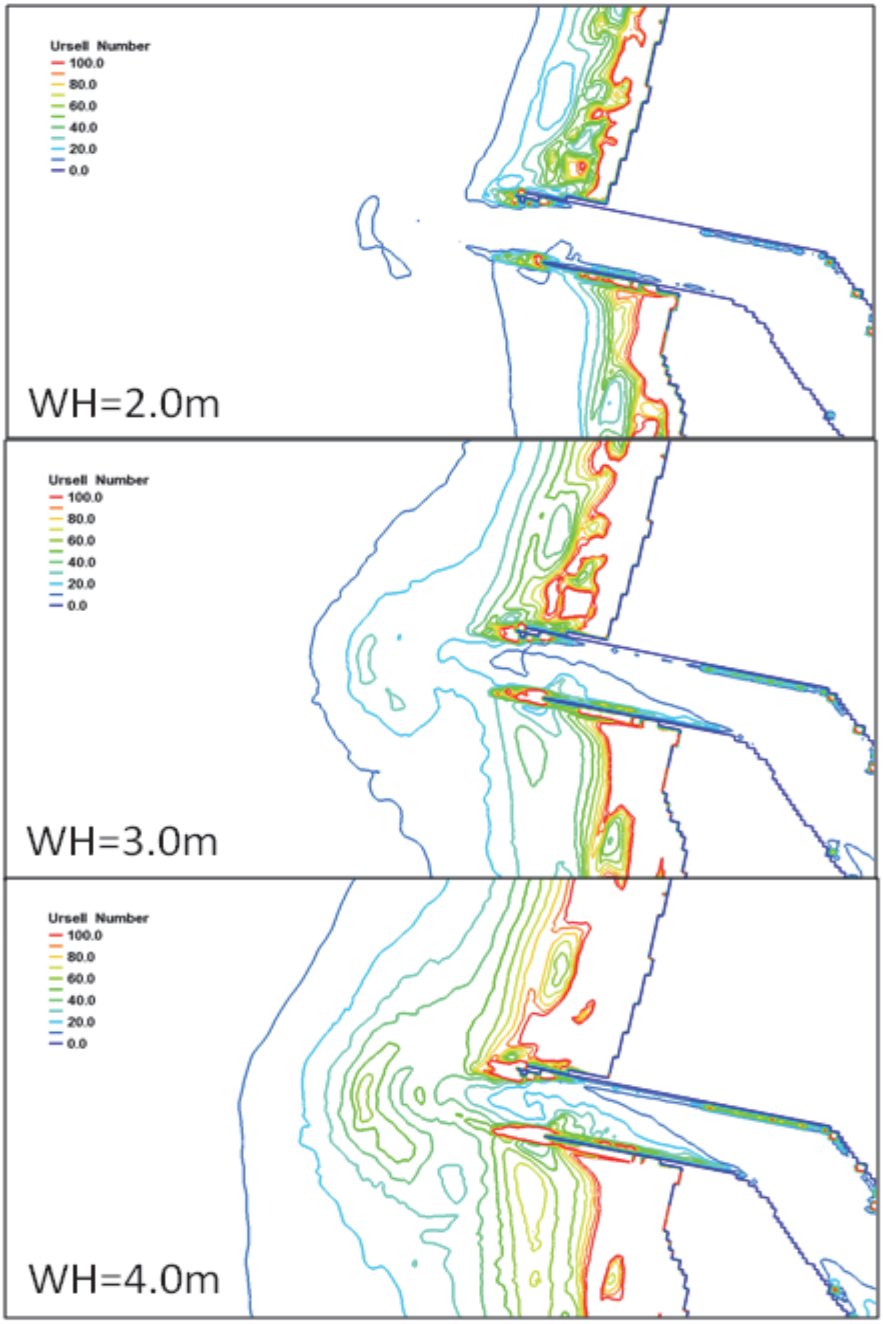

By definition, $U_r = (H_s/h)\,(L_p/h)^2$ is the ratio of wave nonlinearity measured by the relation of waves and water depth. The Ursell parameter is the most accurate measure to characterize linear and nonlinear waves at any water depth. The calculated Ursell number is greater for larger incident waves over the ebb shoal and its surrounding areas, and can be used for risky conditions for navigation. Results show higher Ursell numbers outside the inlet and around the ebb shoal with incident wave heights greater than 3 m. The Ursell numbers greater than 100 immediately seaward of jetty tips indicate strong wave nonlinearity occur in these areas.

4.5.2 Symmetric and Asymmetric Ebb Shoal Simulations for a Summer Month

Figure 4-8 shows the maximum wave steepness fields calculated for the asymmetric (August 2005 simulation) and symmetric (August 2010 simulation) ebb shoal. Figure 4-9 shows the mean wave steepness fields from the same simulations. Both maximum and mean wave steepness fields have higher values for the asymmetric ebb shoal as compared to the symmetric ebb shoal.

Figure 4-10 shows the maximum wave dissipation for asymmetric (August 2005 simulation) and symmetric (August 2010 simulation) ebb shoal. Figure 4-11 shows the mean wave dissipation for the same simulations. While the pattern of the mean wave dissipation for the asymmetric and symmetric ebb shoal bathymetries is similar, the calculated maximum wave dissipation intensity for the asymmetric ebb shoal is greater than the symmetric shoal at the inlet entrance and around the ebb shoal.

Figure 4-12 depicts the maximum Ursell number fields for asymmetric and symmetric ebb shoal bathymetries. Figure 4-13 shows mean Ursell number fields for asymmetric and symmetric ebb shoal bathymetries. The calculated Ursell number is greater at the ebb shoal and surrounding area for the asymmetric ebb shoal. In summary, even though incident wave conditions for the months of August 2005 and 2010 are so strikingly similar, the wave steepness, dissipation and Ursell number parameters for the asymmetric ebb shoal bathymetry with August 2005 waves are greater as compared to the symmetric bathymetry with August 2010 waves. Because the wave conditions for the month of August in 2005 and 2010 are similar, the differences seen for these years are related directly to the symmetry and asymmetry of the ebb shoal geometry.

Figure 4-8. Calculated monthly maximum wave steepness fields for (a) asymmetric ebb shoal bathymetry (August 2005 waves), and (b) symmetric ebb shoal bathymetry (August 2010 waves).

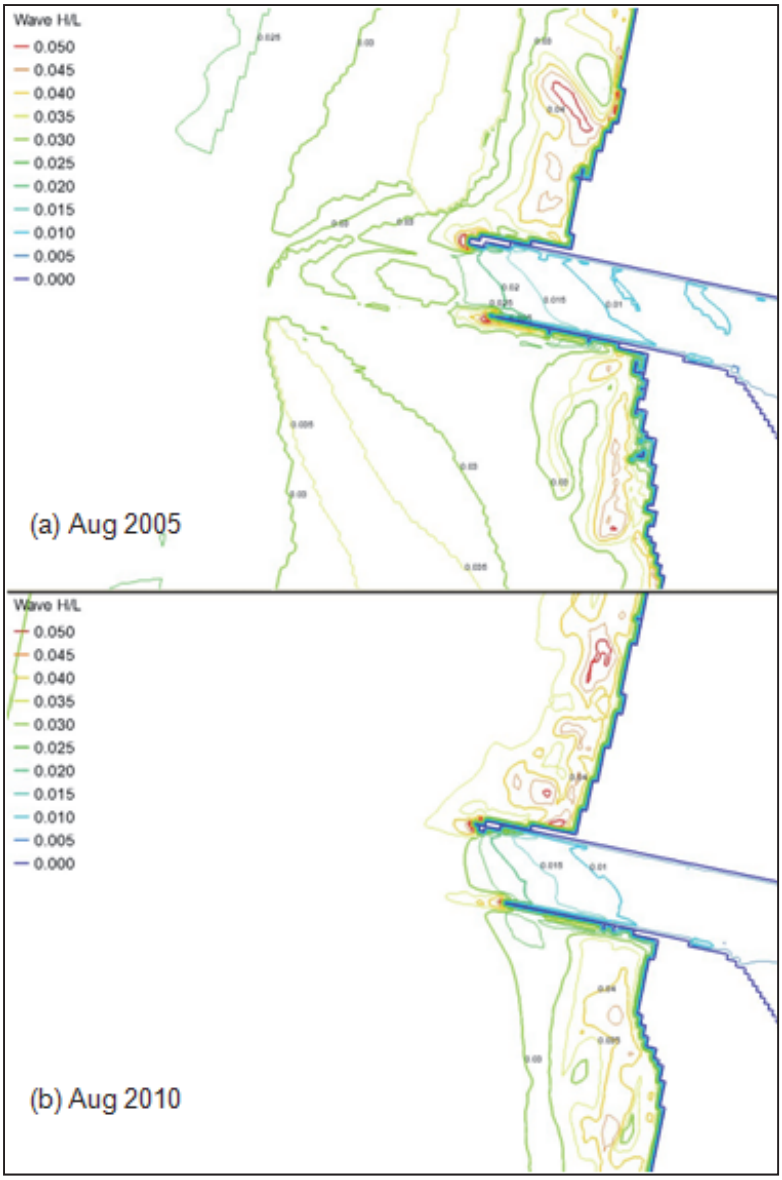

Figure 4-9. Calculated monthly mean wave steepness fields for (a) asymmetric ebb shoal bathymetry (August 2005 waves), and (b) symmetric ebb shoal bathymetry (August 2010 waves).

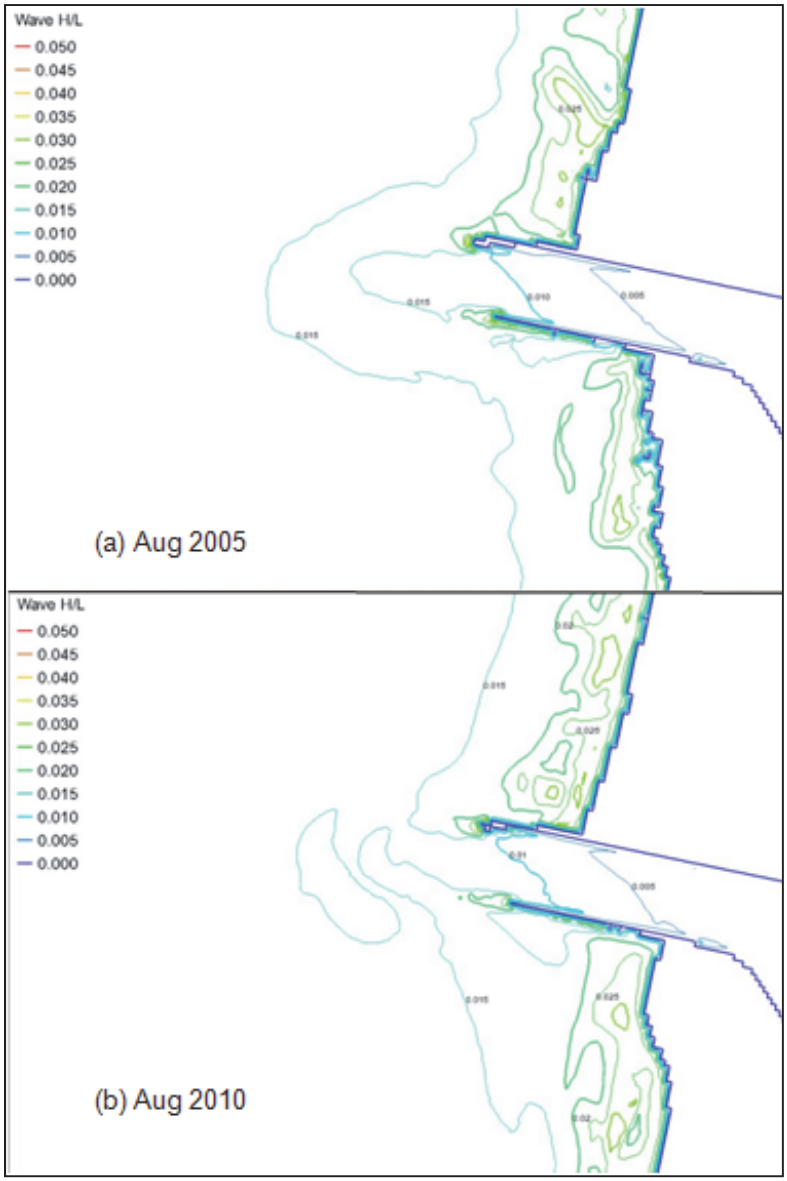

Figure 4-10. Calculated monthly maximum wave dissipation fields for (a) asymmetric ebb shoal bathymetry (August 2005 waves), and (b) symmetric ebb shoal bathymetry (August 2010 waves).

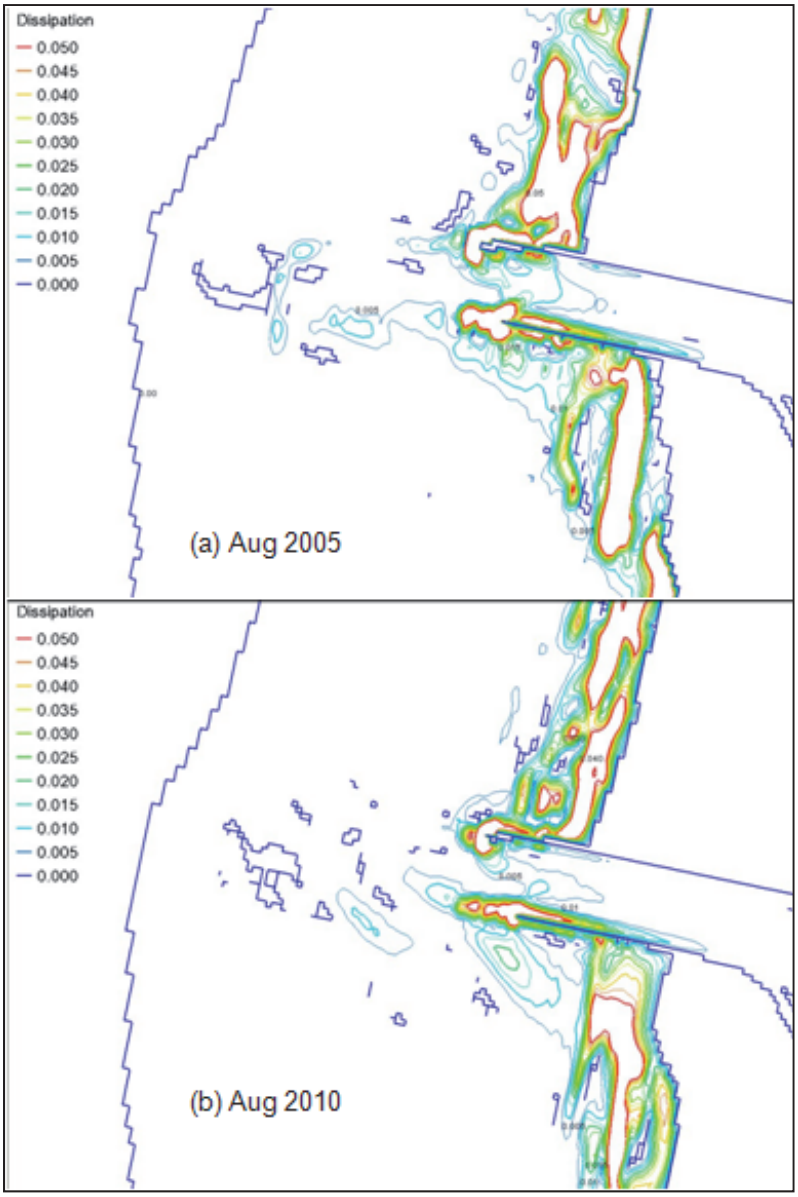

Figure 4-11. Calculated monthly mean wave dissipation fields for (a) asymmetric ebb shoal bathymetry (August 2005 waves), and (b) symmetric ebb shoal bathymetry (August 2010 waves).

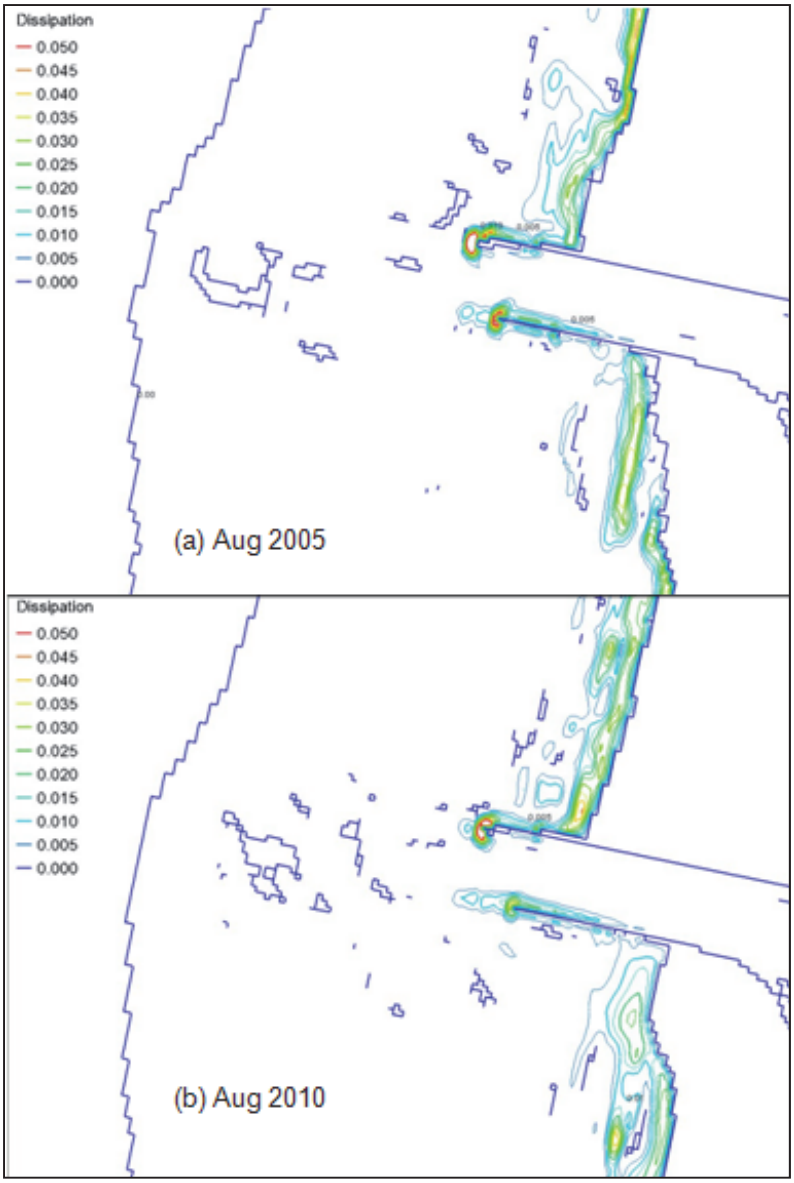

Figure 4-12. Calculated monthly maximum Ursell number fields for (a) asymmetric ebb shoal bathymetry (August 2005 waves), and (b) symmetric ebb shoal bathymetry (August 2010 waves).

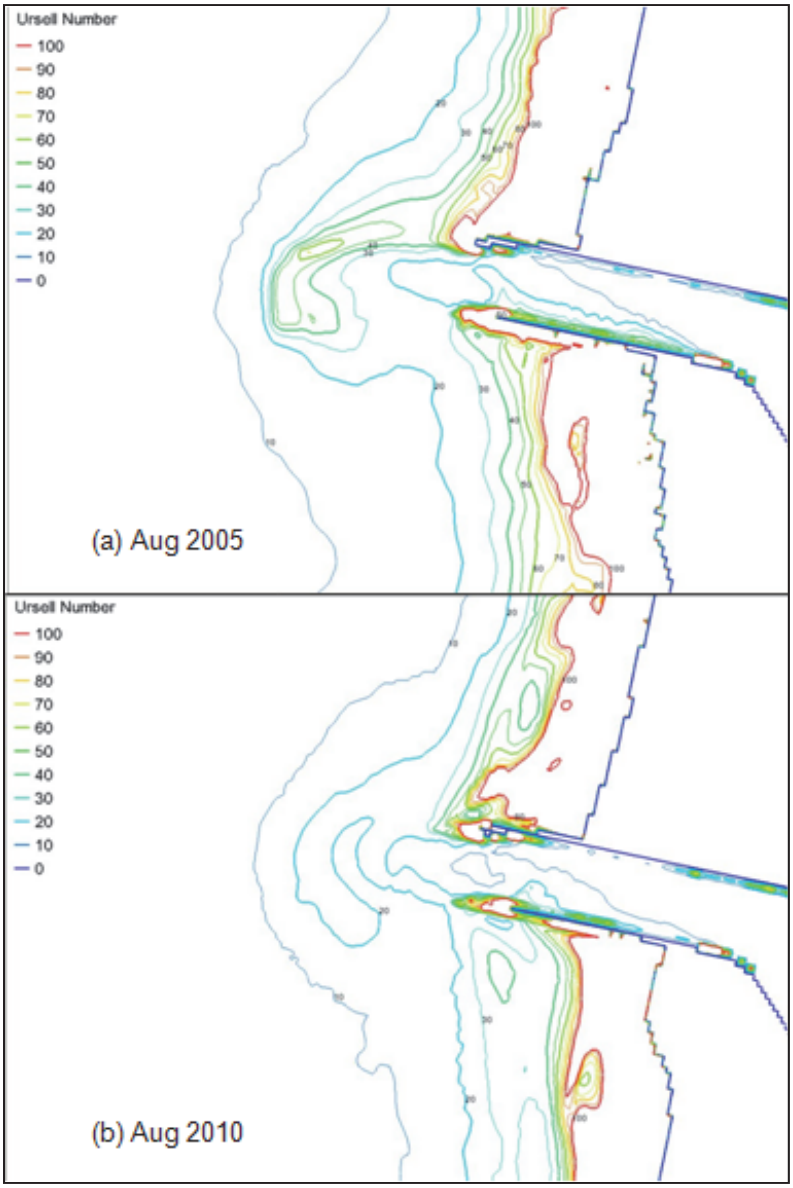

Figure 4-13. Calculated monthly mean Ursell number fields for (a) asymmetric ebb shoal bathymetry (August 2005 waves), and (b) symmetric ebb shoal bathymetry (August 2010 waves).

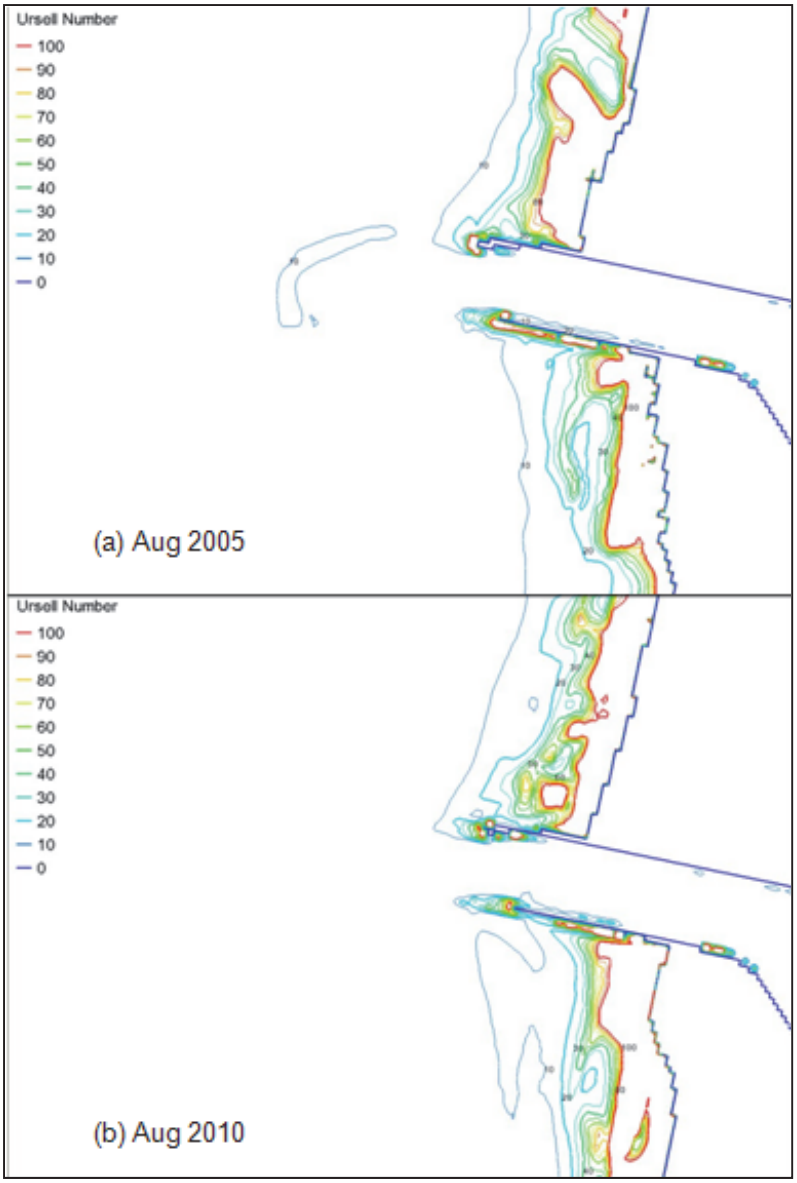

4.5.3 Symmetric and Asymmetric Ebb Shoal Simulations for a Winter Month

Figure 4-14 shows the maximum wave steepness fields calculated for the asymmetric ebb shoal with December 2005 waves and symmetric ebb shoal with December 2010 waves. Figure 4-15 shows the associated mean wave steepness fields for the same month. Both maximum and mean wave steepness fields have higher wave steepness values for the asymmetric ebb shoal than symmetric ebb shoal. Larger wave steepness values occur in the vicinity of asymmetric ebb shoal. The larger steepness values for

asymmetric ebb shoal in the December 2005 could be caused by higher incident waves in that month, with more severe winter storms, than in December 2010.

Figure 4-14. Calculated monthly maximum wave steepness fields for (a) asymmetric ebb shoal bathymetry (December 2005 waves), and (b) symmetric ebb shoal bathymetry (December 2010 waves).

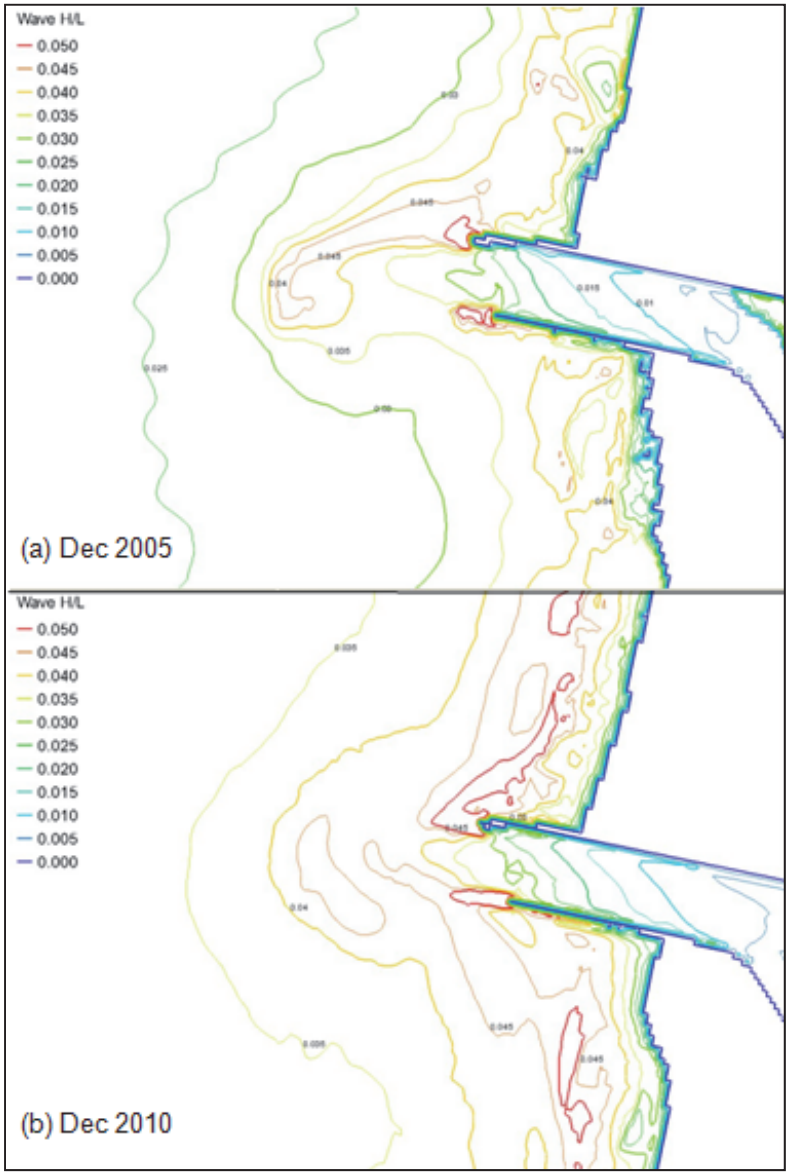

Figure 4-15. Calculated monthly mean wave steepness fields for (a) asymmetric ebb shoal bathymetry (December 2005 waves), and (b) symmetric ebb shoal bathymetry (December 2010 waves).

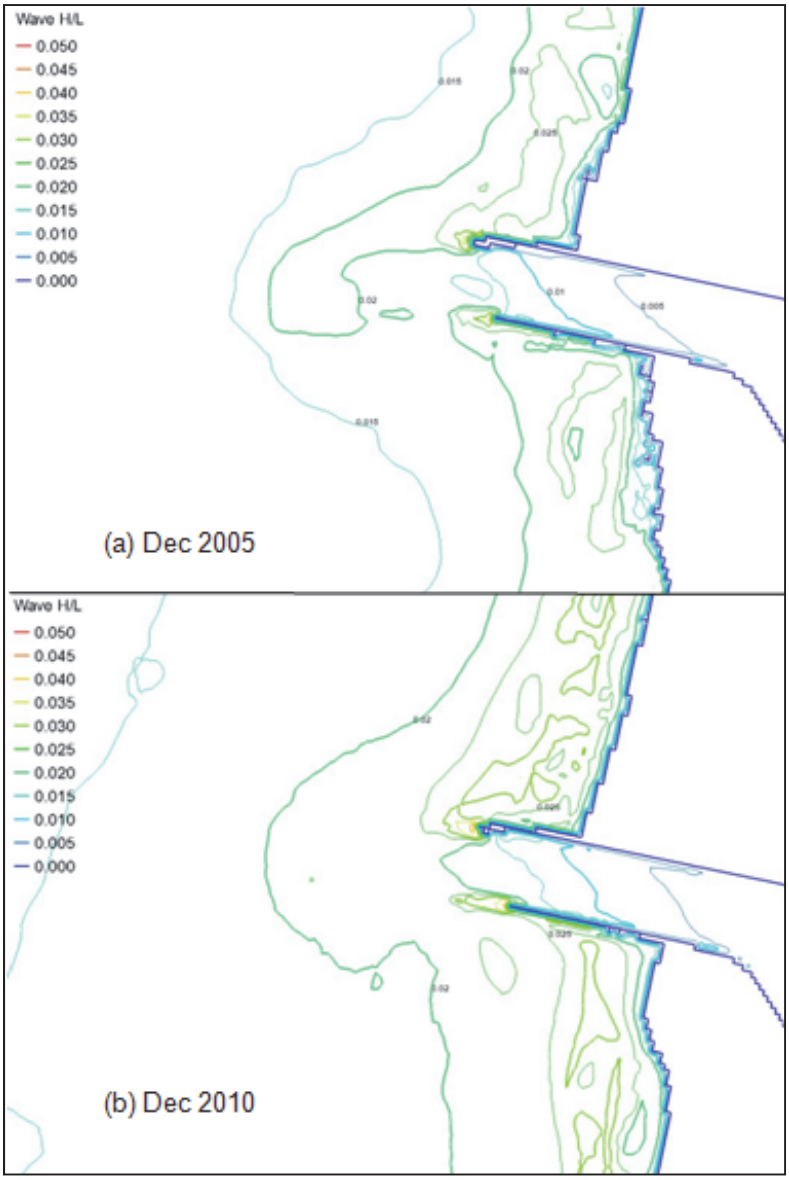

Figure 4-16 shows the maximum wave dissipation for the symmetric and asymmetric ebb shoal. Figure 4-17 shows the associated mean wave dissipation for the same simulations. These results indicate that comparatively much stronger wave breaking and dissipation occur at the inlet entrance and over the ebb shoal in December 2005 than December 2010. This happens because of a combination of the asymmetric ebb shoal and larger incident waves in December 2005.

Figure 4-16. Calculated monthly maximum wave dissipation fields for (a) asymmetric ebb shoal bathymetry (December 2005 waves), and (b) symmetric ebb shoal bathymetry (December 2010 waves).

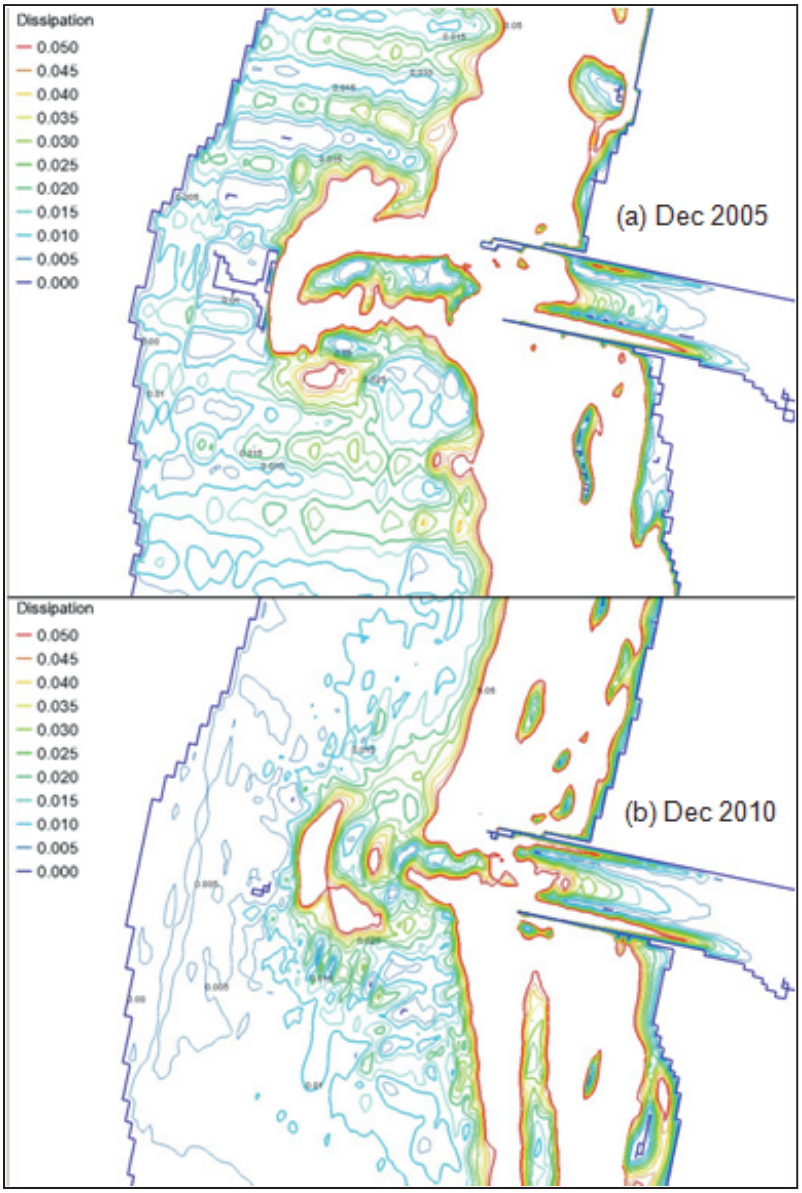

Figure 4-17. Calculated monthly mean wave dissipation fields for (a) asymmetric ebb shoal bathymetry (December 2005 waves), and (b) symmetric ebb shoal bathymetry (December 2010 waves).

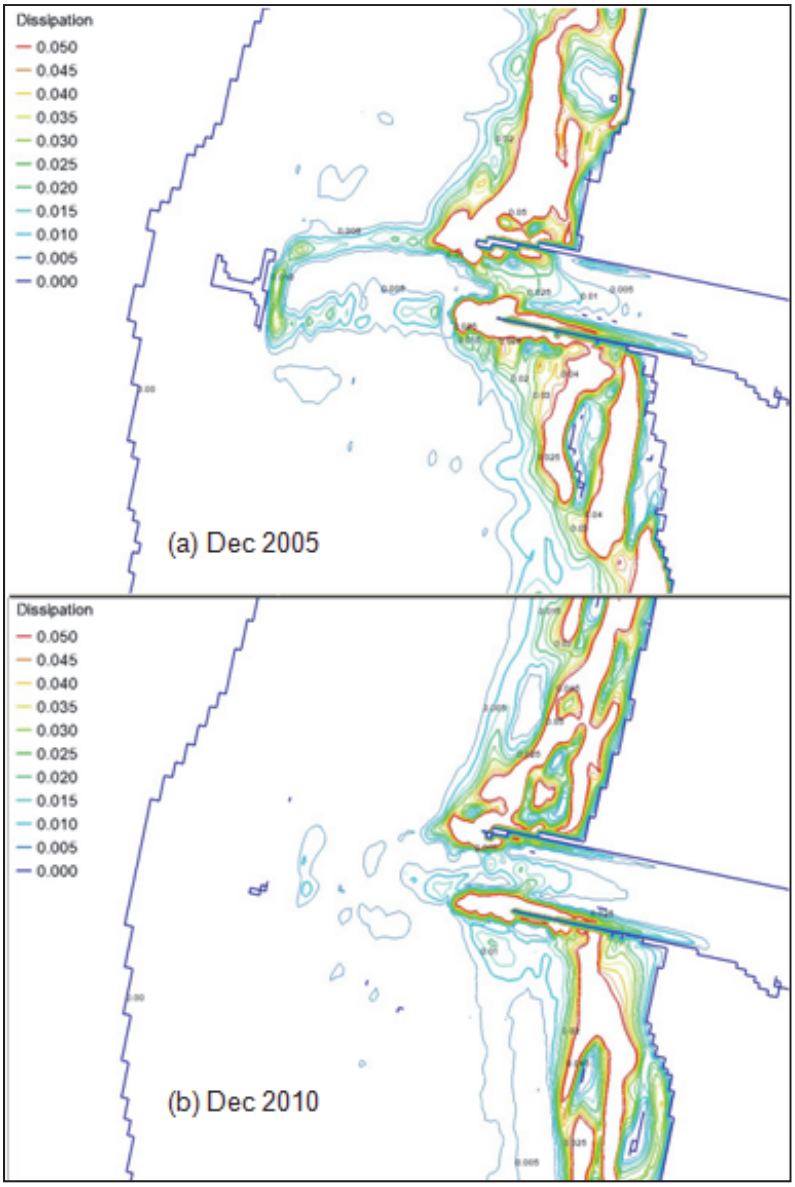

Figure 4-18 shows the maximum Ursell number fields for symmetric and asymmetric ebb shoal. Figure 4-19 shows the associated mean Ursell number fields. The calculated mean and maximum Ursell number values are higher over the ebb shoal and in the inlet entrance for December 2005 than December 2010, which is caused by a combination of the asymmetric ebb shoal and larger incident waves in December 2005.

Figure 4-18. Calculated monthly maximum Ursell number fields for (a) asymmetric ebb shoal bathymetry (December 2005 waves), and (b) symmetric ebb shoal bathymetry (December 2010 waves).

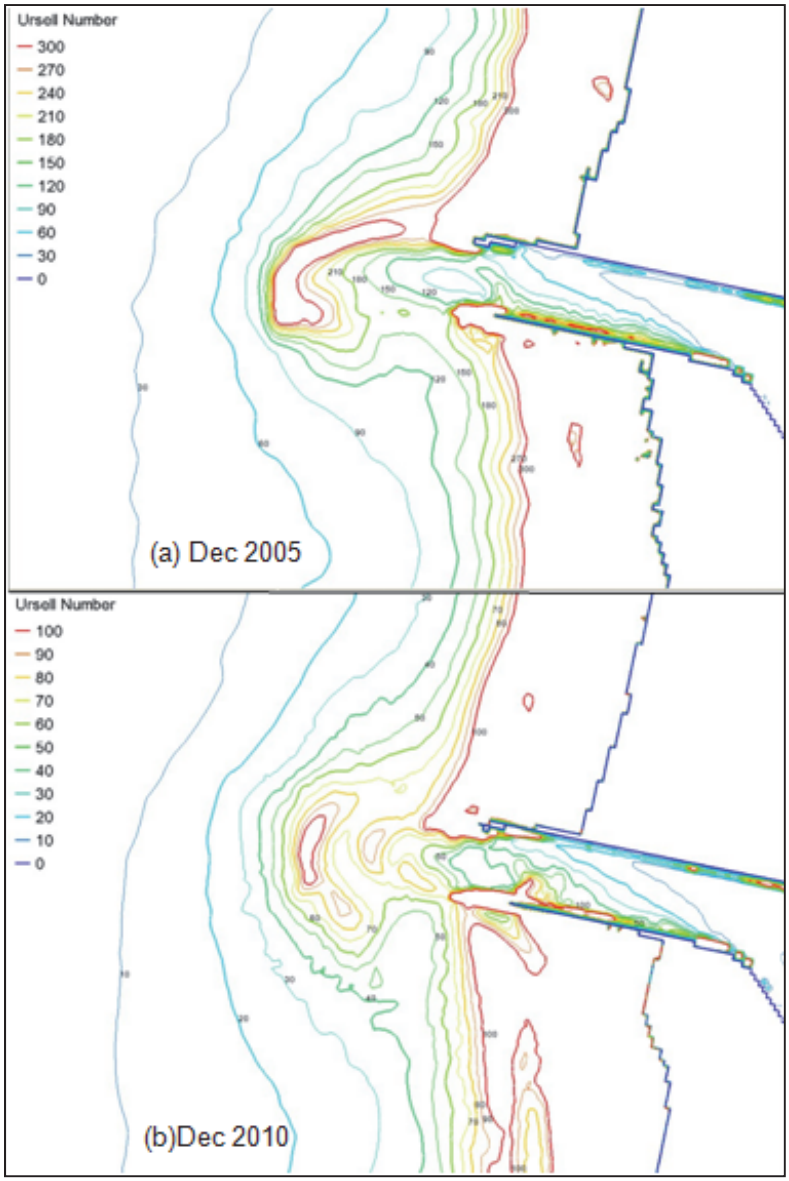

4.6 Hypothetically shortened South Jetty

In collaboration with NWP, a hypothetically shortened South Jetty with a seaward portion of the South Jetty removed was simulated to investigate how such a shortening would affect navigation in Tillamook Inlet. The June 2010 bathymetric grid was modified in the vicinity of the South Jetty tip by smoothing and deepening the depth contours over a 230-m (750 ft) segment of structure. The deepened and smoothed depth contours were matched to neighboring values on both sides of the modified jetty.

Figure 4-19. Calculated monthly mean Ursell number fields for (a) asymmetric ebb shoal bathymetry (December 2005 waves), and (b) symmetric ebb shoal bathymetry (December 2010 waves).

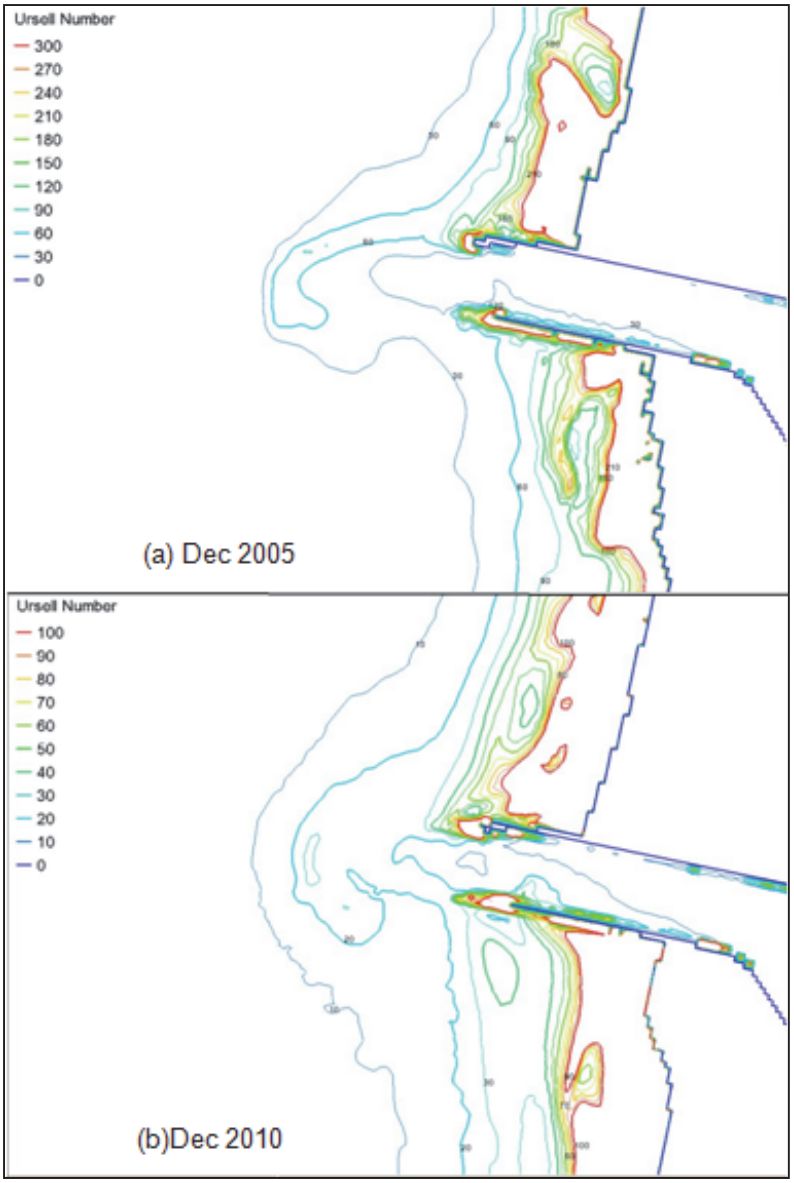

4.6.1 Seasonal Mean Wave Conditions

Three selected incident wave conditions were simulated: (a) H_s = 2 m, T_p = 8 sec, (b) H_s = 3 m, T_p = 10 sec and (c) H_s = 4 m, T_p = 12 sec. Figures 4-20 to 4-22 show the wave steepness, wave dissipation, and Ursell number fields for a hypothetically shortened South Jetty. Comparing these results to the existing South Jetty case (Figures 4-4, 4-5, and 4-7) shows minor changes in wave breaking patterns for these three incident waves occurring adjacent to the recessed South Jetty. The effect of South Jetty shortening is localized to the immediate vicinity of the jetty, and has no visible effect on waves outside

the entrance over the ebb shoal. For 3-m and 4-m waves with a recessed South Jetty, there is a slight increase in wave steepness and dissipation extending into the main channel. Because the South Jetty base was modified slightly, large values of wave steepness and dissipation continued to occur at the same locations regardless of the South Jetty shortening.

Figure 4-20. Calculated wave steepness fields of three incident waves for the hypothetically shortened South Jetty.

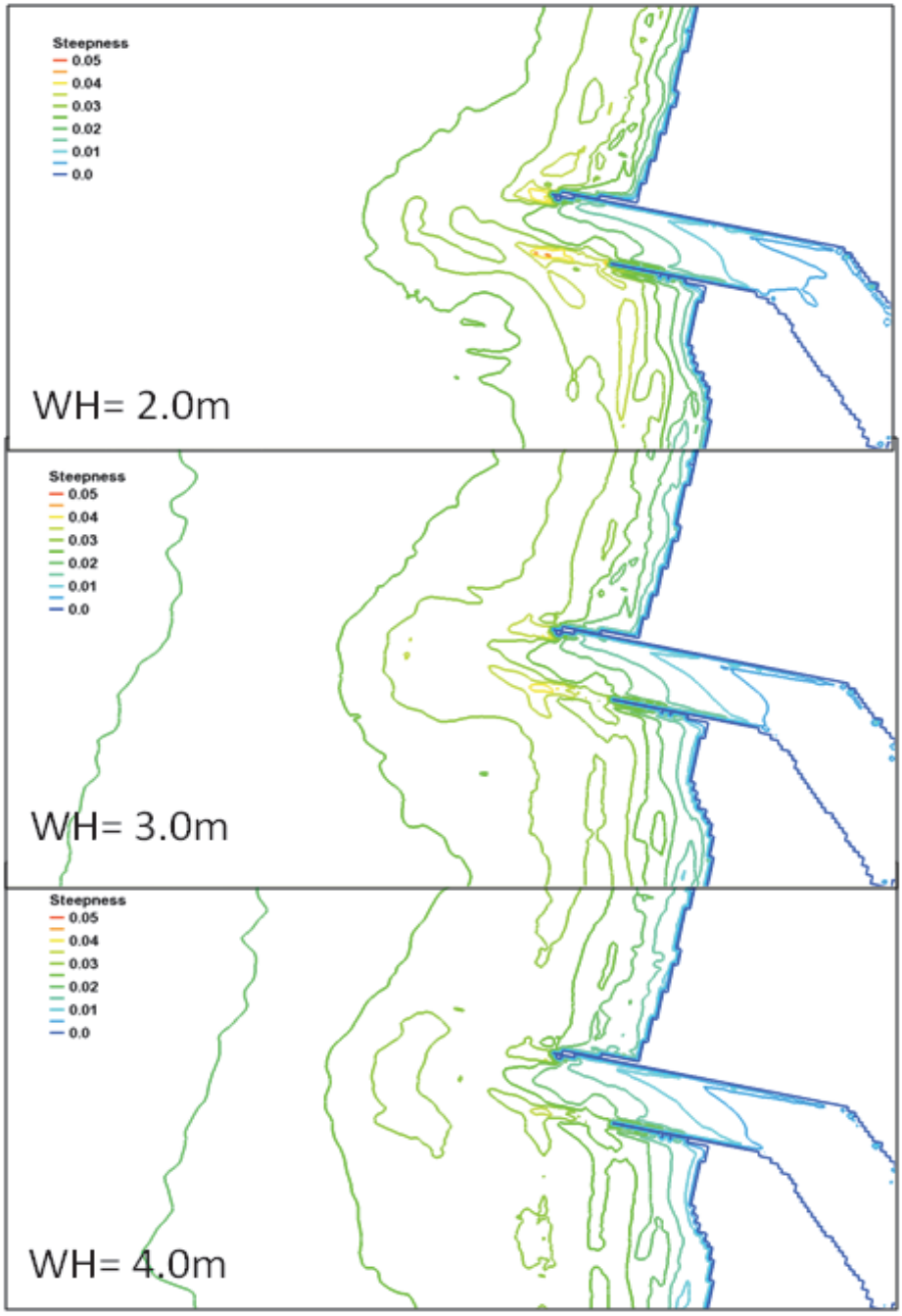

Figure 4-21. Calculated wave dissipation fields of three incident waves for the hypothetically shortened South Jetty.

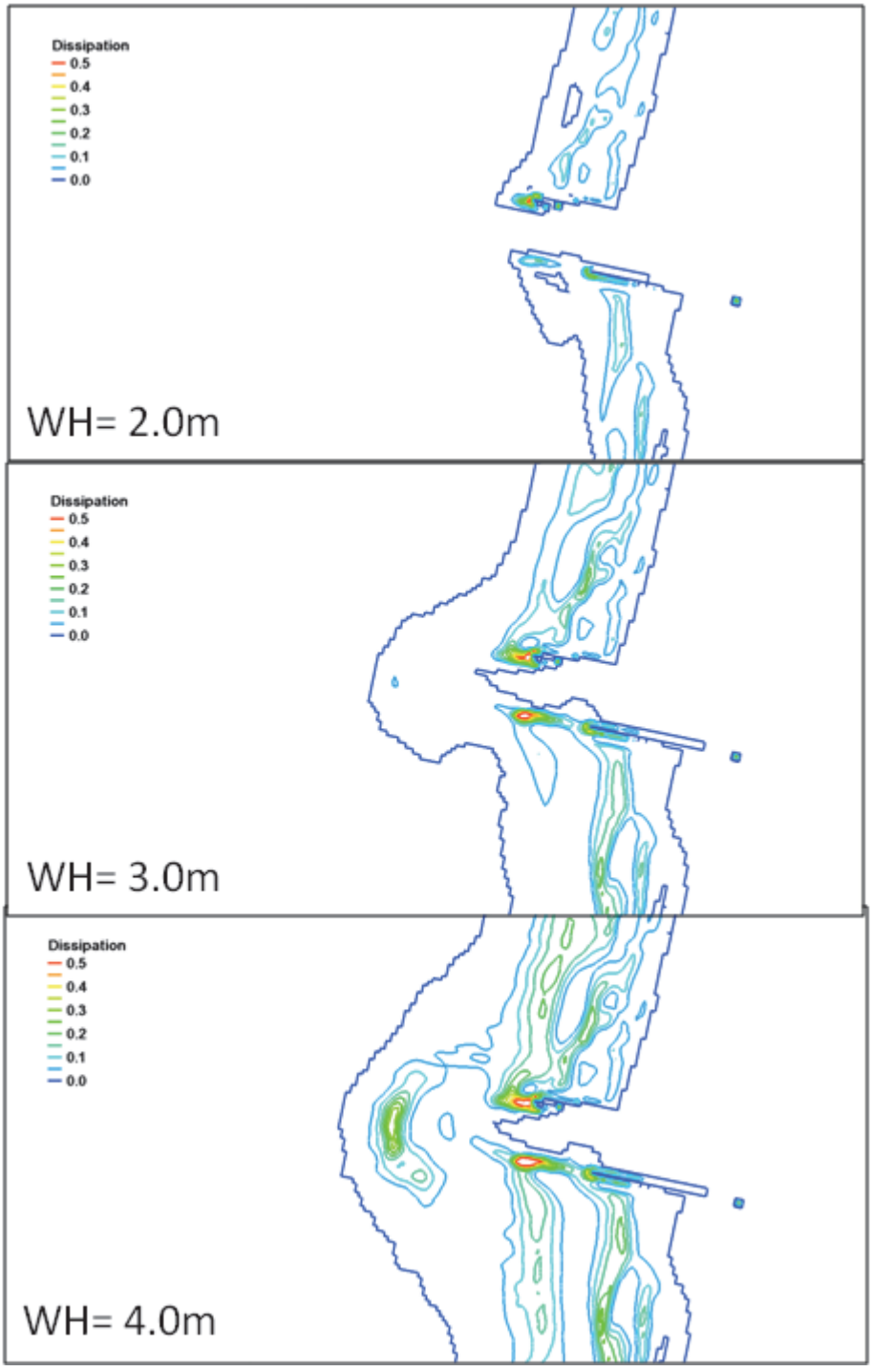

Figure 4-22. Calculated Ursell number fields of three incident waves for the hypothetically shortened South Jetty.

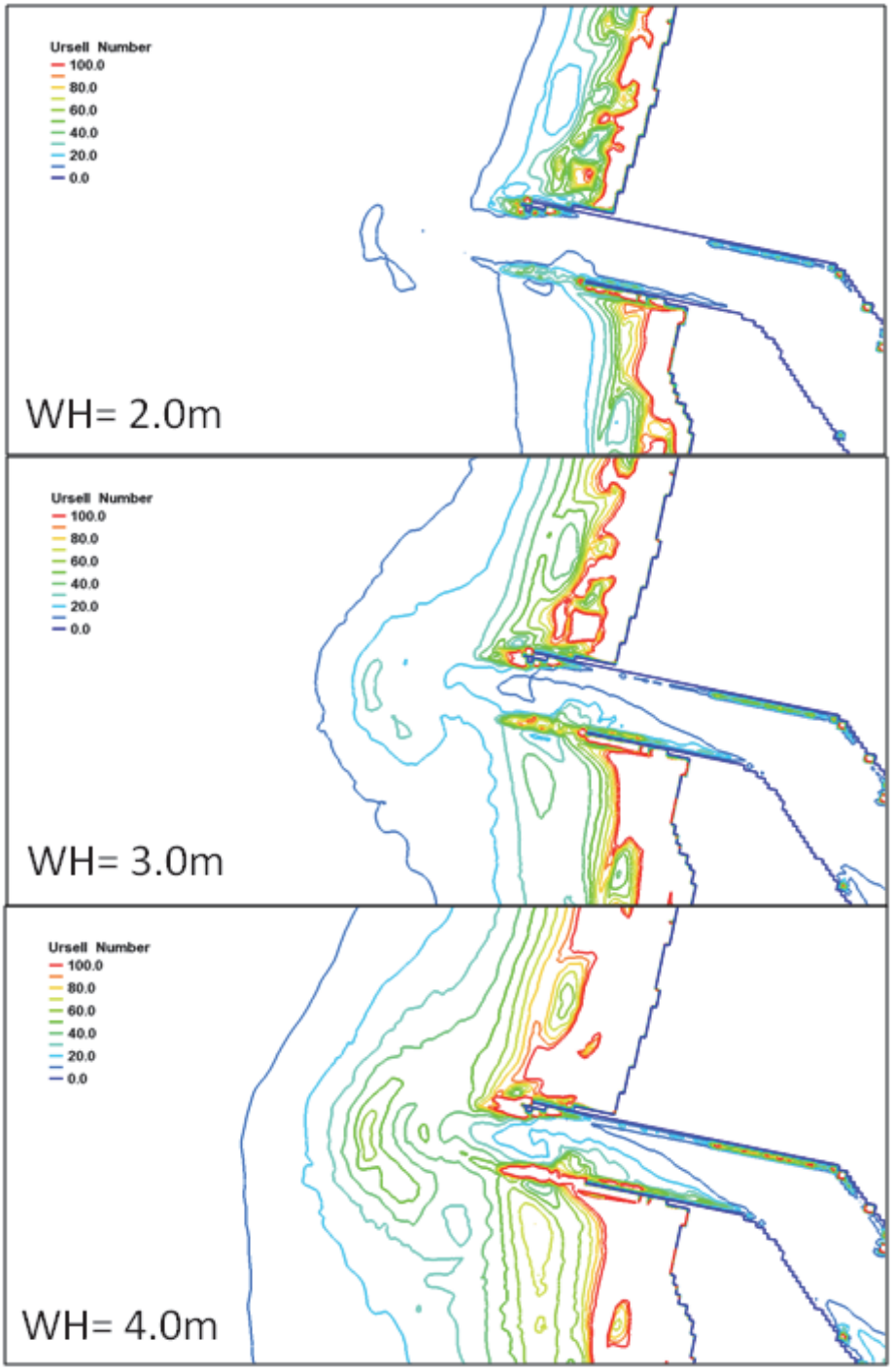

4.6.2 Simulations for August and December 2010

Figure 4-23 shows the calculated maximum wave steepness fields for August and December 2010. For the same simulations, Figures 4-24 and 4-25 show the associated maximum wave dissipation and Ursell numbers,

respectively. Based on these results, which exclude currents in the simulations, the South Jetty shortening did not change waves appreciably in the main channel, in the entrance, or over and beyond the ebb shoal to significantly affect navigation in the entrance channel or on the ebb shoal. Comparison of Figures 4-12(b) and 4-18(b) with Figure 4-25 indicates the values of Ursell number are decreasing over the submerged segment with a shorten South Jetty for August 2005. However, the change of Ursell numbers is negligible for December 2010. Similar changes occurred in the wave steepness and dissipation.

Figure 4-23. Calculated monthly maximum wave steepness fields for symmetric ebb shoal bathymetry with (a) August 2010 waves and (b) December 2010 waves - hypothetically shortened South Jetty.

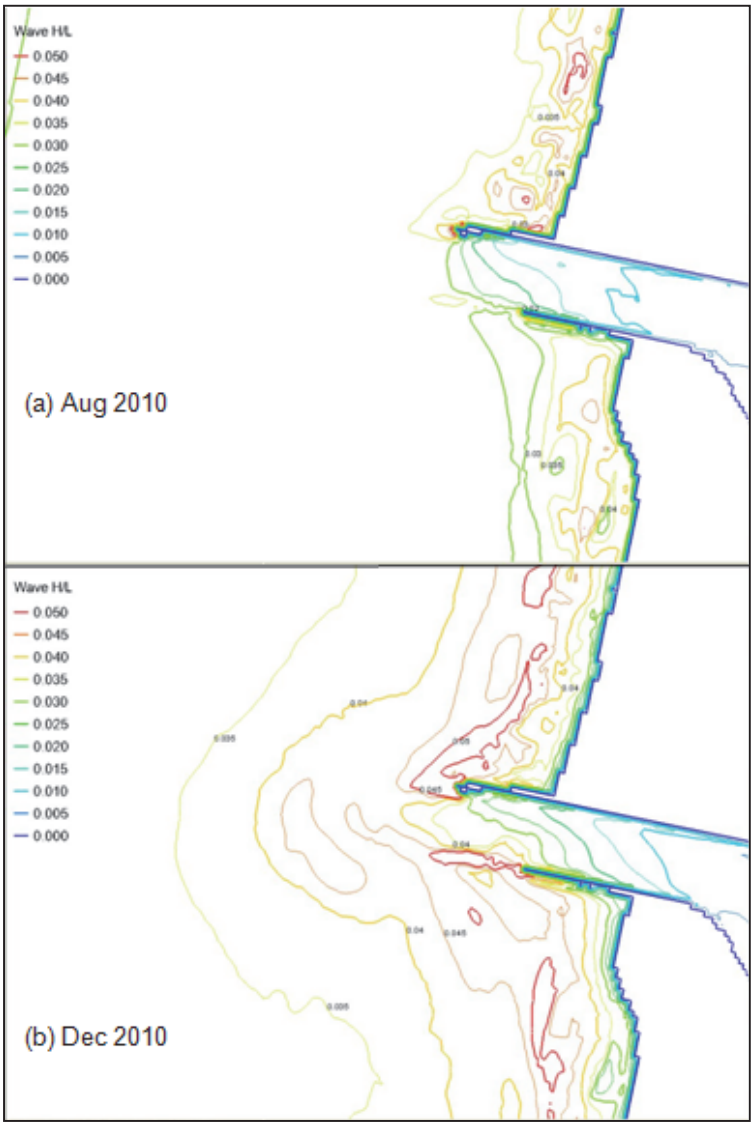

Figure 4-24. Calculated monthly maximum wave dissipation fields for symmetric ebb shoal bathymetry with (a) August 2010 waves and (b) December 2010 waves - hypothetically shortened South Jetty.

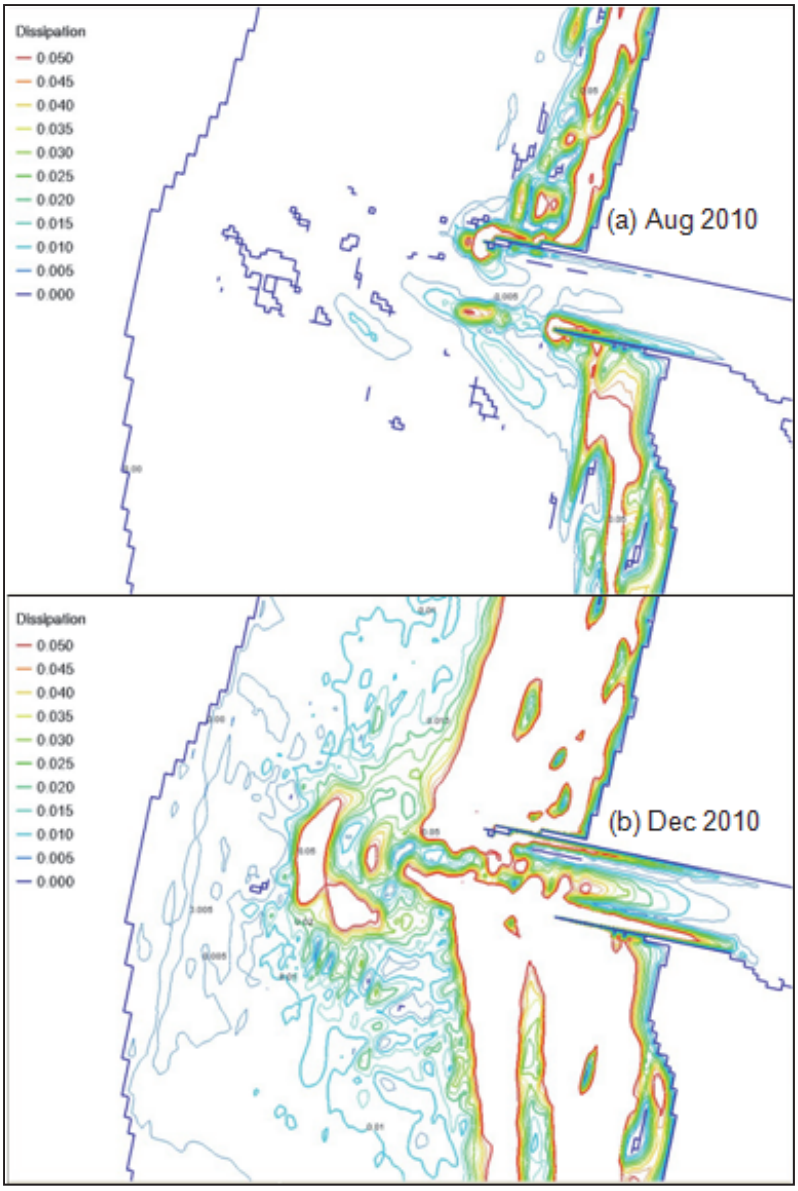

Figure 4-25. Calculated monthly maximum Ursell number fields for symmetric ebb shoal bathymetry with (a) August 2010 waves and (b) December 2010 waves - hypothetically shortened South Jetty.

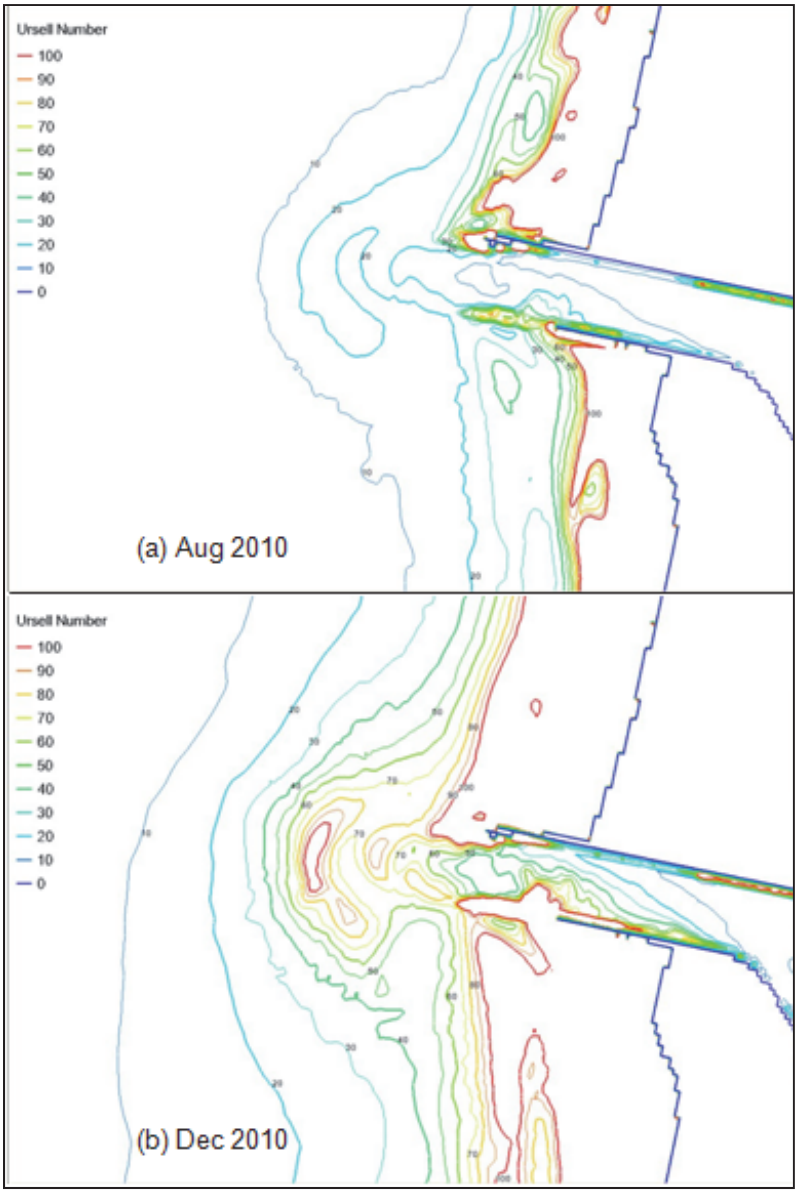

4.7 Discussion and Summary of Results

Wave-only simulations were made with incident waves and wind input. Water level, tides, currents, and river flows were not included in these simulations. These simulations were first conducted for representative seasonal "mean wave conditions," with constant incident wave conditions. Wave simulations were then conducted for a typical summer month (August) and a winter month (December) in 2005 and 2010. Wave-only simulations were run for three model grids: (1) asymmetric ebb shoal grid

based on September 2005 survey, (2) symmetric ebb shoal grid based on June 2010 survey, and (3) hypothetically shortened South Jetty grid based on the symmetric ebb shoal grid.

Four wave-related parameters were initially calculated based on wave simulations: (1) wave steepness, (2) wave dissipation, (3) surf-zone similarity parameter, and (4) Ursell number. The wave steepness is a measure of wave instability that can lead to wave breaking. The wave dissipation is a measure of the intensity of wave breaking caused by the combination of wave instability, bottom friction, whitecaps, and depth-limited breaking. The surf-zone parameter is usually used in the investigation of types of wave breaking and littoral transport processes. The Ursell number which combines both the steepness and depth limited breaking into a single parameter, is a measure of nonlinear wave effects, with larger Ursell numbers corresponding to stronger nonlinearity of waves, intense breaking, and shallowness effects. The calculated surf-zone parameter was found to be not sensitive to the range of incident waves representing seasonal mean wave conditions at Tillamook Inlet. For this reason, this parameter was not pursued further.

Wave steepness, wave dissipation, and Ursell number are all wave-related parameters, and these can be used to identify wave conditions posing increasing hazard to navigation in areas of Tillamook Inlet complex. Wave steepness and dissipation are useful in terms of gaining a better understanding of wave conditions around the navigation channel at the entrance. Wave steepness and dissipation were closely associated with the bathymetry of ebb shoal, and wave dissipation patterns followed the ebb shoal shape.

The calculated Ursell number can attain large values especially for high energy winter storm waves in shallow depths. Ursell number accounts for the effects of wave severity or nonlinearity (wave height), it includes depth-limited wave breaking (wave height to water depth ratio). It also determines the types of waves that could exist at any local depth (ratio of wavelength to water depth). Consequently, this unique parameter could be the best measure among the three to identify conditions that might affect navigation. On the other hand, the safe operational navigation limits at Tillamook would also depend on the moving vessel's size, speed, and her transit course with respect to the direction of waves and currents encountered by the vessel during her transit. To develop a site-specific operational guidance for Tillamook Inlet based on Ursell number, vessel

traffic, speed, and transit route at Tillamook are needed, as well as the records of known accidents as well as the associated waves and currents at the time of such events.

Wave-only simulation results indicated that wave breaking intensity at the inlet entrance and over the ebb shoal region was stronger for the asymmetric ebb shoal (September 2005 bathymetry) than that for the symmetrical ebb shoal (June 2010 bathymetry). Large values of wave steepness, wave dissipation, and Ursell numbers were associated with larger waves prevailing locally. For the majority of simulations performed, values of calculated wave-related parameters were higher in areas away from the navigation channel which were shallow (e.g., along north and south beach faces and on the submerged tips of both jetties). In general, for a limited set of wave conditions evaluated in this study, these calculated parameters have pockets of isolated areas with greater values of wave steepness, wave dissipation and Ursell numbers. On the ebb shoal, these pockets were mostly located along the federal navigation channel and within 100 m (300 ft) of the channel centerline. There were fewer isolated pockets south of the inlet entrance, suggesting that the south entrance channel may be a safer inbound/outbound course for traffic in and out of the inlet.

5 Combined Wave and Flow Modeling

The combined wave and flow modeling for Tillamook Inlet using coupled CMS-Wave and CMS-Flow is described in this Chapter. This modeling includes effects of winds, waves, tides, and river inflows. The calculated quantities of interest includes wave-related engineering parameters including wave height, peak period and direction, wave steepness, dissipation, and Ursell number. These engineering parameters are used to assess wave and current conditions for safe navigation, and preferred entrance and exit courses for boating operations at Tillamook Inlet.

5.1 Details of Combined Wave and Flow Modeling

5.1.1 Model Setup

A telescoping grid was used in the flow modeling that covered a square domain of 17.6 × 17.6 km (same domain as the wave grid), with the offshore boundary located approximately at the 80-m isobaths (Figure 5-1). The grid has finer resolution in areas of high interest such as the ebb shoal, entrance, inlet, and Bay. The red circle denotes the location of NOAA's Garibaldi tide gauge. Two red triangles denote the locations of the inlet entrance (Entrance Channel Station) and Kenchloe Point (Kenchloe Point Station) where high current were calculated. Three flow telescoping grids were generated: (1) an asymmetric ebb shoal grid (based on September 2005 survey), (2) a symmetric ebb shoal grid (based on June 2010 survey), and (3) a hypothetically shortened South Jetty grid. Figure 5-2 shows the symmetric and asymmetric ebb shoal grids.

The South Jetty of the Tillamook Inlet has a recession rate of 40-80 ft/yr. Considering 15 years of the South Jetty recession at a rate of 50 ft/yr, a third grid was developed using the symmetric ebb shoal bathymetry by shortening the South Jetty 230 m (750 ft). Existing and degraded (hypothetically shortened) South Jetty configurations are shown in Figure 5-3.

5.1.2 Model Forcing Conditions

Simulations were conducted for a summer (August) and a winter (December) month for asymmetric ebb shoal (September 2005 bathymetry) and symmetric ebb shoal (June 2010 bathymetry). The hypothetically shortened South Jetty was simulated only for the symmetric ebb shoal. In

Figure 5-1. CMS domain and telescoping grid.

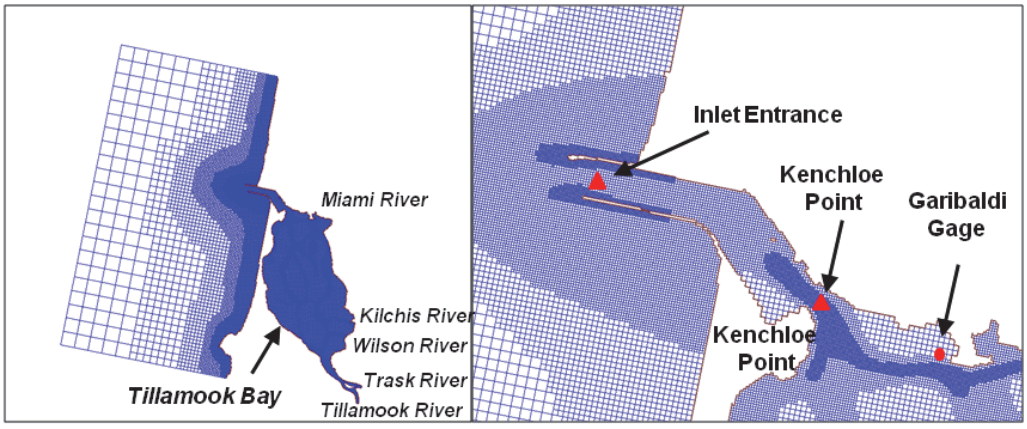

Figure 5-2. The symmetric ebb shoal grid (based on June 2010 bathymetry) and asymmetric ebb shoal grid (based on September 2005 bathymetry).

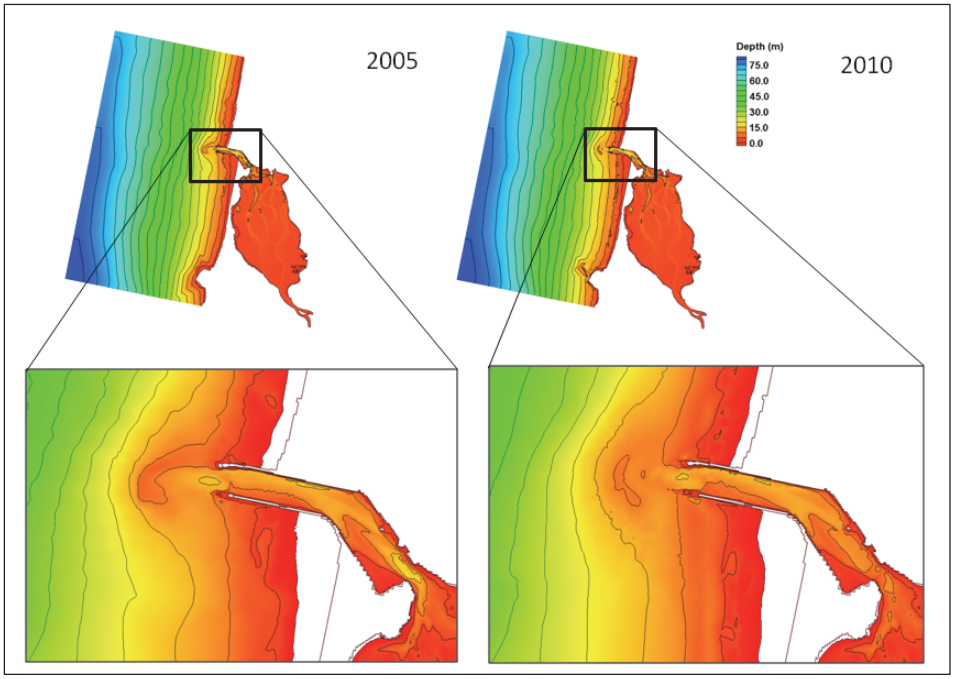

Figure 5-3. Existing (left) and hypothetically shortened (right) South Jetty configurations.

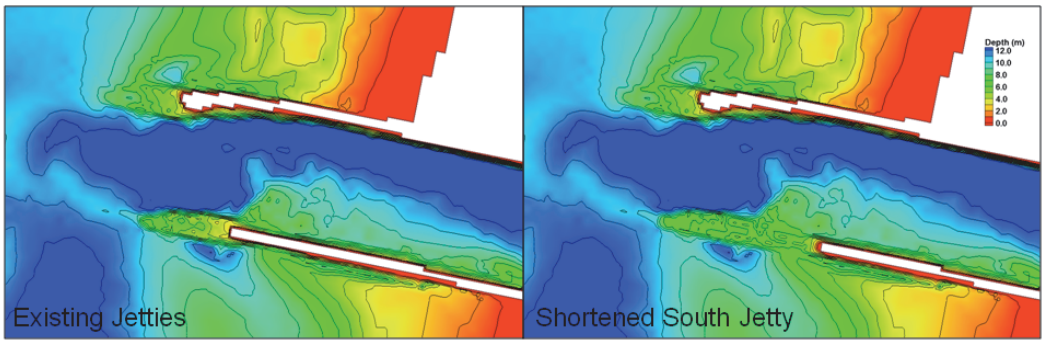

addition to the calculation of monthly mean and maximum parameters, four peak flood and ebb current scenarios were selected to show the strong current effects on wave-related parameters. A monthly maximum estimate could be due to maximum waves or maximum currents or both. These additional scenarios ensure the peak flood and ebb current effects on wave-related parameters are included. For safety of navigation, the peak flood and ebb currents are of primary concern to boating operations.

CMS-Flow was forced with the time-dependent water levels, winds, river discharges, and waves. Water level data (see Figure 5-4 for sample data in August 2005) were obtained from NOAA coastal station (9435380) at South Beach, Yaquina River, Oregon, approximately 105 km south of Tillamook Inlet on the Oregon coast. To account for the distance between the South Beach Station and Tillamook Bay, tidal signals were phase-shifted by 30 minutes at the CMS-Flow open boundary. The data indicate no seasonal changes in tidal signals.

Figure 5-4. Water level data for August 2005 at South Beach and Yaquina River, OR.

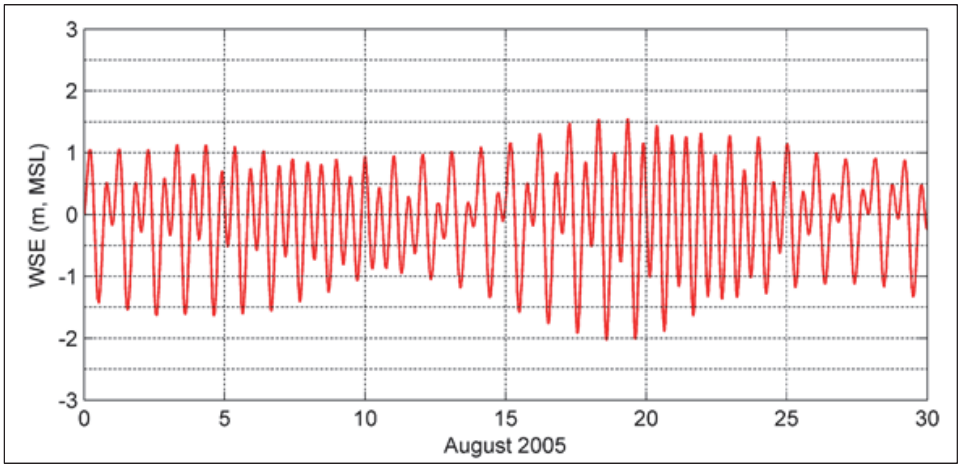

Wind data (see Figure 5-5 for sample data in August and December 2005) were obtained from the offshore NDBC Buoy 46029. River flow data (see Figure 5-6 for sample data in December 2010) were obtained from the USGS gauges at the Trask and Wilson rivers. The flow discharge in summer is 1 to 2 orders of magnitude smaller than the winter. The flow discharges for three other rivers (Tillamook, Kilchis, and Miami rivers) were estimated by a weighted drainage area approach.

Figure 5-5. Wind data for August and December 2005 at NDBC Buoy 46029.

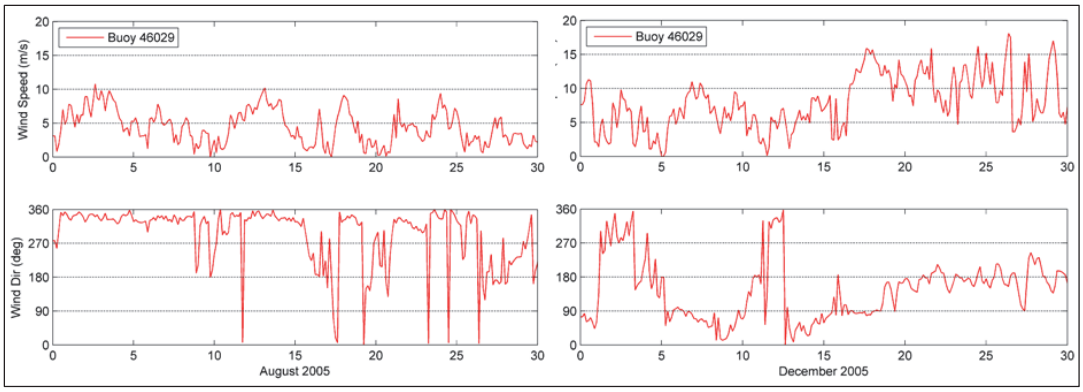

Figure 5-6. River flow discharges for December 2005 and 2010 from USGS gauges at Trask (Sta 14302480) and Wilson (Station 14301500) rivers, OR.

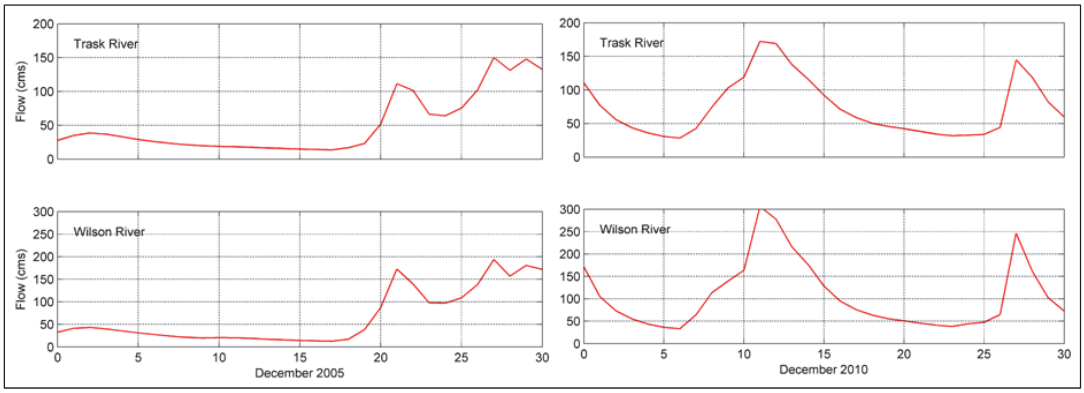

5.2. Modeling Results

5.2.1 Water Levels and Currents

As an example, the calculated and the measured water surface elevations at Garibaldi for August 2010 are shown in Figure 5-7. The calculated results agree with the measurements. Water levels at Garibaldi have a mixed signal that is mainly semi-diurnal tide. The mean tidal range (mean high water – mean low water) is 1.9 m and the maximum tidal range (mean higher high water - mean lower low water (MLLW)) is 2.5 m. Considering the size of Tillamook Bay and the narrowness of the navigation channel through Tillamook Inlet, this tidal range is large enough to generate strong ebb and flood currents at the inlet channel.

Example snapshots of calculated current fields on 12 August 2010 at 21:00 GMT, 13 August 2010 at 03:00 GMT, 27 December 2010 at 12:00 GMT, and 18:00 GMT, are shown in Figures 5-8 and 5-9. In these examples, incident waves are from west-northwest (300 deg azimuth) in

the summer cases, and west-southwest (260 deg azimuth) in the winter cases. The calculated current magnitude reaches 3 m/sec at the Kenchloe Point Station (Figure 5-1). The current pattern at the ebb shoal is mainly controlled by wind, waves, and local bathymetry.

Figure 5-7. Calculated water surface elevation at Garibaldi, August 2010.

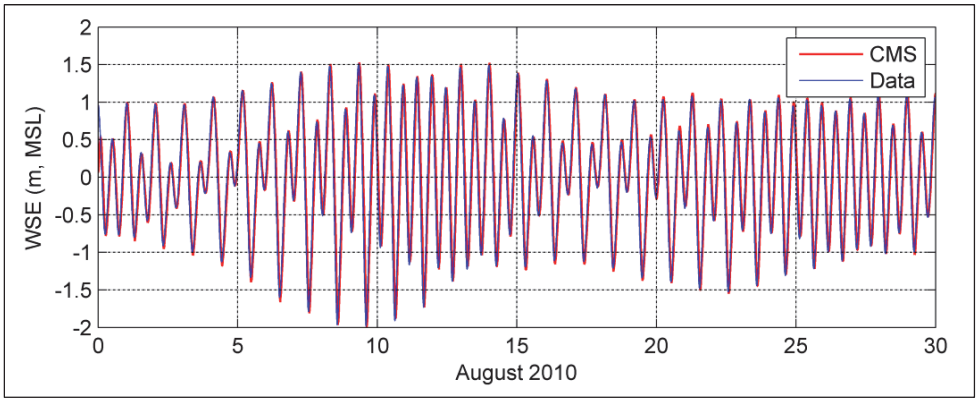

Figure 5-8. Calculated current field on 12 August 2010 at 21:00 GMT (flood current) and on 13 August 2010 at 03:00 GMT (ebb current).

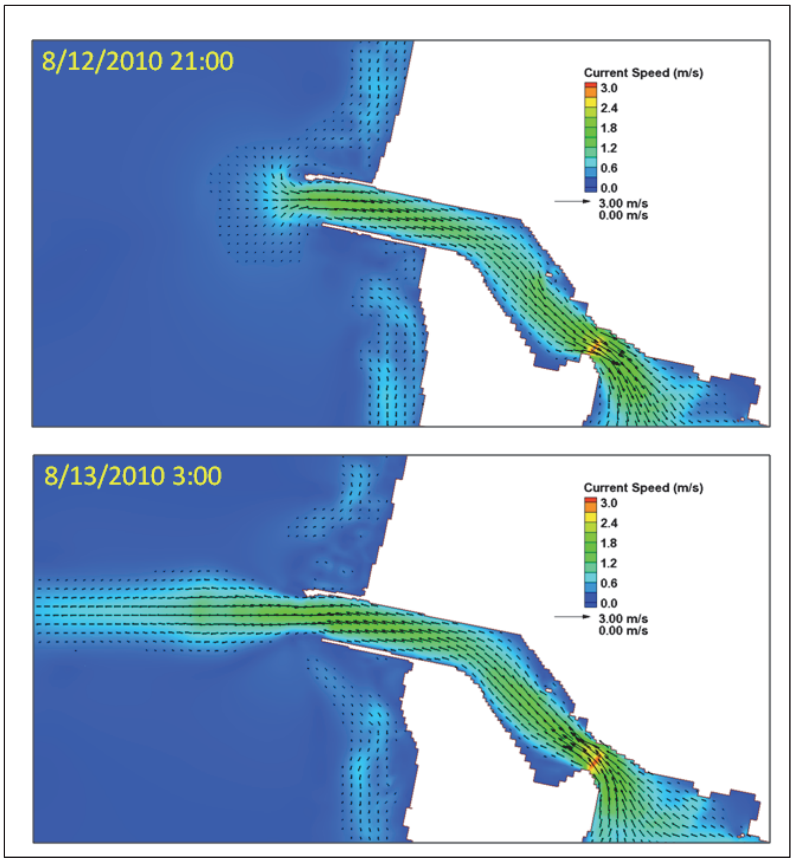

Figure 5-9. Calculated current field on 27 December 2010 at 12:00 GMT (flood current) and 18:00 GMT (ebb current).

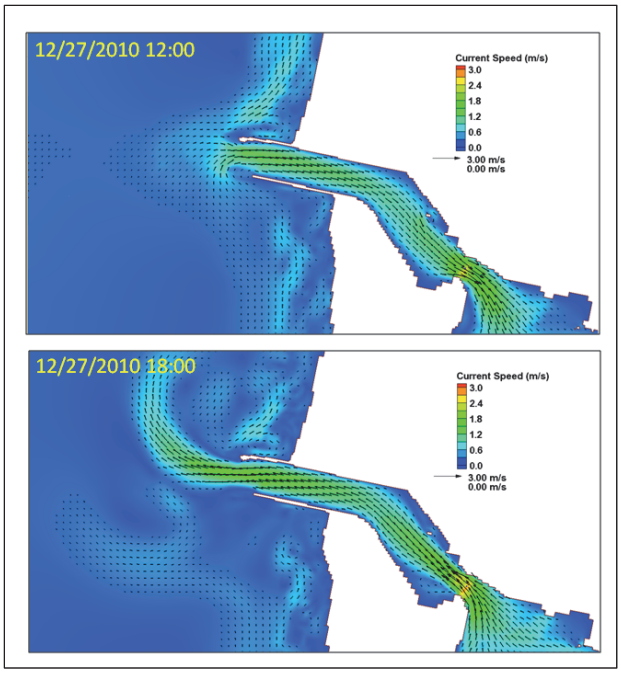

5.2.2 Summer and Winter Monthly Simulations

Calculated monthly mean and maximum wave steepness, wave dissipation, and Ursell number for August and December 2005 are shown in Figures 5-10 and 5-11, respectively. Monthly mean and maximum wave steepness, wave dissipation, and Ursell number for August and December 2010 are shown in Figures 5-12 and 5-13, respectively. The values of these parameters are small in summer but larger in winter as a result of higher waves in winter. For the summer month (August), calculated mean and maximum wave steepness, dissipation and Ursell number results show that stronger wave breaking and wave nonlinearity occur over the ebb shoal in August 2005 than August 2010. Calculated maximum dissipation and Ursell numbers are relatively small in the south entrance channel. For the winter month (December), calculated mean wave steepness, dissipation, and Ursell number results show stronger wave breaking and wave nonlinearity occur over the ebb shoal in December 2005 than December 2010. The values of maximum wave steepness in December 2010 are higher than December 2005 while the maximum dissipation and Ursell number are greater in December 2005 than December 2010. The storm waves in December 2010 have shorter mean wave periods that produce waves with larger wave steepness.

Figure 5-10. Calculated monthly mean wave steepness (top), wave dissipation (middle), and Ursell number (bottom) for August and December 2005.

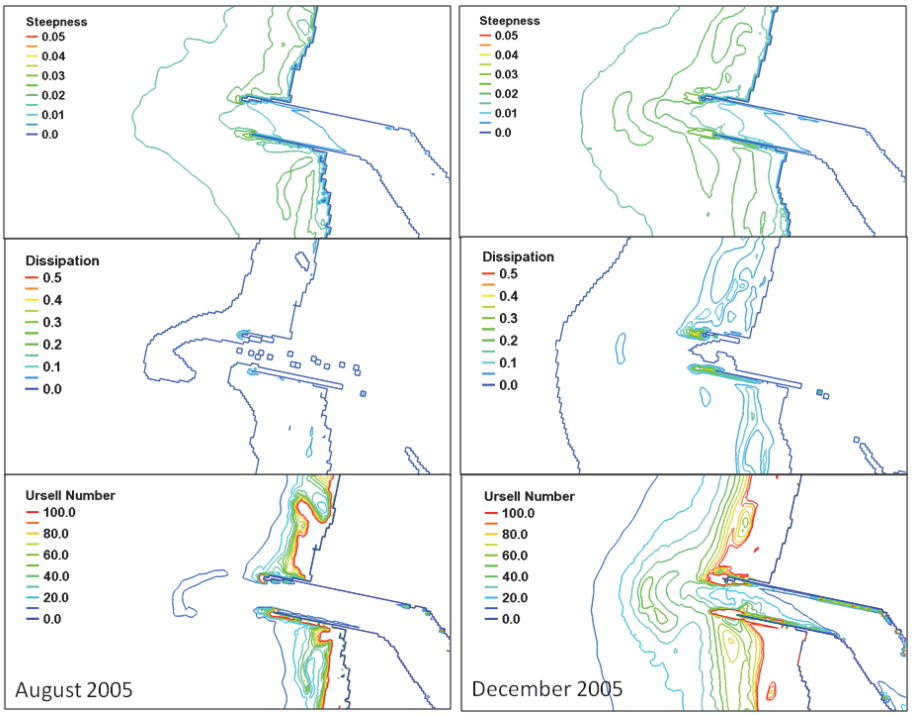

Figure 5-11. Calculated maximum wave steepness (top), wave dissipation (middle), and Ursell number (bottom) for August and December 2005.

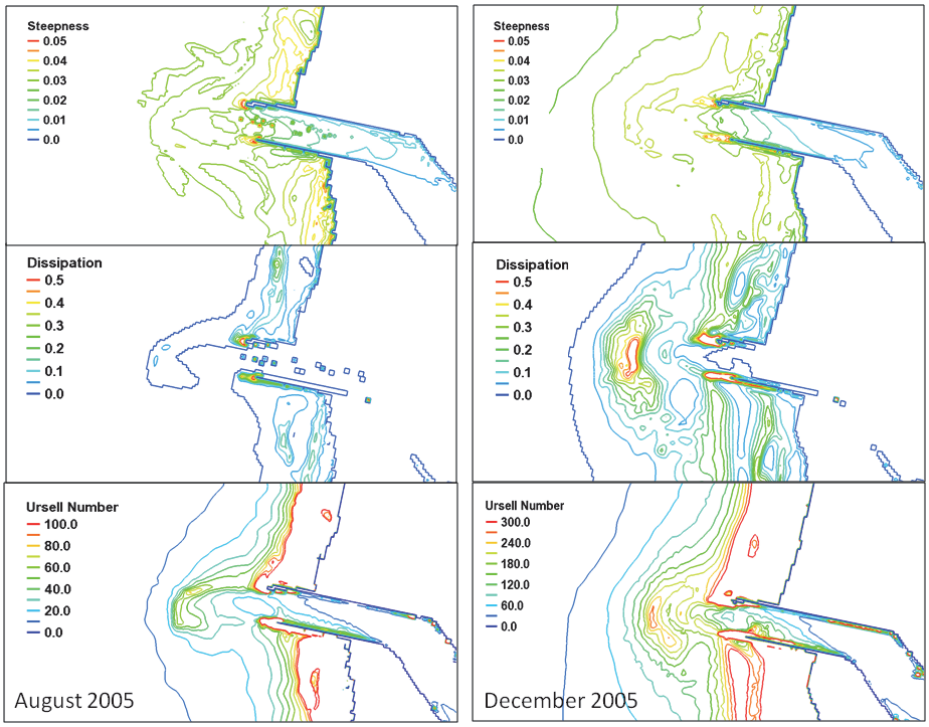

Figure 5-12. Calculated monthly mean wave steepness (top), wave dissipation (middle), and Ursell number (bottom) for August and December 2010.

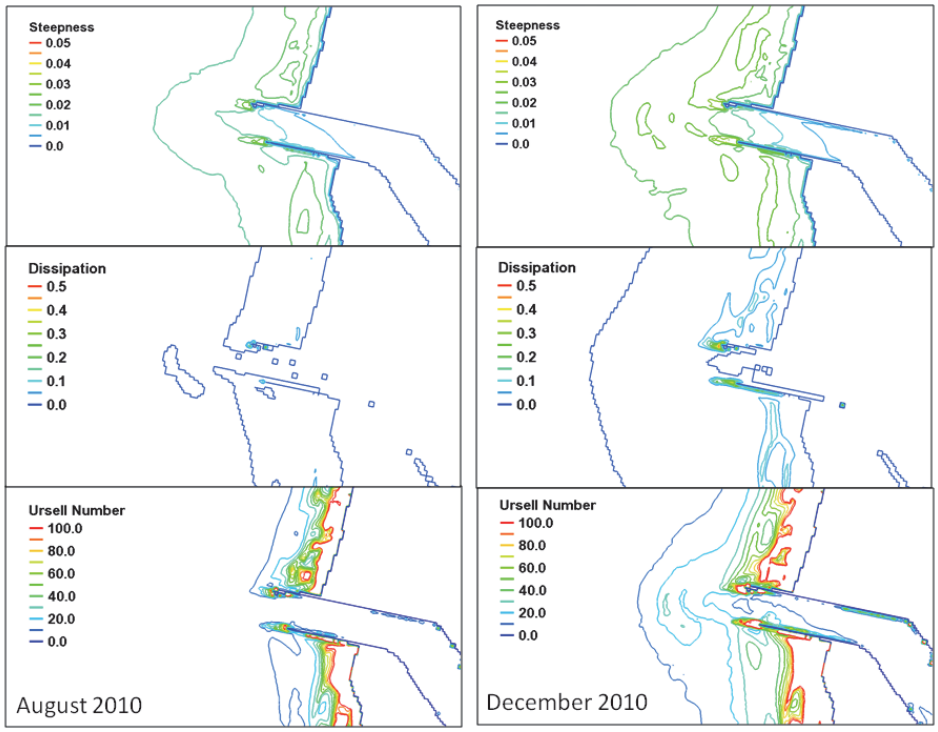

Figure 5-13. Calculated maximum wave steepness (top), wave dissipation (middle), and Ursell number (bottom) for August and December 2010.

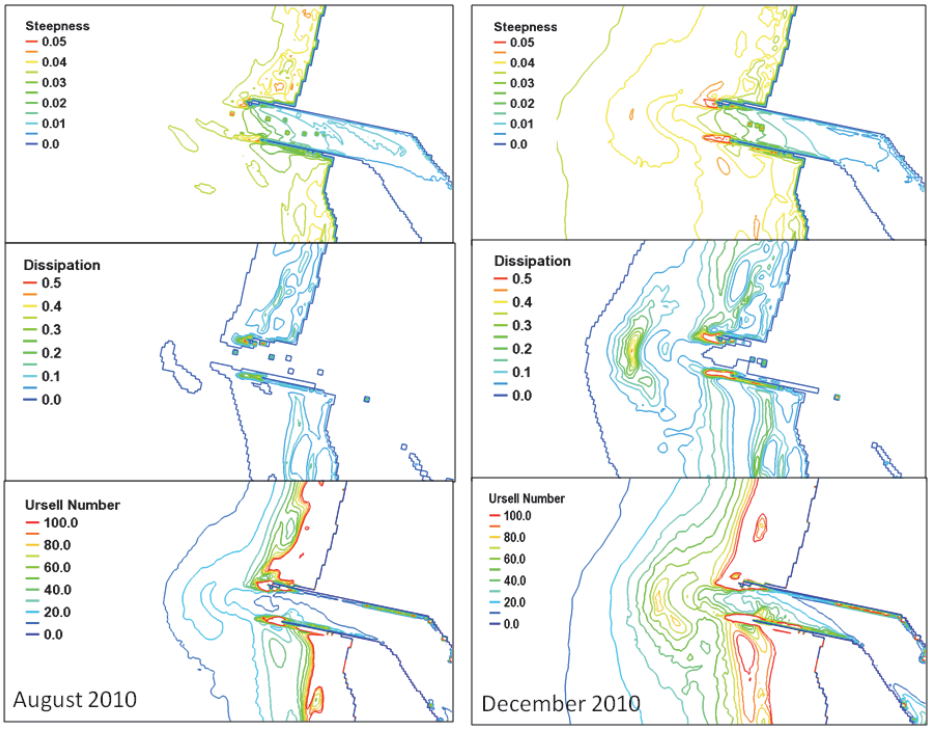

5.2.3 Simulations of Peak Flood and Ebb Conditions

Four scenarios of peak ebb and flood currents with large river inflows are used to investigate the effects of currents on waves. In these scenarios, the largest incident waves were around 2 m in August 2005 and 2010, and 3.4 m and 3.6 m in December 2005 and 2010, respectively. These waves came from northwest for the summer scenarios and southwest for the winter.

Figure 5-14 shows snapshots of calculated wave steepness, wave dissipation, and Ursell number fields for a peak flood current on 12 August 2010 at 21:00 GMT and for peak ebb current on 13 August 2010 at 03:00 GMT. These incident waves are 2 m (9 sec) from northwest (311 deg azimuth) and 2.1 m (9 sec) from west-northwest (294 deg azimuth), respectively. The calculated current magnitudes at the Inlet Entrance Station (Figure 5-1) are around 1.5 m/sec (see Figure 5-8). Calculated wave steepness and dissipation are higher for the peak ebb than the peak flood in the south entrance channel and ebb shoal. Calculated Ursell number fields are similar in both peak flood and ebb scenarios.

Figure 5-14. Calculated wave steepness (top), wave dissipation (middle) and Ursell number (bottom) during a flood current on 12 August 2010 at 21:00 GMT and an ebb current on 13 August 2010 at 03:00 GMT.

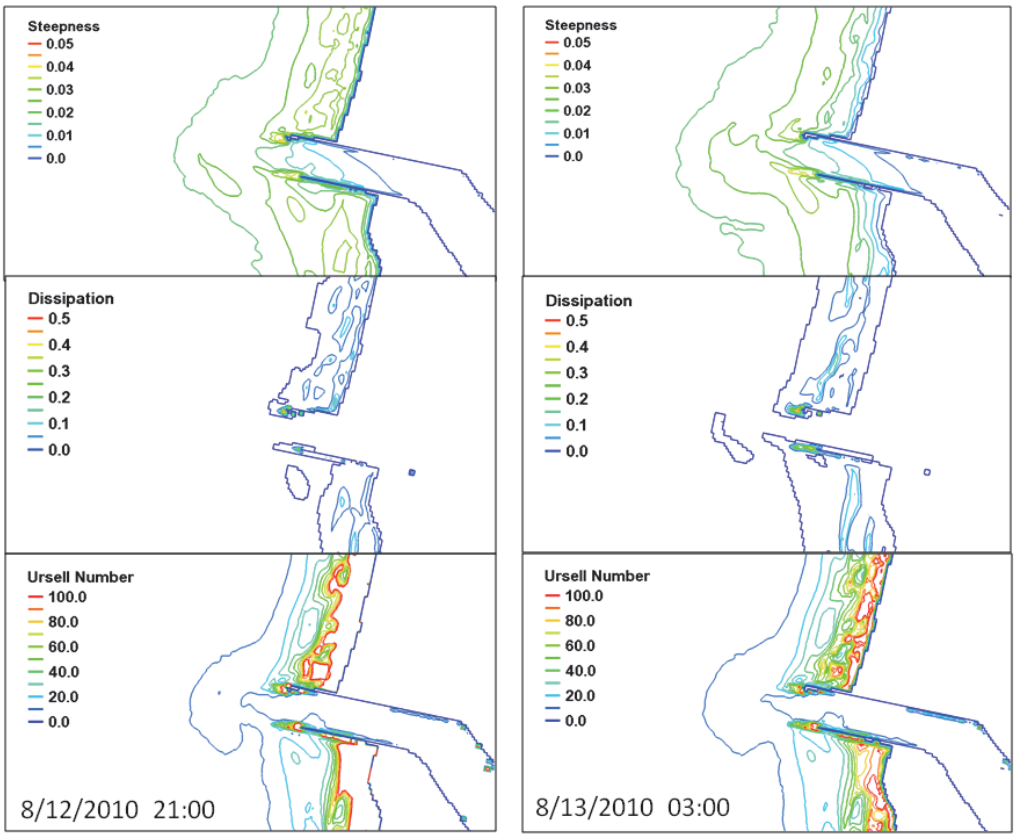

Figure 5-15 shows snapshots of calculated wave steepness, wave dissipation, and Ursell number fields for peak flood and ebb currents on 27 December 2010 at 12:00 GMT and 18:00 GMT, respectively. The incident waves at these times were 3.4 m (11 sec) from west-southwest (259 deg azimuth) and 3.6 m (11 sec) from west-southwest (264 deg azimuth). Calculated current magnitudes at the inlet entrance were around 1.4 m/sec (see Figure 5-9). With ebb current, larger wave steepness, dissipation, and Ursell number occur over the ebb shoal and south entrance channel.

Figure 5-15. Calculated wave steepness (top), wave dissipation (middle), and Ursell number (bottom) during a flood current on 27 December 2010 at 12:00 GMT and an ebb current on 27 December 2010 at 18:00 GMT.

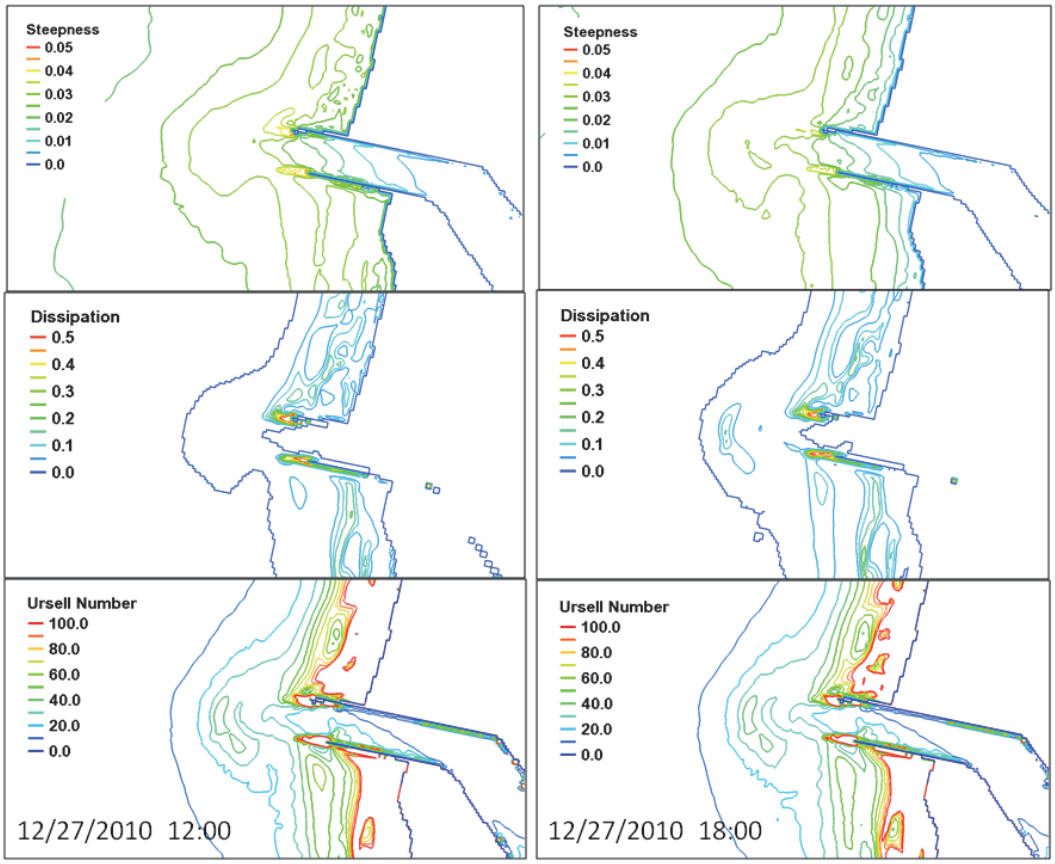

Figure 5-16 shows results for one more scenario for a peak ebb current on 24 December 2010 at 03:00 GMT. The incident waves were 3.2 m and 10 sec from southwest (234 deg azimuth). The calculated ebb current magnitude at the inlet entrance was 1.7 m/sec. Compared to Figure 5-15, this scenario, with a smaller wave height and a larger current, produced smaller values of wave steepness, dissipation, and Ursell number. These results show that waves may have a stronger role than the current at the inlet entrance and ebb shoal.

Figure 5-16. Calculated wave steepness (top), wave dissipation (middle), and Ursell number (bottom) during an ebb current in 24 December 2010 at 03:00 GMT.

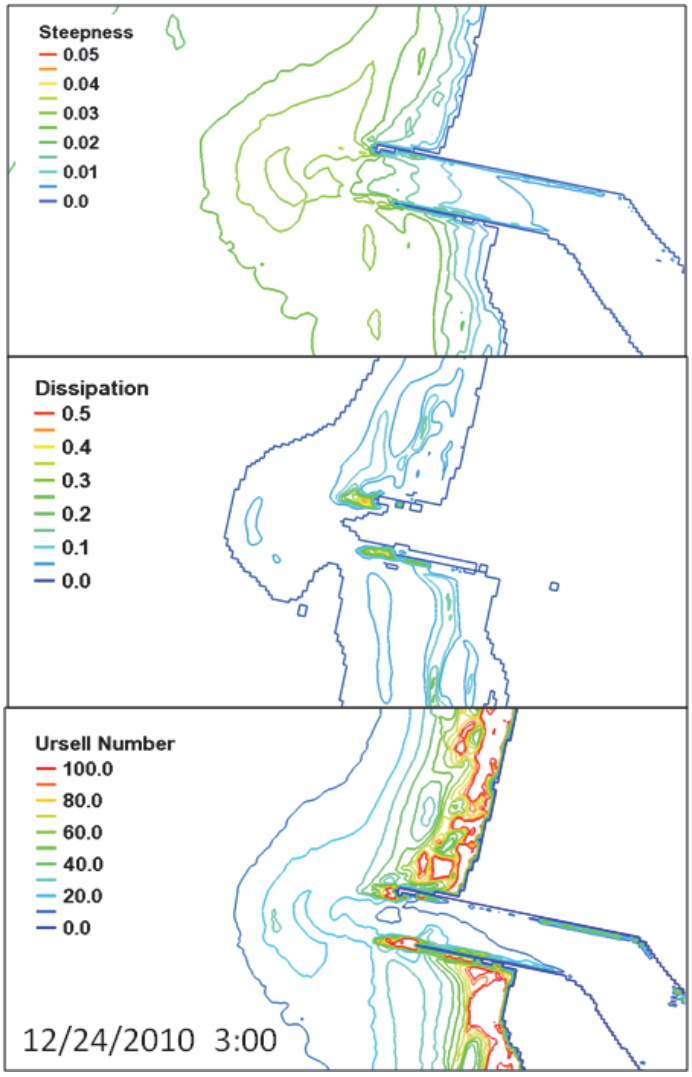

5.3 Simulations for a hypothetically shortened South Jetty

5.3.1 Currents

For the hypothetically shortened South Jetty, simulations were conducted only for August and December 2010 (symmetric ebb shoal). Figure 5-17 shows calculated current fields on 12 August at 21:00 GMT and 13 August at 03:00 GMT. Figure 5-18 shows the current fields on 27 December 2010 at 12:00 and 18:00 GMT. The peak flood and ebb current magnitudes at the Kenchloe Point (Figure 5-1) remained unchanged between existing and hypothetically shortened South Jetty simulations. With or without the South Jetty shortening, the currents at the entrance remained essentially unchanged during the ebb. The peak flood currents over the immersed

section of the hypothetically shortened South Jetty were reduced approximately by 0.2 m/sec (15 percent reduction) at the entrance. Results indicated that with the South Jetty shortening, the entrance becomes wider and this affects the flood current magnitude but not the ebb current magnitude.

Figure 5-17. Calculated current fields for the hypothetically shortened South Jetty on 12 August 2010 at 21:00 GMT (flood current) and 13 August 2010 at 03:00 GMT (ebb current).

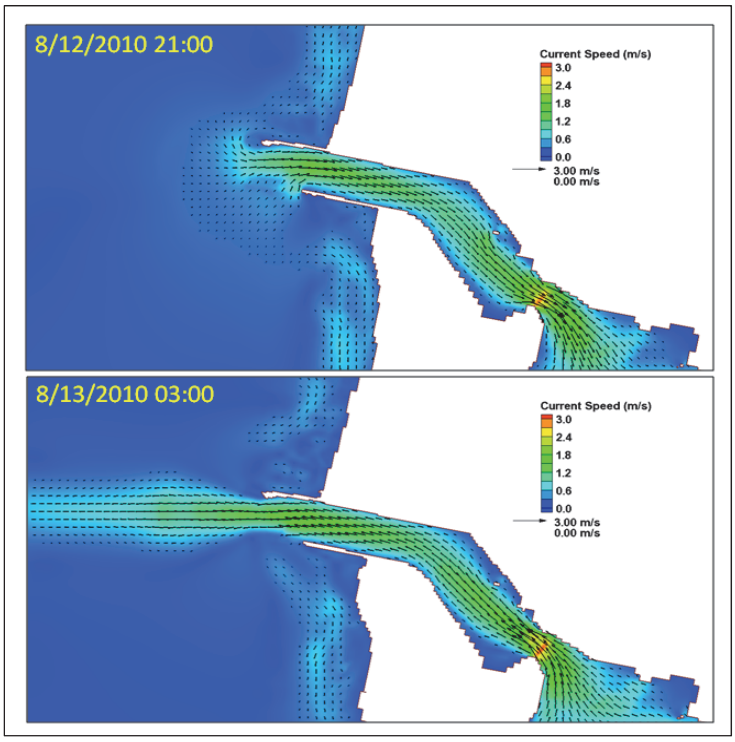

5.3.2 Summer and Winter monthly simulations for hypothetically shortened South Jetty

Monthly mean and maximum wave steepness, wave dissipation, and Ursell number have similar patterns before and after the South Jetty shortening (Figures 5-12, 5-13, 5-19, and 5-20). Both for summer and winter months, minor changes in wave breaking patterns occurred over the submerged section of the recessed South Jetty. Wave steepness, dissipation, and Ursell number increased and further extended into the main channel toward the Bay. This is much more noticeable for winter conditions. As noted earlier for constant incident wave simulations, the peak values of wave steepness, dissipation, and Ursell number for the hypothetically shortened South Jetty occurred approximately at the same locations of the existing (full length) South Jetty configuration.

Figure 5-18. Calculated current fields for the hypothetically shortened South Jetty on 27 December 2010 at 12:00 GMT (flood current) and 18:00 GMT (ebb current).

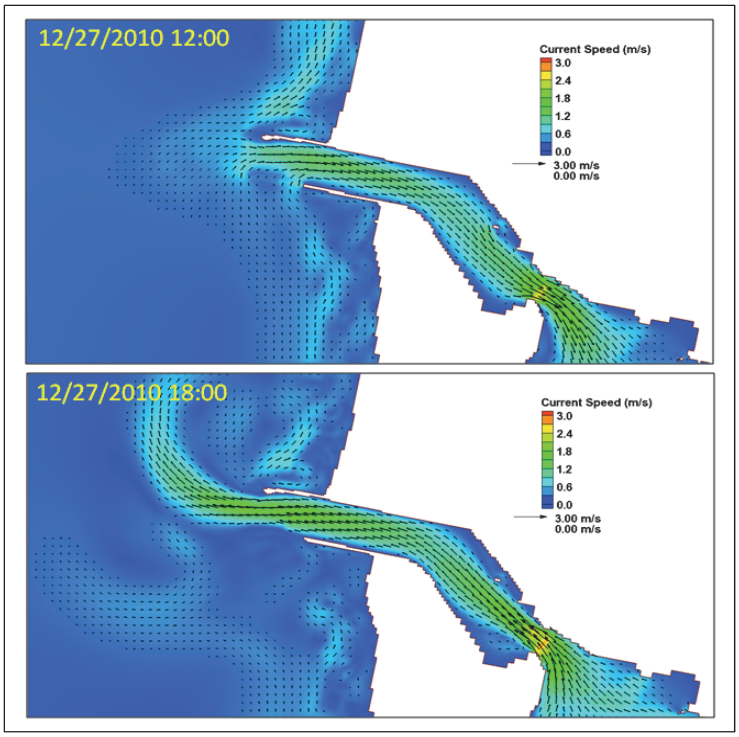

Figure 5-19. Monthly mean wave steepness (top), wave dissipation (middle), and Ursell number (bottom) fields for the hypothetically shortened South Jetty in August and December 2010.

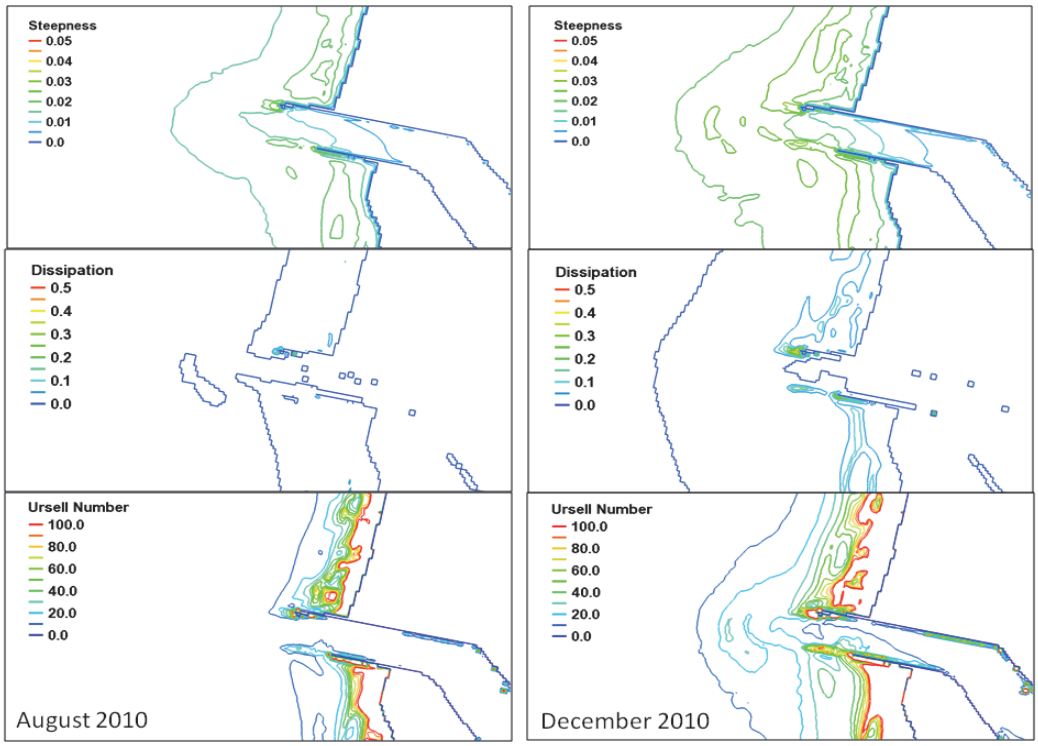

Figure 5-20. Maximum wave steepness (top), wave dissipation (middle), and Ursell number (bottom) fields for the hypothetically shortened South Jetty in August and December 2010.

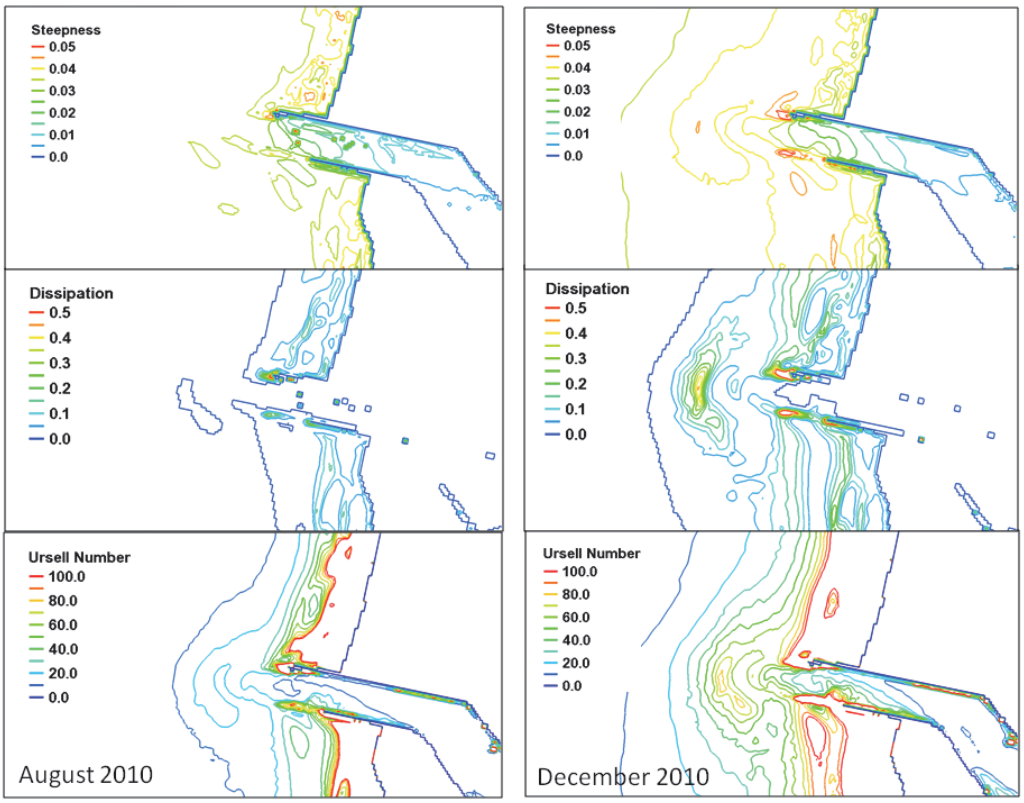

5.3.3 Peak flood and ebb simulations for hypothetically shortened South Jetty

Figure 5-21 shows snapshots of wave steepness, wave dissipation, and Ursell number for the hypothetically shortened South Jetty during a flood current on 12 August 2010 at 21:00 GMT and an ebb current on 13 August 2010 at 03:00 GMT. Figure 5-22 has snapshots of wave steepness, wave dissipation, and Ursell number for the hypothetically shortened South Jetty during peak flood and ebb currents on 27 December 2010 at 12:00 GMT and on 27 December 2010 at 18:00 GMT, respectively. Comparing these to the cases of the existing jetty configuration (Figures 5-14 and 5-15) we find that currents, wave heights, wave steepness, wave dissipation, and Ursell number have increased only over the submerged section of the hypothetically shortened South Jetty. The snapshots in Figure 5-22 correspond to an incident winter wave of 3.6 m from southwest, showing that waves propagate over the submerged South Jetty section to reach the navigation channel and penetrate further into the Bay.

Figure 5-21. Wave steepness (top), wave dissipation (middle), and Ursell number (bottom) for the hypothetically shortened South Jetty: a) flood current in 12 August 2010 at 21:00 GMT and b) ebb current in 13 August 2010 at 03:00 GMT.

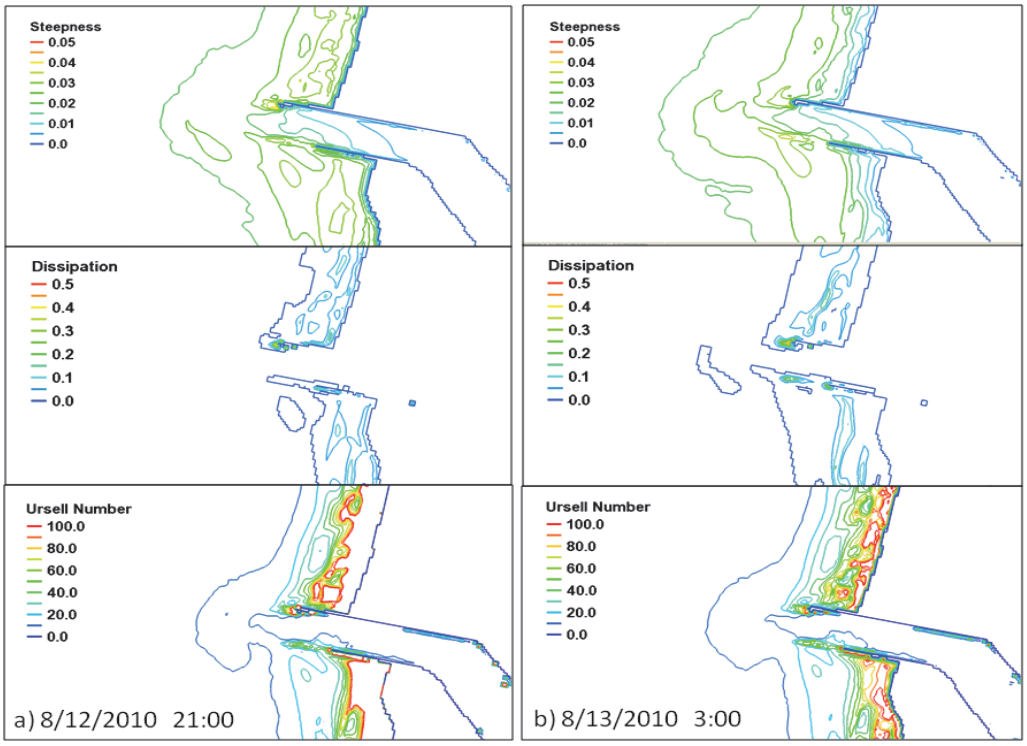

Figure 5-22. Wave steepness (top), wave dissipation (middle), and Ursell number (bottom) for the hypothetically shortened South Jetty: a) flood current on 27 December 2010 at 12:00 GMT and b) ebb current on 27 December 2010 at 18:00 GMT.

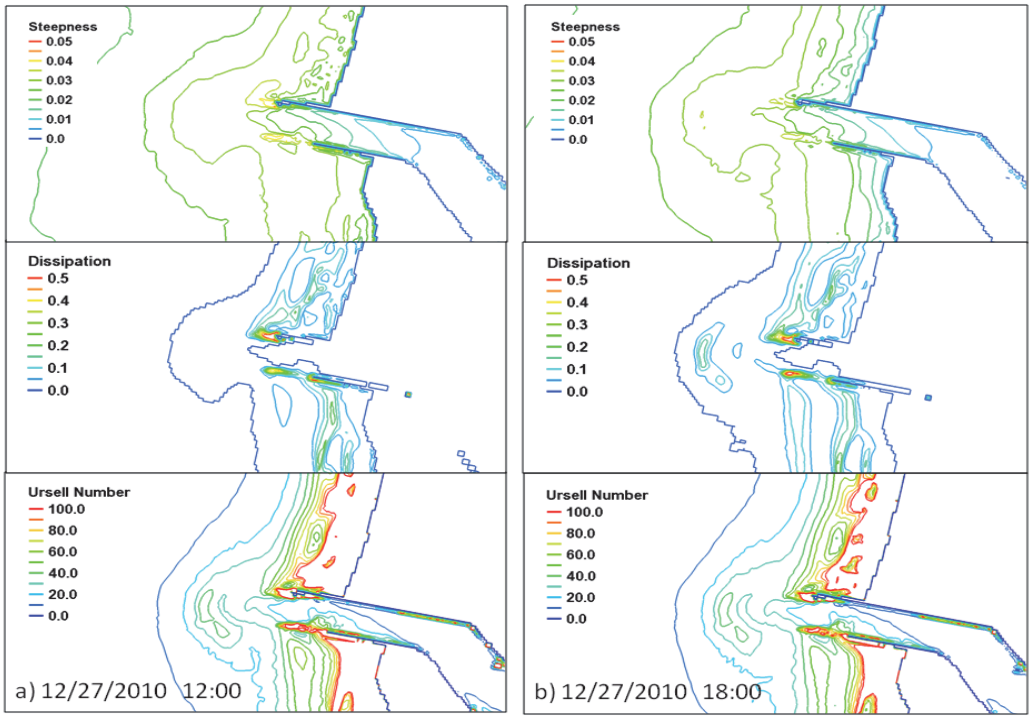

Based on results shown in Figures 5-19 through 5-22, the effect of South Jetty shortening was localized to the immediate vicinity of the jetty. It had little or no visible effect on waves or currents outside the entrance and over the ebb shoal. For the 3-m and 5-m waves with a recessed South Jetty, there was a slight increase in wave steepness and dissipation, and waves extended a little further into the main channel. With both jetty lengths, because the full South Jetty base was modified slightly, the peak values of wave steepness and dissipation occurred at the same locations.

5.4 Discussion and Summary of Results

Winds, waves, tides and river discharges were included in the combined wave and flow simulations described in this chapter. The simulations were performed with three telescoping grids corresponding to the 2005 asymmetric ebb shoal, the 2010 symmetric ebb shoal, and the 2010 hypothetically shortened South Jetty. Three wave-related parameters (wave steepness, wave dissipation, and Ursell number) were calculated and compared to the wave-only simulations presented in Chapter 4. The following observations are made.

The Tillamook Inlet system is affected by combined waves, tides, currents, and river discharges. Incident waves dominate the inlet and wave heights could reach 6 to 8 m during winter storms, and 3 m/sec peak current occur in the main channel. The current direction outside the inlet over the ebb shoal and along north and south beaches is controlled mainly by local winds, wave actions, and local bathymetry. The total freshwater discharges from five rivers into Tillamook Bay can be as high as 28,000 cfs (800 m^3/sec) in the winter, and these affect the ebb current.

Modeling results showed the winter storms produced larger wave steepness and wave dissipation at the inlet complex. Wave steepness and dissipation were closely associated with the bathymetry of ebb shoal, and wave dissipation patterns in the winter followed the ebb shoal shape. The calculated wave steepness and wave dissipation with the 2005 bathymetry indicated that a south passage out of the inlet would be safer than a course straight out passing over the bar or a course turning to the NW direction.

Examination of the patterns produced by combined waves and flow showed that larger waves caused high wave steepness and increasing wave dissipation. The flood currents weakened wave dissipation, while ebb

currents increased wave dissipation over the ebb shoal and across the USCG recommended south passage in/out of the inlet.

The model results show that hypothetically shortened South Jetty reduced the flood current magnitude approximately by 0.2 m/sec (15 percent) at the entrance, but did not change the ebb current magnitude. The effect of South Jetty degradation was localized in the immediate vicinity of the South Jetty. Because morphologic change that could occur over years to decades following degradation of the jetty was not considered, it is likely that the navigation channel would migrate towards the South Jetty, and therefore increasing currents over the degraded portion and potentially increasing the risks to navigation in the entrance area. Jetty degradation would also permit more wave energy to penetrate through the main channel into the Bay.

6 Conclusions

In this study, a preliminary investigation of morphology change and numerical modeling estimates of waves and currents was conducted at the Tillamook Inlet, Oregon. The intent of this limited scope study was to determine possible relationships between the two ebb shoal geometries and their effects on changes to waves and currents in the entrance channel at Tillamook. An ebb shoal initially with an asymmetric orientation relative to the entrance in 2005 and a symmetric ebb shoal in 2010 were used in this study. A limited analysis of these two ebb shoal geometries was performed for one summer and one winter month in each year. Because the numerical modeling analysis was limited to one summer month (August) and one winter month (December), the sole purpose of this study was to better understand how the geometry (shape, footprint, and elevation) of the ebb shoal affects the local wave and current conditions during the two selected months. Numerical modeling results indicated that both the geometry of ebb shoal, as well as the entrance jetties influenced the waves and currents at the inlet area (through the entrance channel and over the shoal). The dual jetties, forming the narrow inlet entrance, plays a critical role by controlling the spatial variation of waves and currents at the entrance and over the ebb shoal.

Based on this limited scope study, while it appears that wave and current conditions at Tillamook Inlet may be improved by changing the geometry of the ebb shoal or jetties or both, the study's results are inadequate to inform future decisions about navigation issues at Tillamook Inlet. A much more comprehensive study is necessary to verify not only the conclusions listed below but also the validity of such short-term (one month) hydrodynamics to infer future responses of this complex inlet system. There are a wide range of meteorological and oceanographic conditions that exist in this part of the Pacific Northwest Coast which have not been considered in this study. It is necessary to perform a much longer and more extensive historical morphology change study at this site to ascertain the utility and validity of the two ebb shoal geometries that have been used in the present study. The ebb shoal geometry was determined based on limited measurements, of which need to be verified with other surveys and data sources. Consequently, the follow up study should be much broader in scope to systematically consider the factors that are expected to modify the short-

and long-term evolution of the ebb shoal, as well as the estimates of the local waves and currents at the Tillamook Inlet complex.

The results described within this report address several complimentary objectives. The first objective of the analysis was to investigate characteristics of short- and long-term morphology changes at Tillamook Inlet using historical bathymetric surveys. The second objective of the study was to quantify the effects of these observed morphologies on representative waves alone and combined waves and currents at the entrance. The third objective was to develop estimates of waves and currents for representative summer and winter months, August and December. These month-long time series of waves were obtained by transforming offshore waves at the 80-m isobath over representative ebb shoal bathymetries. Waves alone and combined waves and currents were calculated for the representative ebb shoal morphologies, as well as a case in which the South Jetty was hypothetically shortened. Details of modeling were described in Chapters 4 and 5, and Conclusions of the study were provided in Chapter 6. The main observations and conclusions derived from this limited scope study are summarized next. However, it is emphasized that these preliminary results should not be extrapolated to beyond the scope of this limited study, and no future decisions should be based on these results until further verified and approved by the Distirct.

6.1 Morphology Change Analysis

The recent changes in the characteristics of the morphology of the ebb shoal at Tillamook Inlet were examined with the goal of understanding the typical bathymetric conditions of the entrance channel from seasonal to decadal time scales. Because seasonal surveys were not available, detailed morphologic change could not be analyzed on a seasonal time scale. The yearly surveys were available for the last three decades, but data were not available for all years and some data were incomplete, had sparse coverage, or did not cover areas of interest. Only ten years of good surveys data could be used in the analysis to understand recent historical trends of Tillamook Inlet and vicinity including the ebb shoal seaward of the jettied entrance. The general characteristics of the ebb shoal were evaluated, including volume, dimensions, and distance offshore from the South Jetty, for the selected surveys decades. The ebb shoal was found to be growing slowly at a rate of 485 KCY/yr, and maintaining its overall dimensions. Overall, the morphology of the ebb shoal does not vary significantly, though there was a clear indication of two characteristic morphologies: a symmetric ebb shoal

with open flood marginal channels to the north and south, and, an asymmetric ebb shoal with a large bar extending off the North Jetty to the end of the ebb shoal.

These two morphologies of the ebb shoal appear to change or alternate every 2 years. This change is caused by tides, river flows, and waves that modify the bathymetry at Tillamook Inlet. The wave climate and tides play a more dominant role in the morphologic change observed in the survey data. Time periods of higher average waves were correlated to the symmetric ebb shoal, and less energetic waves were associated with an asymmetric ebb shoal. The extra-tropical storms that generate high waves from the north and northwest directions produce an asymmetric ebb shoal. Large waves from the south and southwest directions that occur seasonally in some years alter the shape of the ebb shoal. Due to limited historical survey data availability, morphologic analysis could not explain the cause-effect of the ebb shoal changes taking place at Tillamook Inlet, and consequently numerical modeling was necessary to evaluate the navigation conditions experienced at the entrance channel to Tillamook Inlet for any given year. The 2005 asymmetric and the 2010 symmetric bathymetries were chosen to represent the range of bathymetric conditions that occur at the entrance channel for the numerical modeling study.

An alternative case of a hypothetically shortened South Jetty was evaluated in numerical modeling using the 2010 symmetric bathymetry. This case was based on monitoring of the South Jetty head degradation and landward recession will continue and may one day reach a position that poses significant navigation risks to the channel. Although the jetty recession was carefully replicated over a recent bathymetry, additional effects of long-term (decadal) morphologic change could not be added within this limited study scope. The modeling results of wave dissipation and steepness showed only local changes, including slight increase in wave heights between the jetty heads, but the results were not sufficient to determine realistic waves (and, therefore, risk) across the area due to the fixed morphology. From a morphologic perspective, the future case of South Jetty head recession would most likely result in increased currents over the submerged jetty portions, potentially driving the morphology toward a more south-oriented exit channel at the entrance to Tillamook. The potentially increased flooding (and possibly ebbing) currents at the tip of the submerged South Jetty may create conditions that could further undermine the jetty over time. This case may be exacerbated in an

asymmetric bathymetry similar to the 2005 condition, where more current could be channelized southward.

6.2 Numerical Modeling

Numerical modeling was performed for (1) wave-only and (2) combined wave and flow. The purpose of wave-only simulations described in Chapter 4 was to investigate waves as the primary forcing condition and their influence on navigation at Tillamook Inlet. As noted in Chapter 4, wave-only simulations were forced with incident waves and wind, which excluded water levels, tides, currents, and river discharges. Simulations were conducted for selected seasonal mean wave conditions (constant incident wave conditions) as well as for a typical summer month (August) and a winter month (December) in 2005 and 2010.

Three model grids were used in these simulations: an asymmetric ebb shoal grid (based on September 2005 survey), a symmetric ebb shoal grid (based on June 2010 survey), and a hypothetically shortened South Jetty grid (based on symmetric ebb shoal grid). Modeling results in Chapter 4 were presented using four wave-related parameters in the coastal engineering practice: wave steepness, dissipation, surf-zone similarity parameter, and Ursell number. Definition of each parameter and reasons for selecting them were discussed in Chapter 4. The surf-zone similarity parameter was not pursued further as discussed in Chapter 4. General observations based on the wave-only simulations are as follows:

1. Use of the wave steepness, dissipation, and Ursell number were recommended for safe navigation. For incident wave heights greater than 3 m, larger wave steepness was predicted in sections of navigation channel, inlet entrance, over the ebb shoal, and immediately seaward of the jetty tips.
2. Wave dissipation was negligible outside the breaker zone, and increased for larger incident waves over the ebb shoal due to shoaling and breaking. For incident wave heights greater than 3 m, wave dissipation increases in some areas of navigation channel, inlet entrance, and over the ebb shoal.
3. The wave breaking intensity is stronger at the inlet entrance and ebb shoal region for the asymmetric ebb shoal (September 2005 bathymetry) than with the symmetrical ebb shoal (June 2010 bathymetry).
4. Maximum and mean wave steepness fields were greater for the asymmetric ebb shoal as compared to the symmetric ebb shoal. Larger

steepness values obtained for asymmetric ebb shoal in December 2005 can also caused by higher incident waves occurring during that month.

5. In general, the patterns of mean wave dissipation for the asymmetric and symmetric ebb shoals were similar in summer months (August 2005 and 2010). The maximum wave dissipation intensity was greater at the inlet entrance and over the ebb shoal for the asymmetric ebb shoal.
6. Stronger wave breaking and dissipation, larger Ursell numbers occur at the inlet entrance and over the ebb shoal in December 2005 than December 2010. These are caused by combination of the asymmetric ebb shoal and larger incident waves in December 2005.
7. For the hypothetically shortened South Jetty, the effect of shortening was localized to the vicinity of the South Jetty, without visible effects on waves in the entrance and over the ebb shoal. The hypothetically shortened South Jetty did not modify waves significant in the entrance channel and over the ebb shoal to affect navigation.

In summary, the wave-only simulations showed that wave breaking intensity at the inlet entrance and over the ebb shoal was stronger for the asymmetric ebb shoal. Large values of wave steepness, wave dissipation, and Ursell numbers were associated with larger incident waves. Overall, calculated wave-related parameters were higher in areas away from the navigation channel which were not navigable along north and south beach faces and on the submerged tips of both jetties.

There are pockets of isolated areas with greater wave-related parameters for wave conditions evaluated in this study. These pockets were mostly located along the federal channel and within 100 m (300 ft) of the channel centerline on the ebb shoal. There were fewer isolated pockets south of the inlet entrance. This suggests that a south entrance channel would be a safer under these conditions.

For the combined wave and flow simulations in Chapter 5, the effects of winds, waves, tides, and river discharges were included as forcing to models. The flow simulations were performed using three telescoping grids for the 2005 asymmetric ebb shoal bathymetry, the 2010 symmetric ebb shoal bathymetry, and the 2010 hypothetically shortened South Jetty. Three wave-related parameters were calculated: wave steepness, wave dissipation, and Ursell number. The general observations are given as follows:

1. The hydrodynamics of Tillamook Inlet system is affected by the combination of winds, waves, tides, and river discharges. Modeling results indicated river discharges had weak effects on water levels and currents.
2. Monthly mean and maximum wave steepness, wave dissipation, and Ursell number were small in summer (August) but larger in winter (December) due to higher waves occurring in winter. For the summer month, results showed stronger wave breaking and wave nonlinearity over the ebb shoal in August 2005 than August 2010. Maximum dissipation and Ursell numbers were relatively small in the south entrance channel.
3. For the winter month, model results showed a stronger wave breaking and wave nonlinearity over the ebb shoal in December 2005 than December 2010. The values of maximum wave steepness in December 2010 are higher than December 2005. The storm waves in December 2010 have shorter mean wave periods that produce waves with larger wave steepness.
4. Simulations for the peak flood and ebb currents showed wave breaking was affected both by waves and tidal currents, with waves dominate the coastal processes at Tillamook Inlet. The ebb current increased the wave dissipation over the ebb shoal and in the south entrance channel; while the flood current decreased it.
5. With ebb current, larger wave steepness, dissipation, and Ursell number occur over the ebb shoal and in the south entrance channel. Simulations with smaller wave height and larger tidal current produced smaller values of wave steepness, dissipation, and Ursell number. These suggest waves may have a stronger role than the current at the inlet entrance and ebb shoal.
6. The South Jetty shortening reduced the peak flood current locally in the entrance. It did not change the ebb current magnitude. The effect of hypothetically shortened South Jetty was localized to the vicinity of the South Jetty. It has no effect on wave breaking outside the entrance and over the ebb shoal.
7. The peak flood currents over the immersed section of the hypothetically shortened South Jetty were reduced by about 15 percent at the entrance because the entrance becomes wider and this affects the flood current magnitude, but not the ebb current magnitude.

The conclusions provided above have been based on a limited number of wave and wave-flow modeling simulations. To develop definitive recommendations to improve the navigation at Tillamook Inlet, a more thorough, systematic study with an in-depth numerical modeling effort would be required. This involves more extensive analyses of wave and flow

conditions, sensitivity analyses of wave-related parameters, and long-term simulations. In addition to waves and circulation modeling, comprehensive sediment transport and morphology modeling would help to better understand the dynamics of Tillamook Inlet. Lastly, field data are needed for verification and validation of numerical model results for confidence in calculated estimates. The present study results must be viewed as preliminary and unverified estimates.

References

Bouws, E., H. Gunther, W. Rosenthal, and C. L. Vincent. 1985. Similarity of the wind wave spectrum in finite depth water: 1. Spectral form. *Journal of Geophysical Research*, 90 C1: 975-86.

Carr-Betts, E., T. M. Beck, and N. C. Kraus. (2012). "Tidal Inlet Morphology Classification and Empirical Determination of Seaward and Down-Drift Extents of Tidal Inlets," *Journal of Coastal Research*, Coastal Education and Research Foundation, Inc., 28(3)m 547-556.

Demirbilek, Z., and Vincent, C. L. 2010. Water Wave Mechanics. Chapter 1 in EM 1110-2-1100 Part 2, Coastal Engineering Manual, US Army Corps of Engineers, 121pp. Vicksburg, MS: US Army Research and Development Center.

Demirbilek, Z., and J. Rosati. 2011. Verification and validation of the Coastal Modeling System, Report 1: Summary Report, ERDC/CHL Technical Report 11-10.Vicksburg, MS: US Army Corps of Engineers Research and Development Center.

Komar, 1997. “Sediment Accumulation in Tillamook Bay, Oregon, A Large Drowned-River Estuary.” Report for the Tillamook Bay National Estuary Project, Oregon.

Lin, L., Z. Demirbilek, R. Thomas, and J. Rosati. 2011a. Verification and validation of the Coastal Modeling System, Report 2: CMS-Wave, ERDC/CHL Technical Report 11-10. Vicksburg, MS: US Army Corps of Engineers Research and Development Center.

Lin, L., Z. Demirbilek, and H. Mase. 2011b. Recent capabilities of CMS-Wave: A coastal wave model for inlets and navigation projects. Proceedings, Symposium to honor Dr. Nicholas Kraus. Journal of Coastal Research, Special Issue 59,7-14.

Lin, L., Z. Demirbilek, and F. Yamada. 2008. CMS-Wave: A nearshore spectral wave processes model for coastal inlets and navigation projects. Coastal and Hydraulics Laboratory Technical Report ERDC/CHL TR-08-13. Vicksburg, MS: US Army Engineer Research and Development Center.

Longuet-Higgins, M. S., and R. W. Stewart. 1963. The changes in amplitude of short gravity waves on steady non-uniform currents. *Journal of Fluid Mechanics* 10(4):529-549.

Miche, M. 1951. Le pouvoir reflechissant des ouvrages maritimes exposes a 1’action de la houle. Annals des *Ponts et Chau.ssess*. 121e Annee: 285-319 (translated by Lincoln and Chevron, University of California, Berkeley, Wave Research Laboratory, Series 3, Issue 363, June 1954).

National Oceanographic and Atmospheric Administration (NOAA). 2012a. *NOS Hydrographic Survey Data*, National Geophysical Data Center. Office of Coast Survey, National Oceanic and Atmospheric Administration, http://www.ngdc.noaa.gov/mgg/bathymetry/hydro.html, accessed 3 August 2012.

National Oceanographic and Atmospheric Administration (NOAA). 2012b. Tides and currents. National Oceanographic and Atmospheric Administration, http://tidesandcurrents.noaa.gov/, accessed 3 August 2012.

National Data Buoy Center (NDBC). 2012. National Data Buoy Center, National Oceanographic and Atmospheric Administration, http://ndbc.noaa.gov/, accessed 3 August 2012.

Sakai, S., N. Kobayashi, and K. Koike. 1989. Wave breaking criterion with opposing current on sloping bottom: an extension of Goda's breaker index. *Annual Journal of Coastal Engineering* 36:56-59, JSCE (in Japanese).

Sanchez, A., W. Wu, T. M. Beck, H. Li, J. Rosati III, R. Thomas, J. D. Rosati, Z. Demirbilek, M. Brown, and C. Reed. 2011a. Verification and Validation of the Coastal Modeling System, Report 3: Hydrodynamics, ERDC/CHL Technical Report 11-10. Vicksburg, MS: US Army Corps of Engineers Research and Development Center.

Sanchez, A., W. Wu, T. M. Beck, H. Li, J. D. Rosati, Z. Demirbilek, and M. Brown. 2011b. Verification and Validation of the Coastal Modeling System, Report 4: Sediment Transport and Morphology Change, ERDC/CHL Technical Report 11-10. Vicksburg, MS: US Army Corps of Engineers Research and Development Center.

US Army Corps of Engineers (USACE). 2007. "Tillamook Bay and Bar." *Internal USACE document*. Portland , Oregon: US Army Corps of Engineers, Portland District.

US Army Corps of Engineers (USACE). 2011. EC 1165-2-212 (1 Oct 2011). Sea Level Change Considerations for Civil Works Programs. http://140.194.76.129/publications/eng-circulars/EC_1165-2-212.pdf.

US Army Corps of Engineers (USACE). 2013. EC 11-2-204 (31 Mar 2013). Army Programs: Corps of Engineers Civil Works Direct Program: Budget Development Guidance Fiscal Year 2015. http://140.194.76.129/publications/eng-circulars/EC_11-2-204/.

Walton, T. L., and W. D. Adams. 1976. Capacity of inlet outer bars to store sand. *Proceedings 15th Coastal Engineering Conference*, ASCE, 1,919-1,937.

Zundel, A. K.. 2006. *Surface-water modeling system reference manual - Version 9.2*. Provo, UT: Brigham Young University Environmental Modeling Research Laboratory.

Appendix A: Description of CMS

The Coastal Modeling System (CMS) was used for the numerical modeling estimates of waves and currents at Tillamook Inlet. Tasks 2 through 4 in Chapter 1 describe the purpose of numerical modeling tasks, while the implementation details of the wave and combined wave and flow modeling tasks are provided in Chapters 4 and 5. A brief description of the CMS is provided here for completeness.

As shown in Figure A-1, the CMS is an integrated suite of numerical models for waves, flows, and sediment transport and morphology change in coastal areas. This modeling system includes representation of relevant nearshore processes for practical applications of navigation channel performance, and sediment management at coastal inlets and adjacent beaches. The development and enhancement of CMS capabilities continues to evolve as a research and engineering tool for desk-top computers. CMS uses the Surface-water Modeling System (SMS) interface for grid generation and model setup, as well as plotting and post-processing. The Verification and Validation (V&V) Report 1 (Demirbilek and Rosati 2011) and Report 2 (Lin et al. 2011a) have detailed information about the CMS-Wave features, and evaluation of model's performance skills in a variety of applications. The Report, Report 3, and Report 4 by Sanchez et al. (2011a and 2011b) describe coupling of wave-flow models, and hydrodynamic and sediment transport and morphology change aspects of CMS-Flow. The performance of CMS for a number of applications is summarized in Report 1 and details are described in the three companion V&V Reports 2, 3, and 4.

The CMS-Wave, a spectral wave model, is used in this study given the large extent of modeling domain over which wave estimates were required. Details of the wave modeling are described in Chapter 4 of this report. Wind wave generation and growth, diffraction, reflection, dissipation due to bottom friction, white-capping and breaking, wave-current interaction, wave run-up, wave setup, and wave transmission through structures are the main wave processes included in the CMS-Wave. The height and direction of waves approaching the Tillamook Inlet navigation channel change due to wave shoaling, refraction, diffraction, reflection, and breaking. Waves propagating through the entrance interact with bathymetry, surrounding land features, currents, and coastal structures. These changes to waves affect bed shear stresses and sediment mobility around this inlet.

Figure A-1. The CMS framework and its components.

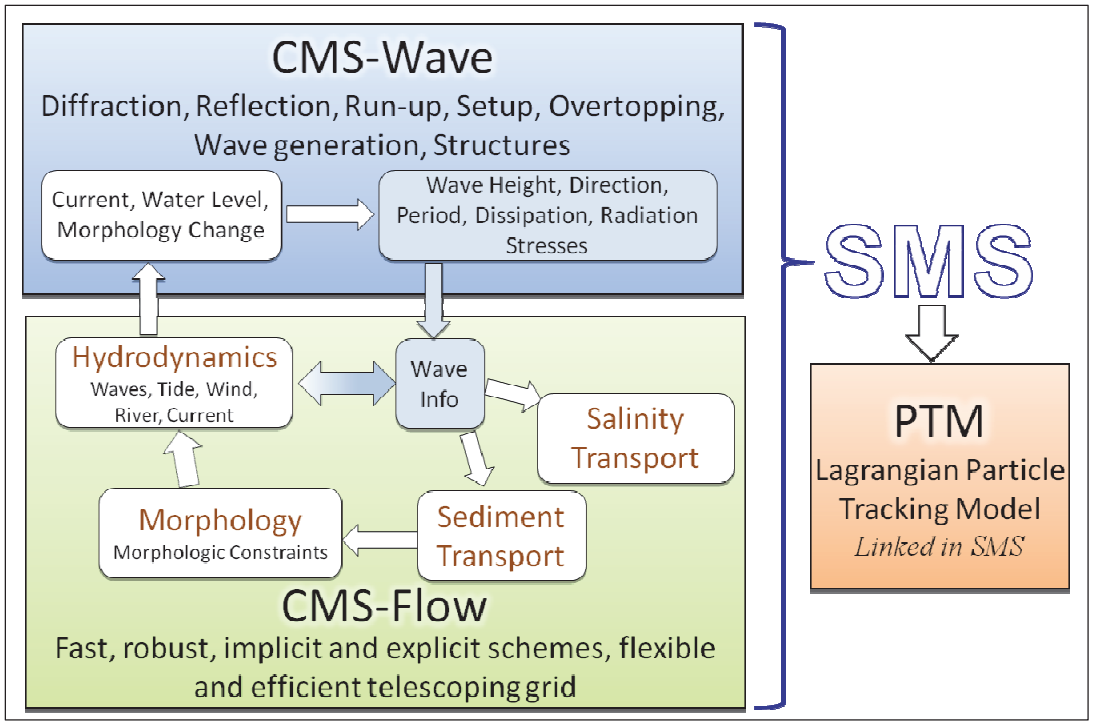

CMS-Wave model solves the steady-state wave-action balance equation on a non-uniform Cartesian grid to simulate steady-state spectral transformation of directional random waves at and around the Tillamook Inlet. CMS-Wave is designed to simulate wave processes with ambient currents at coastal inlets and in navigation channels. The model can be used either in half-plane or full-plane mode for spectral wave transformation (Lin et al. 2008). The half-plane mode is default because in this mode CMS-Wave can run more efficiently as waves are transformed primarily from the seaward boundary toward shore. See Lin et al. (2011b and 2008) for features of the model and step-by-step instructions with examples for application of CMS-Wave to a variety of coastal inlets, ports, structures, and other navigation problems. Publications listed in the V&V reports and this report provide additional information about the CMS-Wave and its engineering applications. Additional information about CMS-Wave is available from the CIRP website: http://cirp.usace.army.mil/wiki/CMS-Wave

The CMS-Flow, a two-dimensional shallow-water wave model, was used for hydrodynamic modeling (calculation of water level and current) in this study. The implicit solver of the flow model was used in this study. This circulation model provides estimates of water level and current given the tides, winds, and river flows as boundary conditions. CMS-Flow calculates

hydrodynamic (depth-averaged circulation), sediment transport and morphology change, and salinity due to tides, winds, and waves.

The hydrodynamic model solves the conservative form of the shallow water equations that includes terms for the Coriolis force, wind stress, wave stress, bottom stress, vegetation flow drag, bottom friction, wave roller, and turbulent diffusion. Governing equations are solved using the finite volume method on a non-uniform Cartesian grid. Finite-volume methods are a class of discretization schemes, and this formulation is implemented in finite-difference for solving the governing equations of coastal wave, flow and sediment transport models. See the V&V Reports 3 & 4 by Sanchez et al. (2011a and 2011b) for the preparation of model at coastal inlet applications. Additional information about CMS-Flow is available from the CIRP website: http://cirp.usace.army.mil/wiki/CMS-Flow

In this study, the coupled CMS-Flow and CMS-Wave models used the same grid domains. CMS-Flow modeling task included specification of winds, tides, and river flows (discharges) to the model. The effects of waves on the circulation were input to the CMS-Flow and have been included in the simulations performed for this study. For investigation of wave-current interaction, the CMS-Flow modeling considered three constant wave heights (H_s = 2 m, 3 m, and 4 m) to investigate the effects of flow on waves. These test runs were done in part for setting up the CMS-Flow for simulations using the actual field conditions in 2005 and 2010 for the months of August (summer) and December (winter). Details of these simulations are presented in Chapter 5.

Although sediment transport and morphology change modeling were not considered in this study, we note for future reference that there are three sediment transport models available in CMS-Flow: a sediment mass balance model, an equilibrium advection-diffusion model, and a non-equilibrium advection-diffusion model. Depth-averaged salinity transport is simulated with the standard advection-diffusion model and includes evaporation and precipitation. The V&V Report 1, Report 3 and Report 4 describe the integrated wave-flow-sediment transport and morphology change aspects of CMS-Flow. The performance of CMS-Flow is described for a number of applications in the V&V reports.

REPORT DOCUMENTATION PAGE

Form Approved
OMB No. 0704-0188

1. REPORT DATE *(DD-MM-YYYY)*	2. REPORT TYPE	3. DATES COVERED *(From - To)*
September 2013	Final Report	

4. TITLE AND SUBTITLE

Preliminary Analysis of Morphology Change, Waves, and Currents for Navigation at Tillamook Inlet, Oregon

5a. CONTRACT NUMBER

5b. GRANT NUMBER

5c. PROGRAM ELEMENT NUMBER

6. AUTHOR(S)

Zeki Demirbilek, Honghai Li, Lihwa Lin, Tanya M. Beck,and Hans R. Moritz

5d. PROJECT NUMBER

5e. TASK NUMBER

5f. WORK UNIT NUMBER

7. PERFORMING ORGANIZATION NAME(S) AND ADDRESS(ES)

Coastal and Hydraulics Laboratory
US Army Engineer Research and Development Center
3909 Halls Ferry Road
Vicksburg, MS 39180-6199

8. PERFORMING ORGANIZATION REPORT NUMBER

ERDC/CHL TR-13-13

9. SPONSORING / MONITORING AGENCY NAME(S) AND ADDRESS(ES)

US Army Engineer District, Portland
333 SW First Avenue
10th Floor
Portland, OR 97204-3495

10. SPONSOR/MONITOR'S ACRONYM(S)

11. SPONSOR/MONITOR'S REPORT NUMBER(S)

12. DISTRIBUTION / AVAILABILITY STATEMENT

Approved for public release; distribution is unlimited.

13. SUPPLEMENTARY NOTES

14. ABSTRACT

This report documents preliminary investigations of morphologic change and numerical modeling of wave and current conditions that affect entrance channel navigation at Tillamook Inlet, Oregon. It is believed that unfavorable conditions are caused by a combination of three primary factors: a large ebb shoal, the Pacific coast high-energy wave climate, and a narrow dual-jetty entrance that forms a high current environment. A limited analysis of two bathymetry surveys for representative summer and winter months in 2005 and 2010 indicated that the geometry of ebb shoal outside the entrance of the inlet has been changing, exhibiting an asymmetric orientation relative to the entrance in 2005 which became symmetric by 2010. The historical morphologic evolution of the ebb shoal was evaluated in an attempt to determine possible relationships between the ebb shoal changes and changes to waves and currents in the entrance channel at Tillamook. The numerical modeling analysis was limited to one selected summer month and one winter month, with the sole purpose being the investigation of potential relationships between the geometry (shape, footprint, and elevation) of the ebb shoal and local wave and current conditions during these two selected months. Results indicated that both the geometry of ebb shoal and the entrance jetties together influence the magnitude of waves and currents at the inlet area (through the entrance channel and over the shoal). The two jetties forming the narrow inlet entrance played a critical role in the evolution of the ebb shoal, controlling the spatial variation and severity of waves and currents at the entrance and over the ebb shoal. Wave conditions at Tillamook Inlet may be improved by changing the geometry of the ebb shoal or jetties or both.

15. SUBJECT TERMS

Inlet
Jetty
DUAL jetties
CURRENTS
Waves
Tides
Bathymetry
EBB shoal

16. SECURITY CLASSIFICATION OF:			17. LIMITATION OF ABSTRACT	18. NUMBER OF PAGES	19a. NAME OF RESPONSIBLE PERSON
a. REPORT	b. ABSTRACT	c. THIS PAGE			19b. TELEPHONE NUMBER *(include area code)*
unclassified	unclassified	unclassified		101	